Oxides for thermoelectricity

Sylvie Hébert
Laboratoire CRISMAT
UMR6508 CNRS et ENSICAEN

UCSB – ICMR Summer School on Inorganic Materials
for Energy Conversion and Storage
August 2012

Laboratoire CRISMAT

Cristallographie et Sciences des Matériaux

Caen

ENSICAEN

ÉCOLE NATIONALE SUPÉRIEURE D'INGÉNIEURS DE CAEN
& CENTRE DE RECHERCHE

✓ **CRISMAT : some figures**

- **120 persons**
- **47 researchers**
- **15 post-doc**
- **42 Ph-D students**
- **125 publications per year**

Search for new oxides : high Tc superconductors, colossal magneto-resistance, thermoelectrics, multiferroics…
And Beyond oxides

Thermoelectric Activities

7 permanent staff + 1 engineer + students / postdocs + the rest of the lab!

Ramzy Daou, Franck Gascoin, Christophe Goupil, Emmanuel Guilmeau, Sylvie Hébert, Antoine Maignan, Jacques Noudem

→ Synthesis / Processing

→ Low and high T thermoelectric properties

→ Modelization of the thermoelectric properties

→ Module and module testing

Techniques

Cristallography (8 diffractometers)

<u>80 furnaces</u>

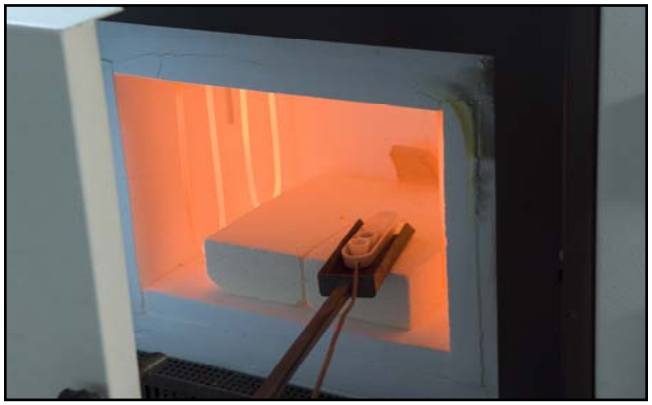

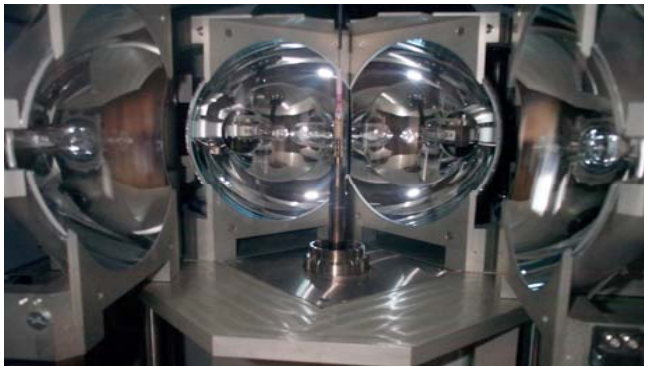

Thin-films (PLD's)

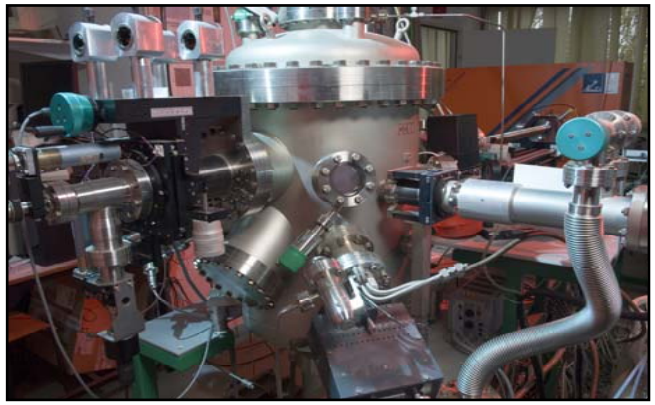

5 TEM, 3 SEM

thermomechanical tests

+ SPS

Low T properties

Thermopower and thermal conductivity measurements developped by Jiri Hejtmanek (Prague), using PPMS environment

4 ‘PPMS’
H_{max} = 14T
2K < T < 400K

DC and AC magnetization
Magnetization up to 1000K (VSM)
Resistivity
Specific heat
Seebeck coefficient
Thermal conductivity

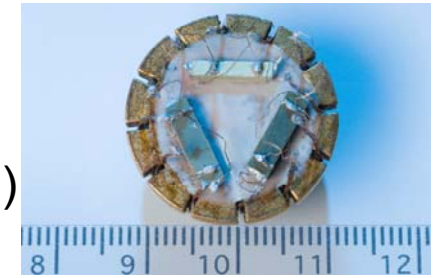

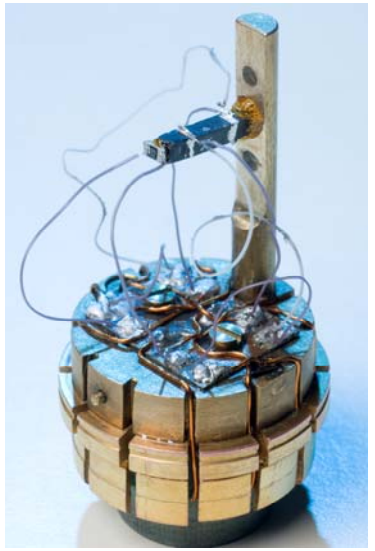

F. Janin, Photothèque CNRS

3 SQUID magnetometers
H_{max} =5.5T
2K < T < 400K

DC and AC magnetization

High T properties

$$ZT = \alpha^2 T/\rho\kappa$$

seebeck

Electrical resistivity

Thermal conductivity

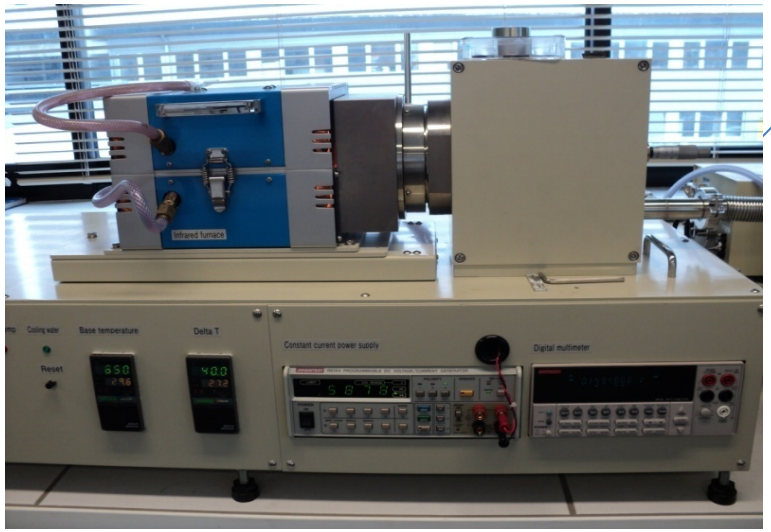

ZEM 3 Ulvac Riko
Combined Seebeck and resistivity measurement
(RT to 700°C)

κ = diffusivity x density x Cp

Netzsch

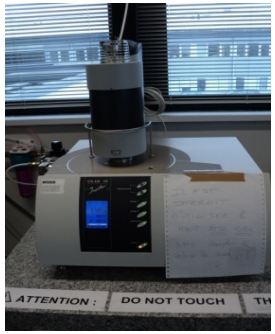

Modules

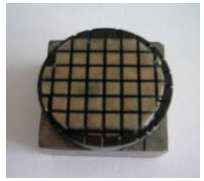

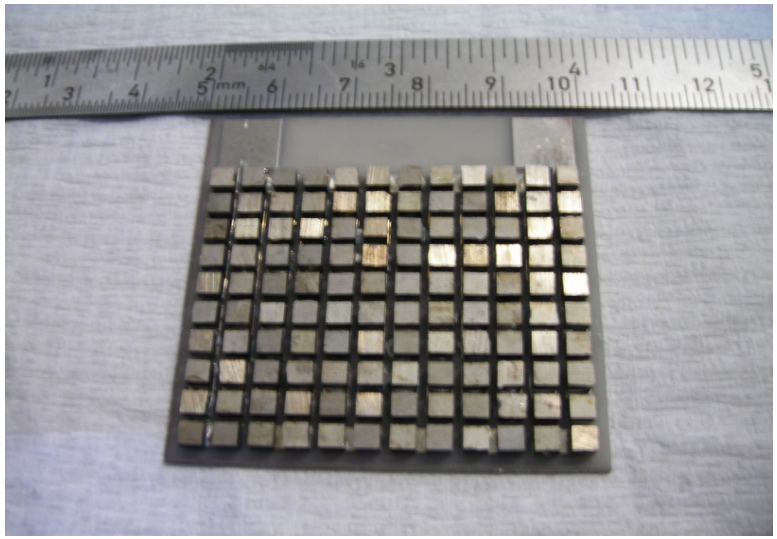

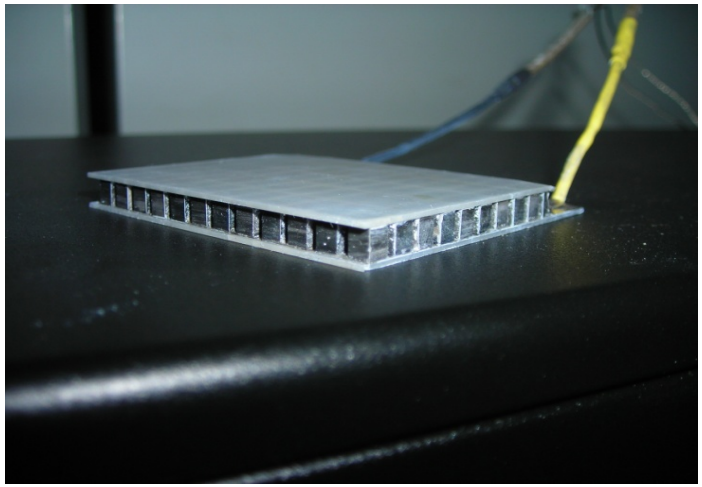

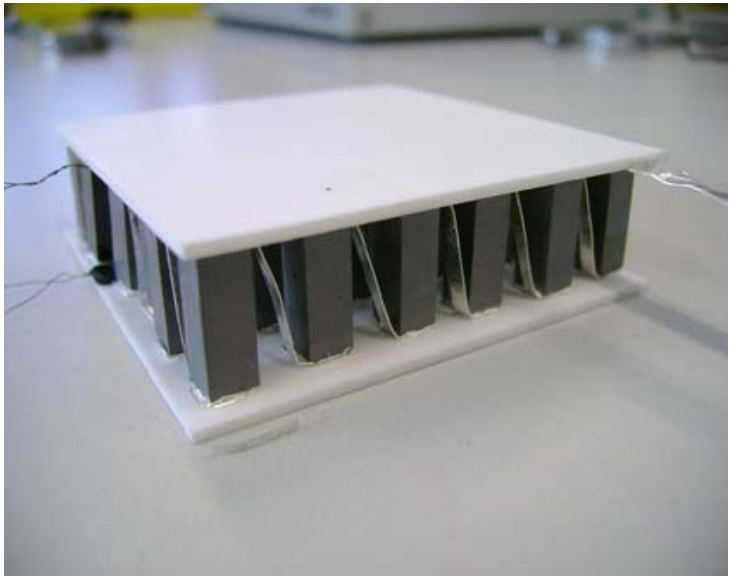

Oxides for thermoelectricity

Aim of this tutorial :
Best thermoelectric oxides /
show the specificities of oxides

- Introduction :
Oxides specificities / Models for oxides /
Best thermoelectric oxides

Increase of the carrier density ↓

- Semi – conductors : the Heikes formula
- Degenerate semi-conductors : best n type oxides
- Na_xCoO_2 and misfit compounds

- Nanostructuration
- Modules
- Conclusion

Introduction

Why oxides?

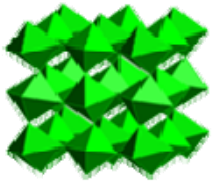

Strong interplay between spin/charge/lattice

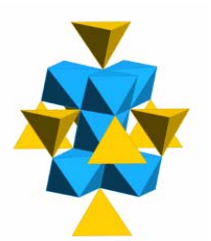

Property	Materials
Metals	CrO_2, Fe_3O_4, $SrRuO_3$
Insulators	Cr_2O_3, CoO, Fe_2O_3, Al_2O_3
Metal-Insulator Transition	VO_2, V_2O_3
Superconductors	$Ba(Bi,Pb)O_3$, $YBa_2Cu_3O_7$
Piezo- and Ferroelectrics	$Pb(Zr,Ti)O_3$, $BaTiO_3$
Catalysts (chemical, photo-)	TiO_2 , $LaCoO_3$, $BiMoO_4$
Ferro-, Antiferro-, Ferrimagnets	CrO_2, MnO, $MnFe_2O_4$
Pigments	TiO_2, $CoAl_2O_4$, $Co_3(PO_4)_2$
Sensors	$Ca_xZr_{1-x}O_{2-x}$, SnO_2
Negative Thermal Expansion	ZrW_2O_8
Ionic Conductors (battery, SOFC)	Li_xMnO_2, $Ca_xZr_{1-x}O_{2-x}$
Thermoelectrics	Na_xCoO_2
Non-Linear Optics	$LiNbO_3$

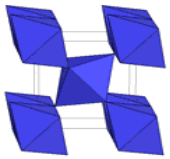

Rutile, TiO_2

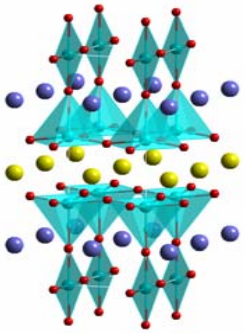

$YBa_2Cu_3O_7$

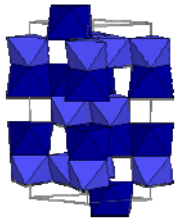

$LiNbO_3$

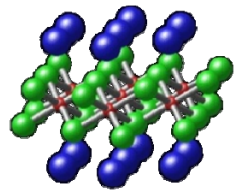

$LiMnO_2$

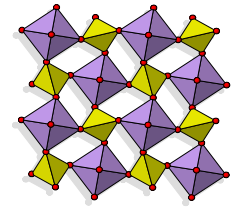

ZrW_2O_8

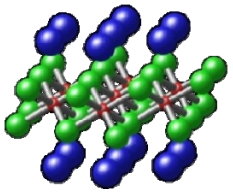

Na_xCoO_2

From M. Subramanian, OSU

Large family of compounds,
Can be cheap, environment friendly and resistant in air

Specificities of oxides

High T synthesis and synthesis possible in oxydizing environment
Oxides can be stable at high T and in air
Non toxic elements, abundance of elements…

Strong electronic correlations
→ Difficult to calculate the band structure
→ **But** could be interesting for the Seebeck!

Kinetic energy ~ Repulsive Coulomb energy

Strong renormalization of effective masses
Narrow bands

Possible tuning of the electronic correlations

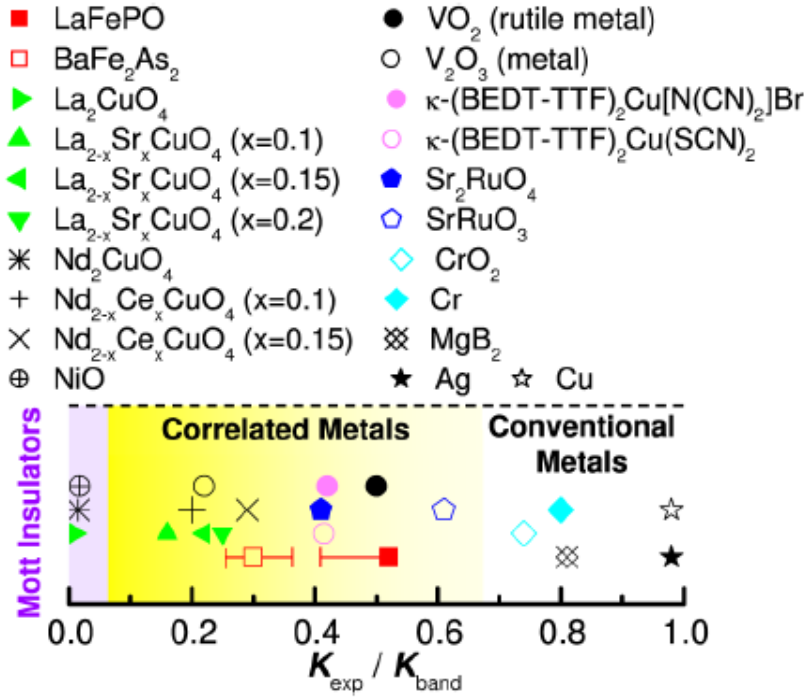

FIG. 1 (color online). The ratio of the experimental kinetic energy and the kinetic energy from band theory K_{exp}/K_{band} for various classes of correlated metals and also for conventional metals. The data points are offset in the vertical direction for clarity. From Qazilbash, Hamlin *et al.*, 2009.

D. Basov et al., Rev. Mod. Phys. 83, 471 (2011)
A. Georges et al., Rev. Mod. Phys. 68, 13 (1996)

Influence of electronic correlations

DOS

Metal

U increasing

Insulator

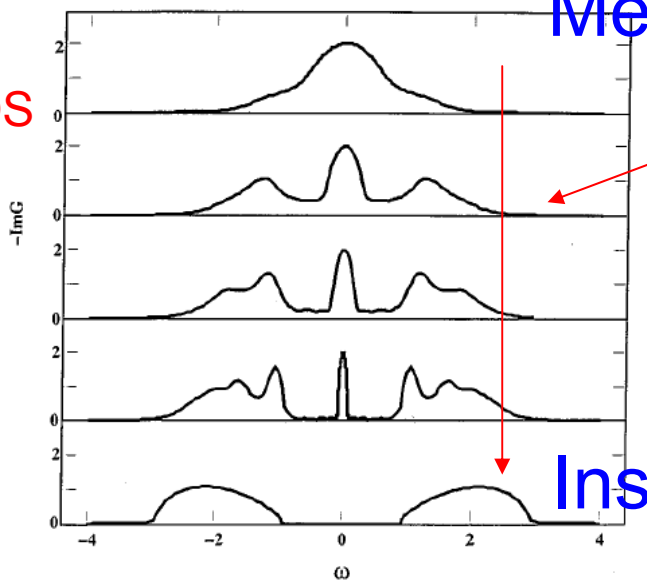

FIG. 30. Local spectral density $\pi D\rho(\omega)$ at T=0, for several values of U, obtained by the iterated perturbation theory approximation. The first four curves (from top to bottom, U/D =1,2,2.5,3) correspond to an increasingly correlated metal, while the bottom one (U/D=4) is an insulator.

Seebeck

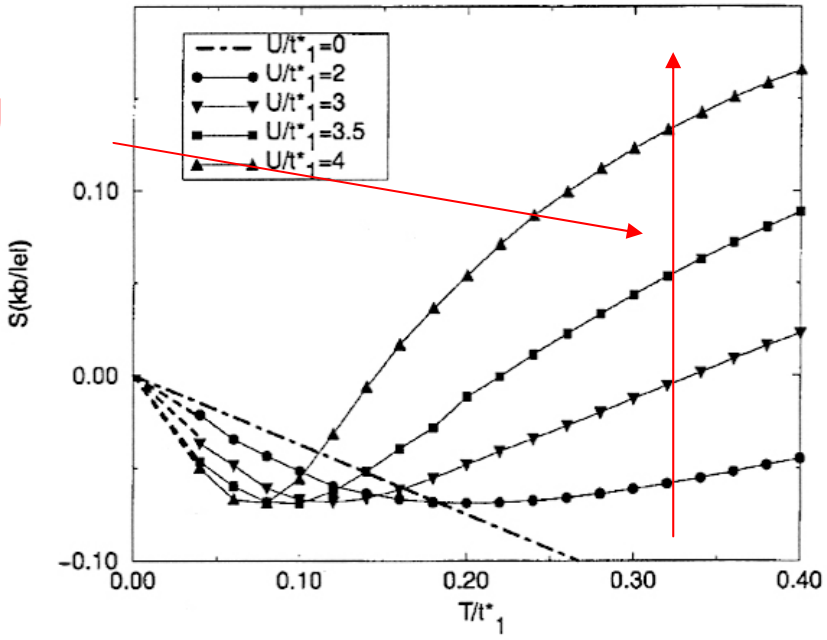

Modification of DOS
→ Increase of S?

A. Georges et al., Rev. Mod. Phys. 68, 13 (1996)

Calcul of U impact on the Seebeck coefficient

J. Merino et al., PRB61, 7996 (2000)

Bibliography : Thermoelectric oxides

•First papers in the 60's : SnO_2, SbO_2…
Degenerate n type semi-conductors

•1980's : thermopower is used as a probe for the cuprates

•1990's : Doped ZnO as best n type thermoelectric oxide (Ohtaki et al.)

•1997 : Na_xCoO_2 (Terasaki et al.)

Web of Science®

<< Back to previous page

Citation Report Topic=(thermoelectric oxides)
Timespan=All Years. Databases=SCI-EXPANDED, SSCI, A&HCI, CPCI-S, CPCI-SSH, IC.

This report reflects citations to source items indexed within Web of Science. Perform a Cited Reference Search to include citations to items not indexed within Web of Science.

Published Items in Each Year

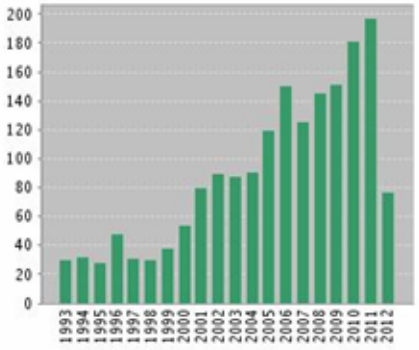

The latest 20 years are displayed.
View a graph with all years.

Citations in Each Year

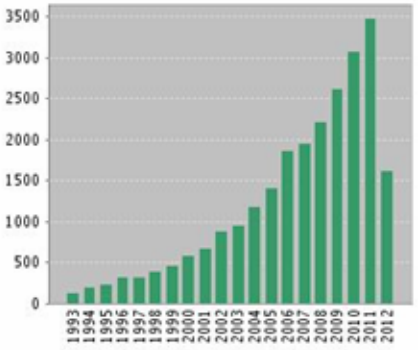

The latest 20 years are displayed.
View a graph with all years.

Results found:	1896
Sum of the Times Cited [?] :	25136
Sum of Times Cited without self-citations [?] :	17567
Citing Articles [?] :	14137
Citing Articles without self-citations [?] :	12757
Average Citations per Item [?] :	13.26
h-Index [?] :	63

Results: 1896 Page 1 of 190 Go Sort by: Times

Introduction

PRB46, 14928 (1992)

High Tc superconductors

Systematics in the thermoelectric power of high-T_c oxides

S. D. Obertelli and J. R. Cooper*
Interdisciplinary Research Centre in Superconductivity, Madingley Road, Cambridge CB3 OHE, United Kingdom

J. L. Tallon
New Zealand Institute for Industrial Research and Development, P.O. Box 31310, Lower Hutt, New Zealand

(Received 2 September 1992)

Many superconducting cuprates show a parabolic variation of T_c with hole concentration p, there being a minimum and a maximum hole concentration for superconductivity. Thermoelectric power (TEP) measurements reported here as a function of p for a number of oxides reveal several important trends: (1) close similarities in the TEP of several compounds and a change in sign of the room-temperature TEP near the maximum T_c, (2) continuity in the TEP when doping across the two superconducting-nonsuperconducting boundaries, and (3) a universal correspondence of the room-temperature TEP with p over the whole range of doping.

Correlation between Seebeck / doping / Critical temperature

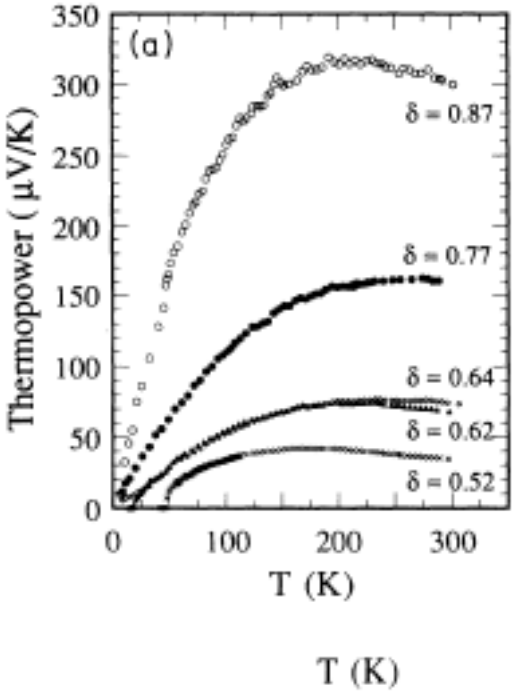

T (K)

FIG. 2. (a) Thermoelectric power vs temperature for underdoped $YBa_2Cu_3O_{7-\delta}$ with $0.52 \leq \delta \leq 0.87$. For $\delta > 0.5$ the es-

$YBa_2Cu_3O_{7-\delta}$

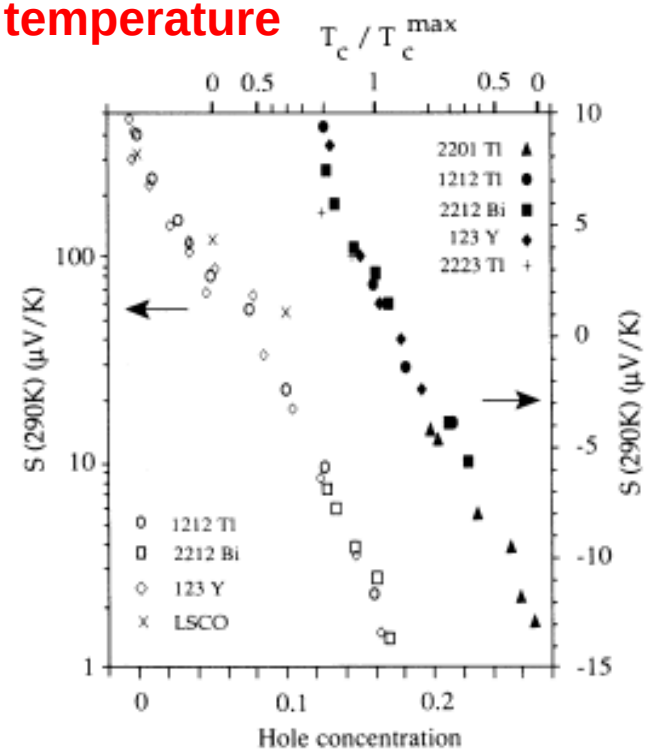

FIG. 3. Room-temperature thermoelectric power $S(290\ \mathrm{K})$ vs hole concentration (and T_c/T_c^{max}) for various high-T_c cuprates in both the underdoped (logarithmic scale) and overdoped (linear scale) regions. $La_{2-x}Sr_xCuO_4$ (LSCO) data from Ref. 33.

$Zn_{1-x}Al_xO$ (x = 0 – 0.1)

ZT = 0.3

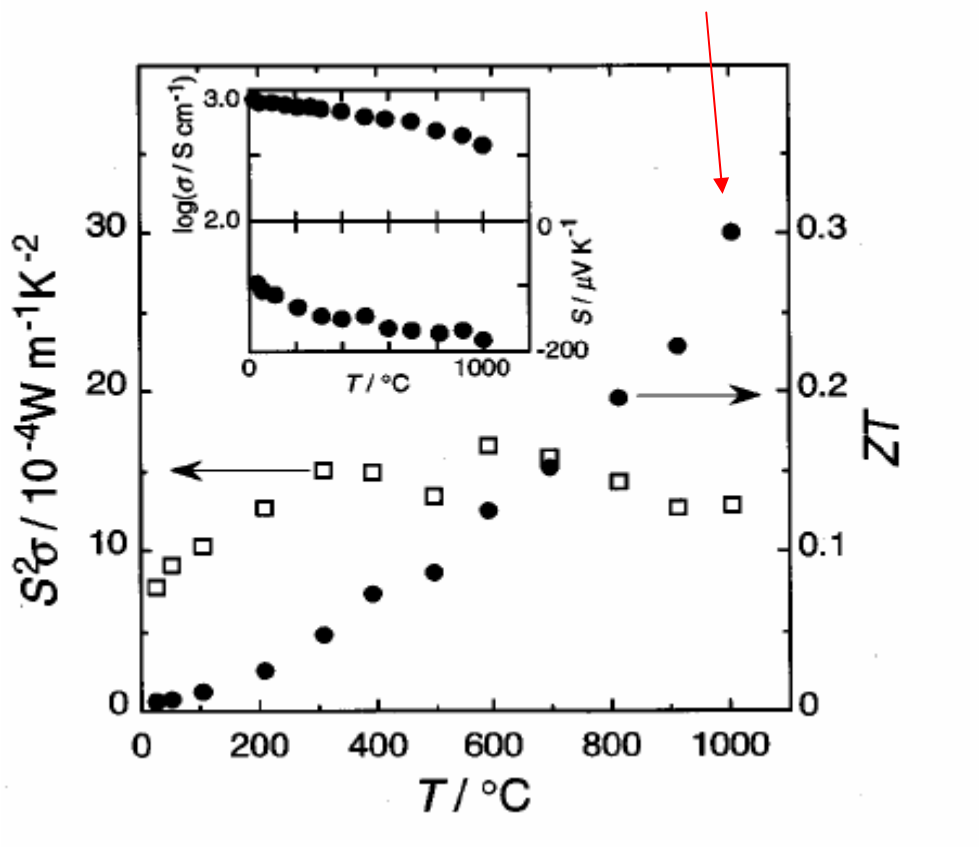

But κ is too high !!!

M. Ohtaki et al., JAP79, 1816 (1996)

Broadband model for extrinsic n type semiconductor

$$\sigma = n e \mu,$$

$$S = -(k/e)[\ln(N_v/n) + A],$$

Large mobility of the carriers : 3 – 7cm^2/Vs

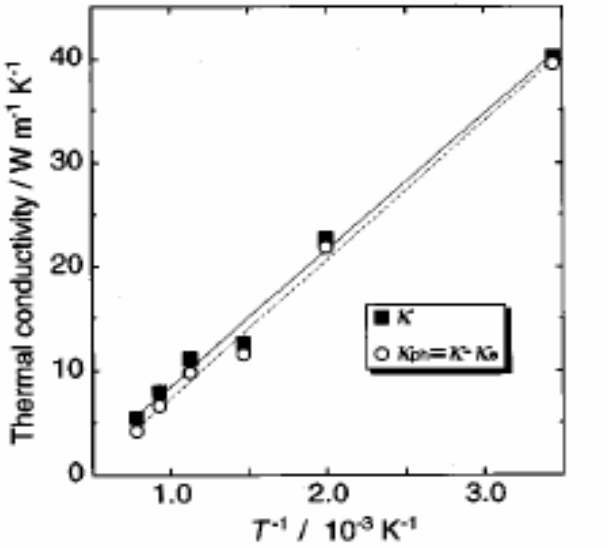

κ = 40Wm^{-1}K^{-1} at 300K

κ=5.4 Wm^{-1}K^{-1} at 1000°C

$Na_{0.7}CoO_2$

' Phonon Glass / Electron crystal '

I. Terasaki et al., Phys. Rev. B 56, R12685 (1997)

$Na_xCoO_2 : Na^+_x Co^{3+}_x Co^{4+}_{1-x} O_2$

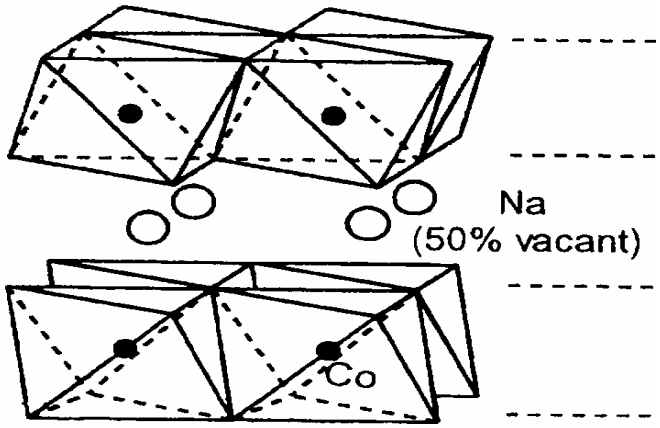

Co^{3+} ($3d^6$) / Co^{4+} ($3d^5$)

Measurements on polycrystals

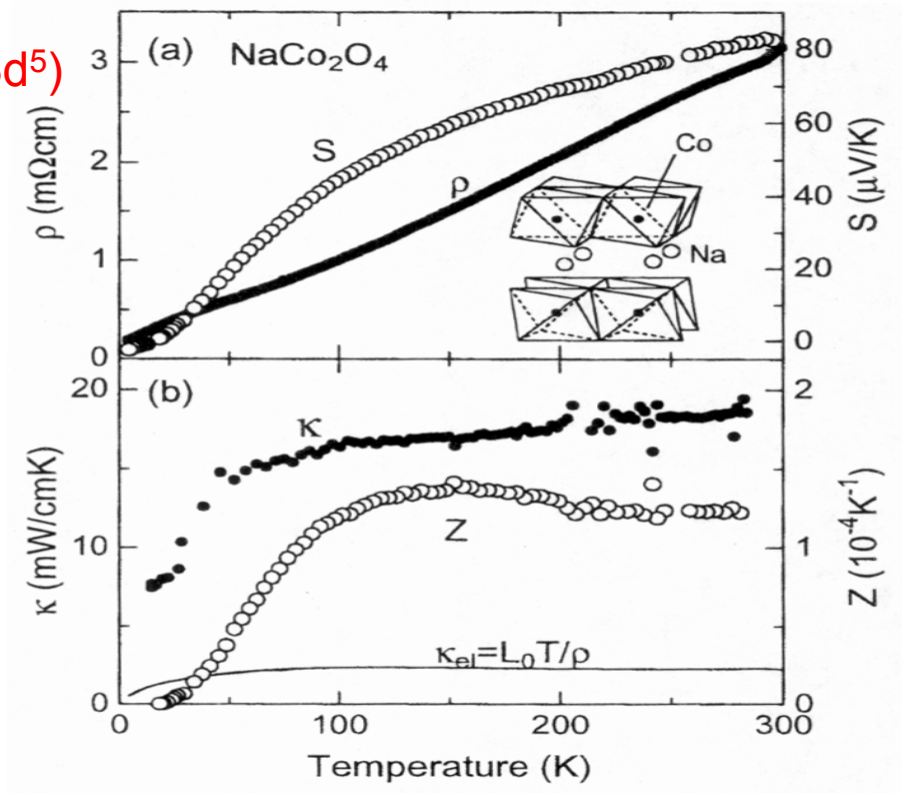

At 300K

Metallicity (crystals) $\rho \sim 0.2\ m\Omega\ cm$

Large S $S \sim +80\ \mu V/K$

Small κ (polycrystals) $\kappa \sim 2 Wm^{-1}K^{-1}$

(crystals) $\kappa \sim 5 Wm^{-1}K^{-1}$

Power factor $P=S^2/\rho$ at 300K

$Na_{0.7}CoO_2$

$P= 50\ 10^{-4}\ WK^{-2}m^{-1}$

Bi_2Te_3

$P= 40\ 10^{-4}\ WK^{-2}m^{-1}$

ZT of oxides

2 different families for the best thermoelectric oxides

- Type p : oxides related to Na_xCoO_2, metallic and large S
- Type n : 'transparent conducting oxides', degenerate semi-conductors

ZT (type p) > ZT (type n)

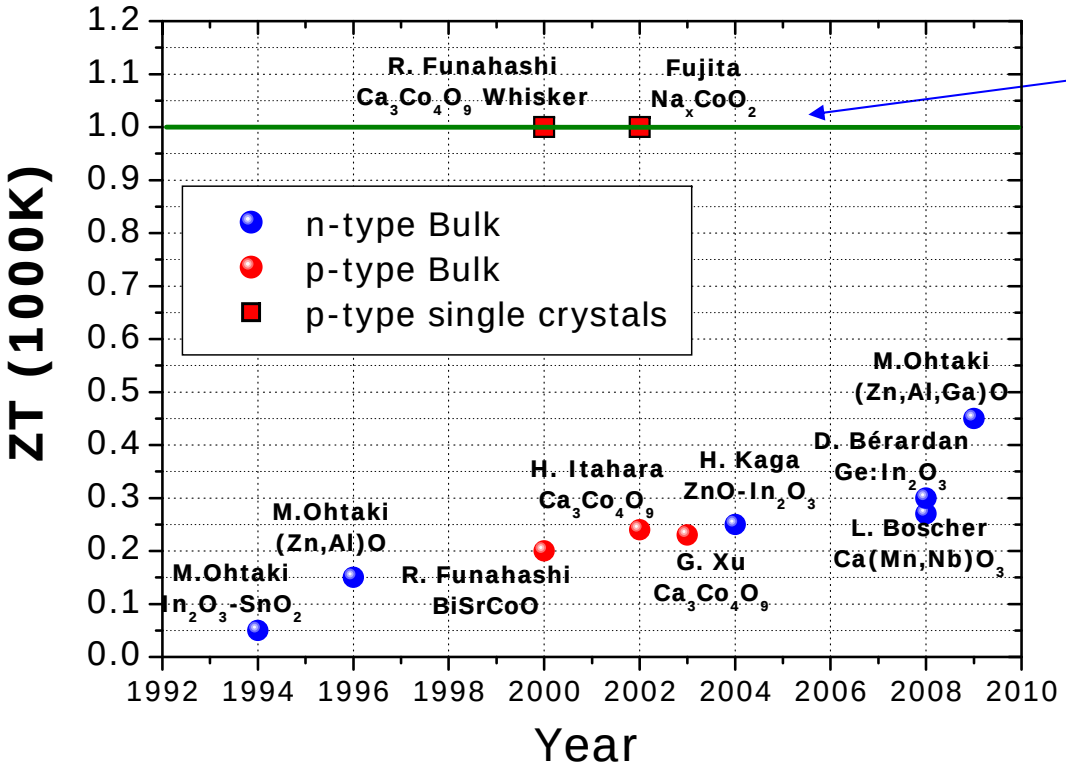

p type : Na_xCoO_2, Misfit oxides

n type : TCOs

High T properties of Na_xCoO_2

K. Fujita et al. JJAP40, 4644 (2001)

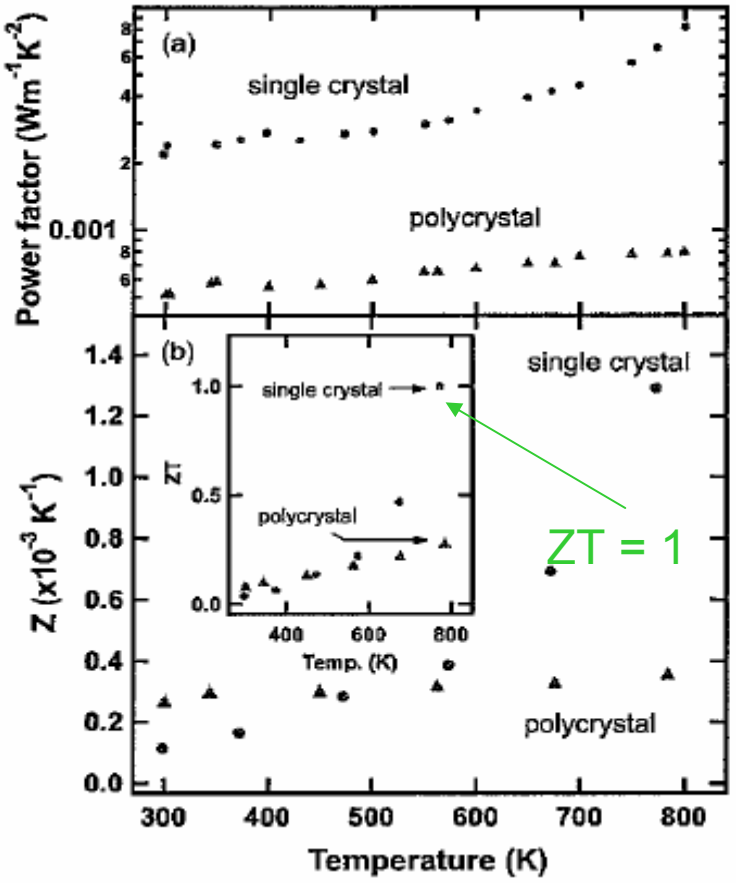

Crystal and polycrystal measurements

Crystals : 1.5 ×1.5 × 0.03 mm^3

ZT ~ 1 for crystals only at 800K

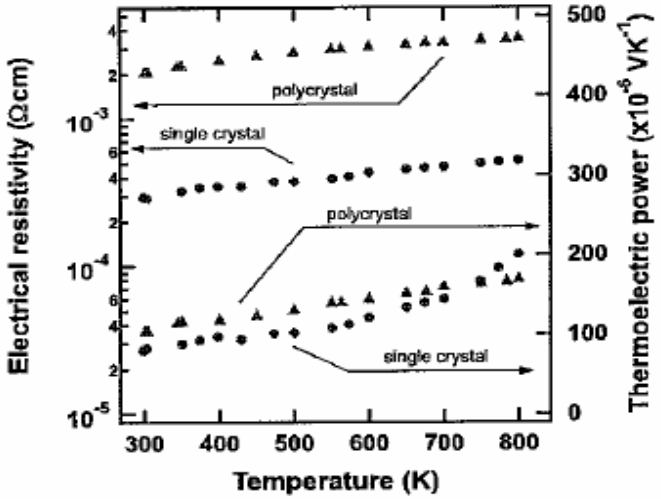

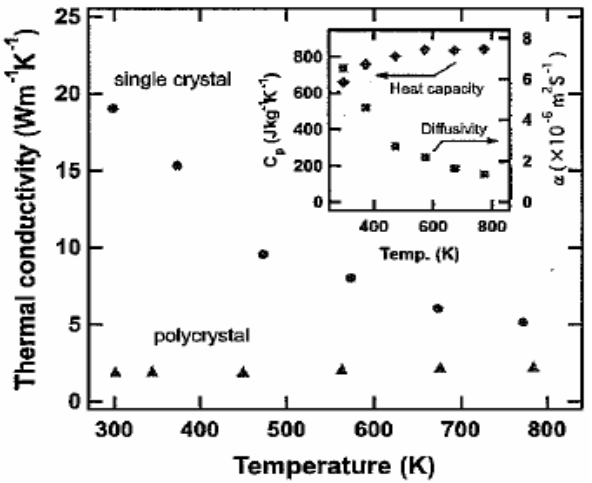

Oxides

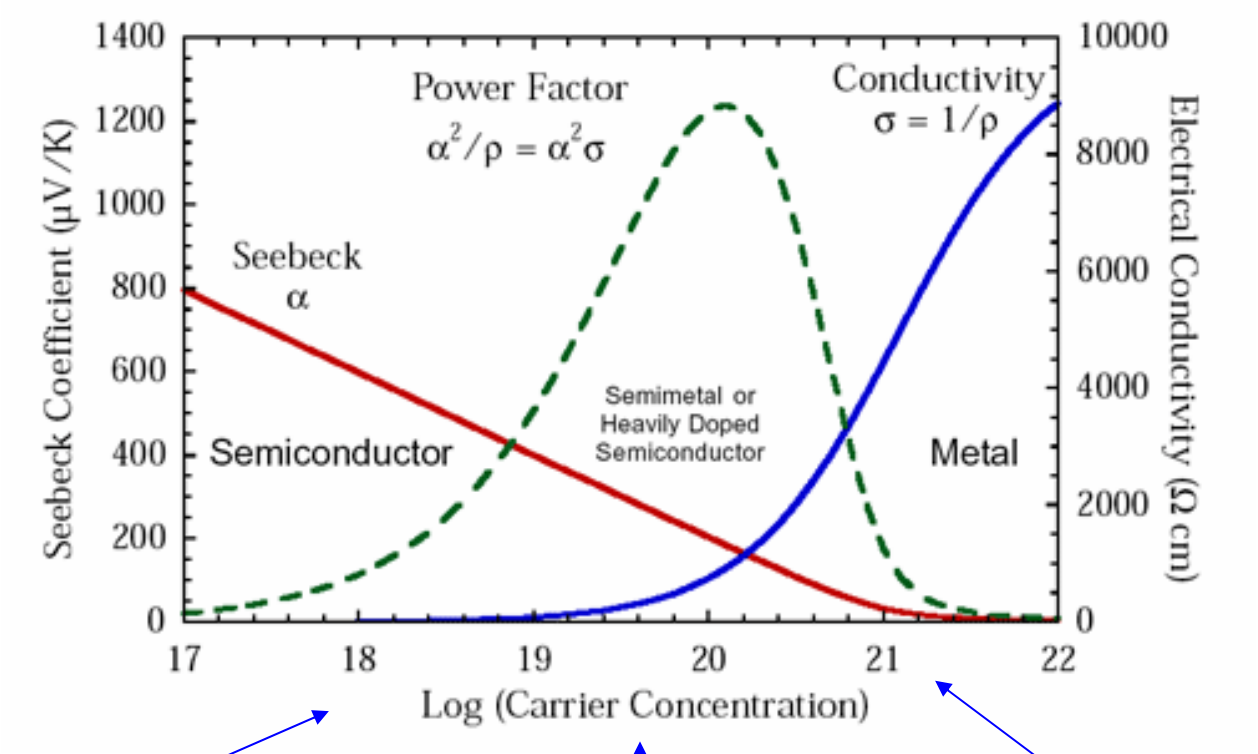

Semi-conductors
Large
S
Large ρ
n and p type
Increase of S
through Heikes?

Transparent conductors, Delafossites
Large S, small ρ
Large κ
Mostly n type (some p type)
Reduction of κ
through nanostructuration?

Misfits
Na_xCoO_2
Large S
+ metallic ρ
small κ
p type
Model system
Texturation problems

Modelization of thermoelectric properties in oxides

Models

$$ZT = \frac{S^2 T}{\rho\kappa} = \frac{S^2 T}{\rho(\kappa_e + \kappa_l)}$$

- **Mott's formula** :

$$S = \frac{\pi^2 k_B^2}{3e} T \left(\frac{\partial \ln \sigma(E)}{\partial E}\right)_{E=E_F}$$

$$\sigma(E) = en(E)\,\mu(E)$$

DOS

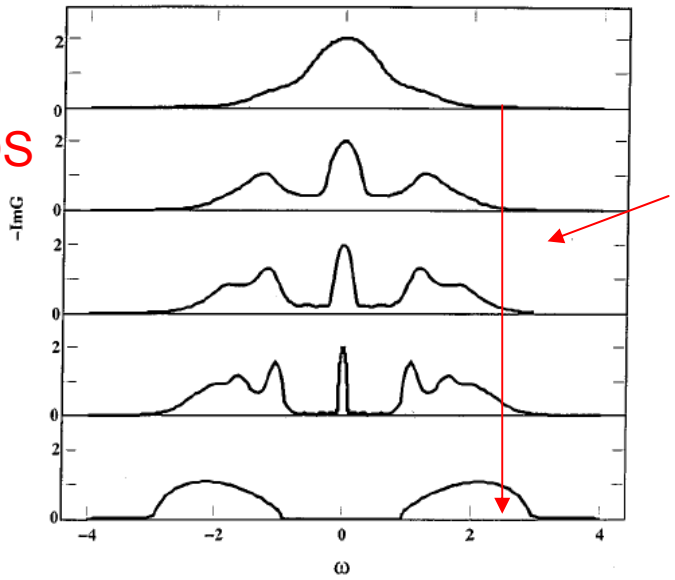

FIG. 30. Local spectral density $\pi D\rho(\omega)$ at T=0, for several values of U, obtained by the iterated perturbation theory approximation. The first four curves (from top to bottom, U/D =1,2,2.5,3) correspond to an increasingly correlated metal, while the bottom one (U/D=4) is an insulator.

U increasing

Seebeck

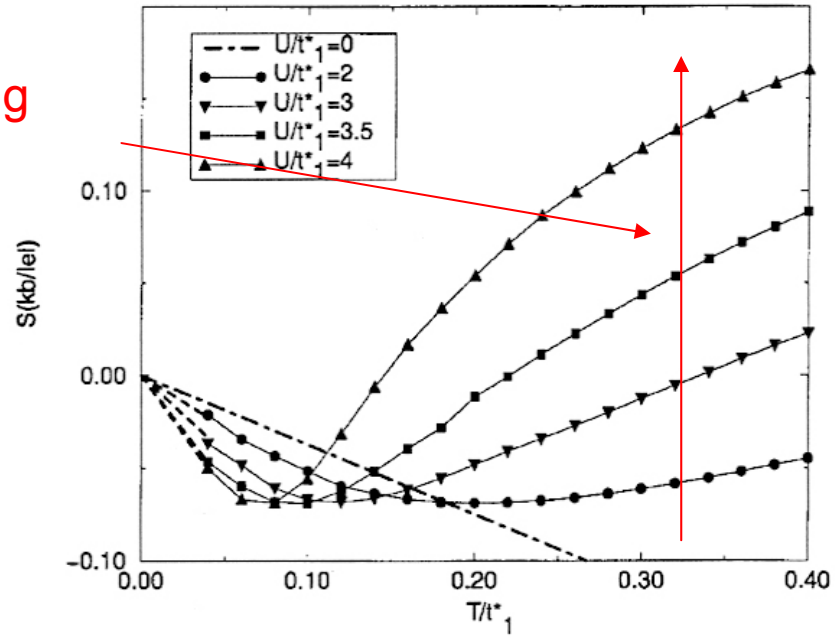

Possible increase of S due to strong correlations?

$$ZT = \frac{S^2 T}{\rho\kappa} = \frac{S^2 T}{\rho(\kappa_e + \kappa_l)}$$

- **Resistivity** : $\rho^{-1} = \mathrm{en(E)}\mu\mathrm{(E)}$

A large mobility is required (difficult for oxides!)

- **Thermal conductivity**

Electronic part related to ρ^{-1} (Wiedemann Franz), usually small

Lattice part has to be minimized

Mott's formula : influence of electronic correlations

$$S = \frac{\pi^2 k_B^2}{3e} T \left(\frac{\partial \ln \sigma(E)}{\partial E}\right)_{E=E_F}$$

Free electron gas

$$S = -\frac{\pi^2}{3}\frac{k_B^2 T}{e}\frac{N(\epsilon_F)}{n}\left(1 + \frac{2\zeta}{3}\right).$$

Scattering parameter

Carrier density

Very similar to the electronic specific heat

$$C_{el}/T = \gamma = \frac{\pi^2}{3} k_B^2 N(E_F)$$

γ is a probe of electronic correlations

Relationship between Seebeck and specific heat at low T??

K. Behnia et al. JPCM 16, 5187 (2004)

Low T limit

$$S = -\frac{\pi^2}{3}\frac{k_B^2 T}{e}\frac{N(\epsilon_F)}{n}\left(1+\frac{2\zeta}{3}\right).$$

$$C_{el}/T = \gamma = \frac{\pi^2}{3}k_B^2 N(E_F)$$

Universal value for the ratio of S / γ

Limit T→ 0

$$q = \frac{S}{T}\frac{N_{Av}e}{\gamma} = \text{cste}$$

$$0.5 < |q| < 2$$

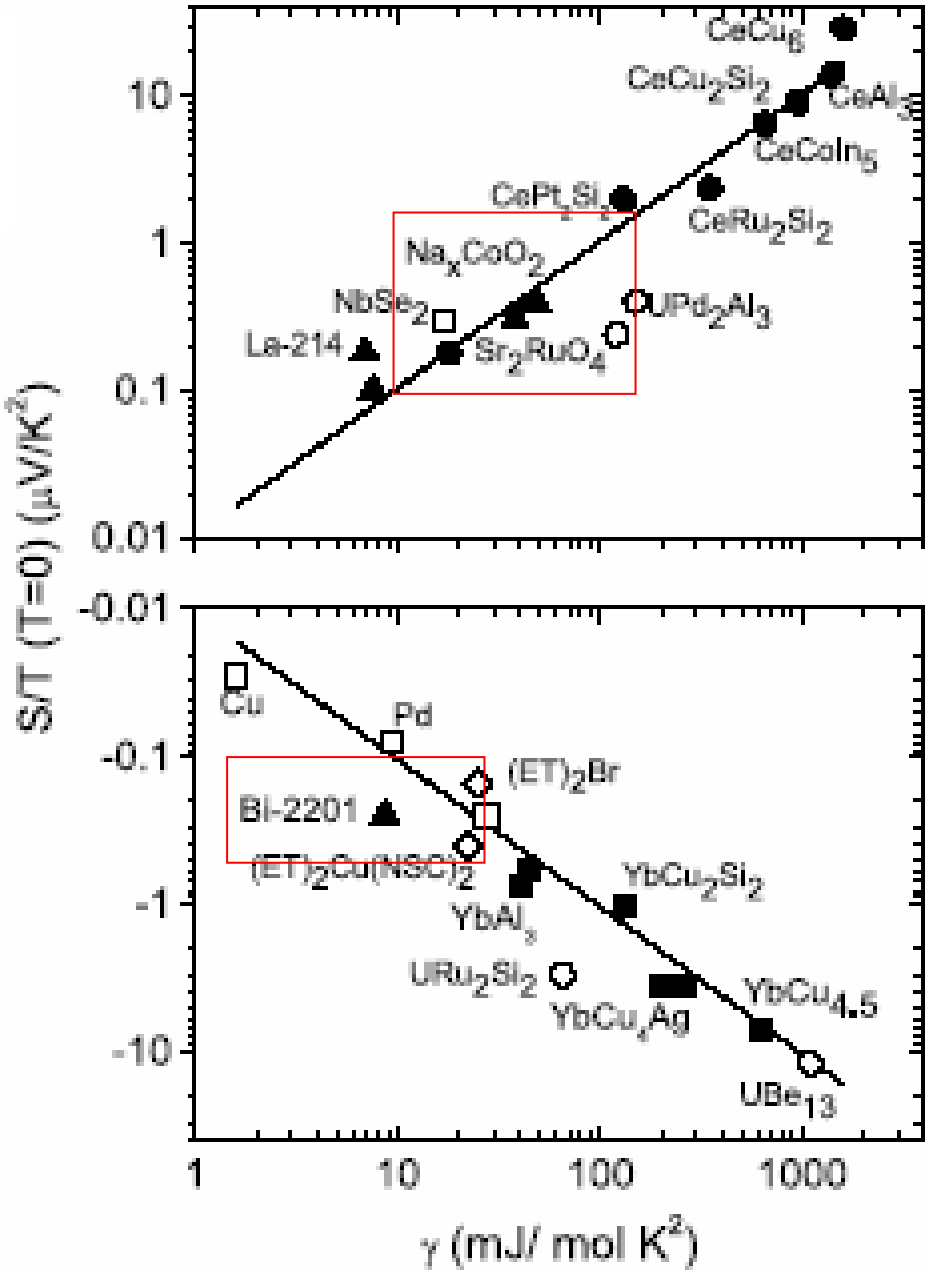

K. Behnia et al. JPCM 16, 5187 (2004)

Models

The Heikes formula

High T limit

PHYSICAL REVIEW B VOLUME 13, NUMBER 2 15 JANUARY 1976

Thermopower in the correlated hopping regime

P. M. Chaikin*
Department of Physics, University of California, Los Angeles, California 90024

G. Beni
Bell Laboratories, Murray Hill, New Jersey 07974

(Received 16 June 1975)

The high-temperature limit for the thermopower of a system of interacting localized carriers is governed entirely by the entropy change per added carrier. The calculation of this quantity reduces to a simple combinatorial problem dependent only on the density of carriers and the interactions stronger than the thermal energy. We have thus been able to generalize the Heikes formula to include several cases of interacting Fermi systems with spin.

'Simple combinatorial problem'

Calculated for organic thermoelectrics

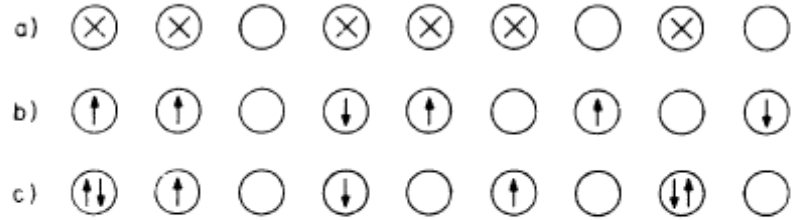

FIG. 1. Possible high-temperature site configuration of (a) spinless fermions; (b) electrons with an infinite on-site repulsion; and (c) electrons with no interactions.

P. M. Chaikin et al. Phys. Rev. B 13, 647 (1976)

The Heikes formula

Hubbard model

$$S = \frac{-S^{(2)}/S^{(1)} + \mu/|e|}{T} \rightarrow \frac{\mu/|e|}{T} \qquad \text{for } T \rightarrow \infty$$

$S^{(1)}$, $S^{(2)}$: depend on v and Q, velocity and energy operators

Valid for narrow band systems (localized correlated particles)

Limit $T \rightarrow \infty$: S ~ entropy / carrier

$$S = \frac{-k_B}{|e|} \ln\left(\frac{1-x}{x}\right)$$

x = concentration of carriers

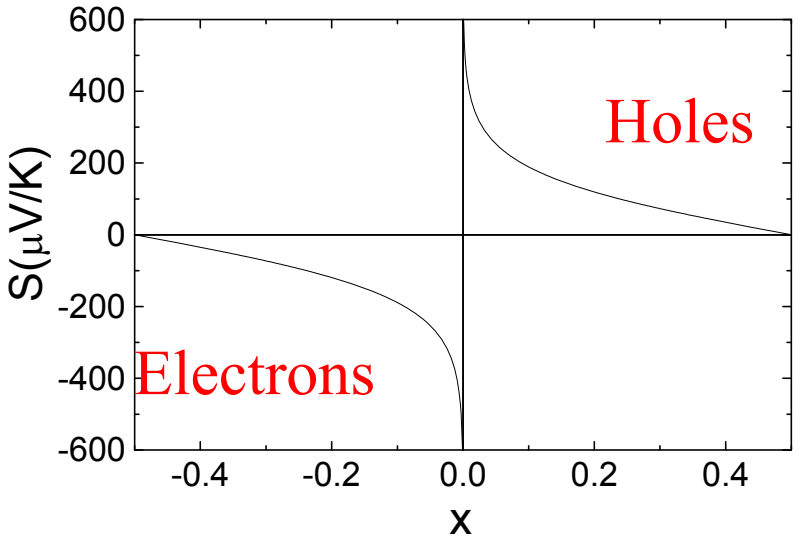

P. M. Chaikin et al. Phys. Rev. B 13, 647 (1976)

Spin entropy

Extra term in the Heikes formula due to the spin degeneracy

Mixed valency cation M^{n+} / $M^{(n+1)+}$:

$$\beta = \frac{2S_n + 1}{2S_{n+1} + 1}$$

$$S = -\frac{k_B}{|e|} \ln(\beta \frac{1-x}{x})$$

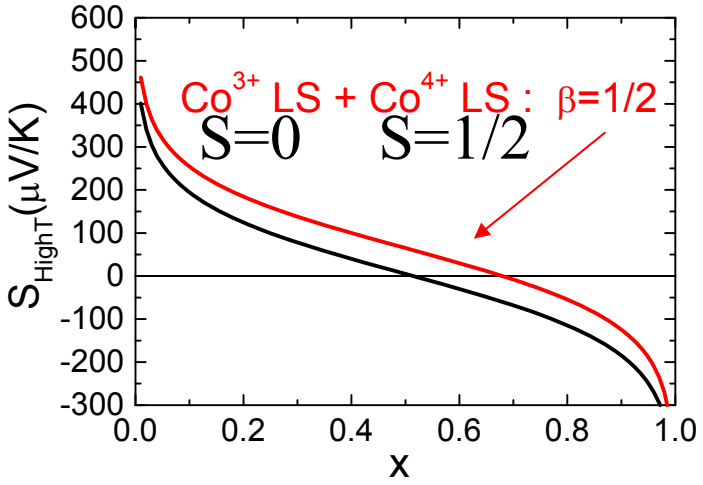

J. P. Doumerc JSSC 110, 419 (1994)

Na_xCoO_2 :

Spin and orbital degeneracy $Co^{3+}(3d^6)/Co^{4+}(3d^5)$

J. P. Doumerc JSSC 109, 419 (1994)

W. Koshibae et al., Phys. Rev. B 62, 6869 (2000)

$$S = -\frac{k_B}{e}\ln\left(\frac{g_3}{g_4}\frac{x}{1-x}\right)$$

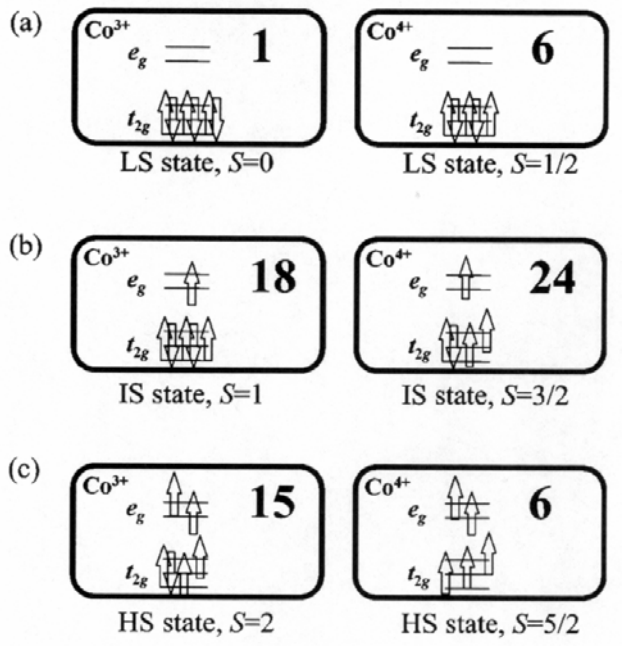

$g_4/g_3 = 6$

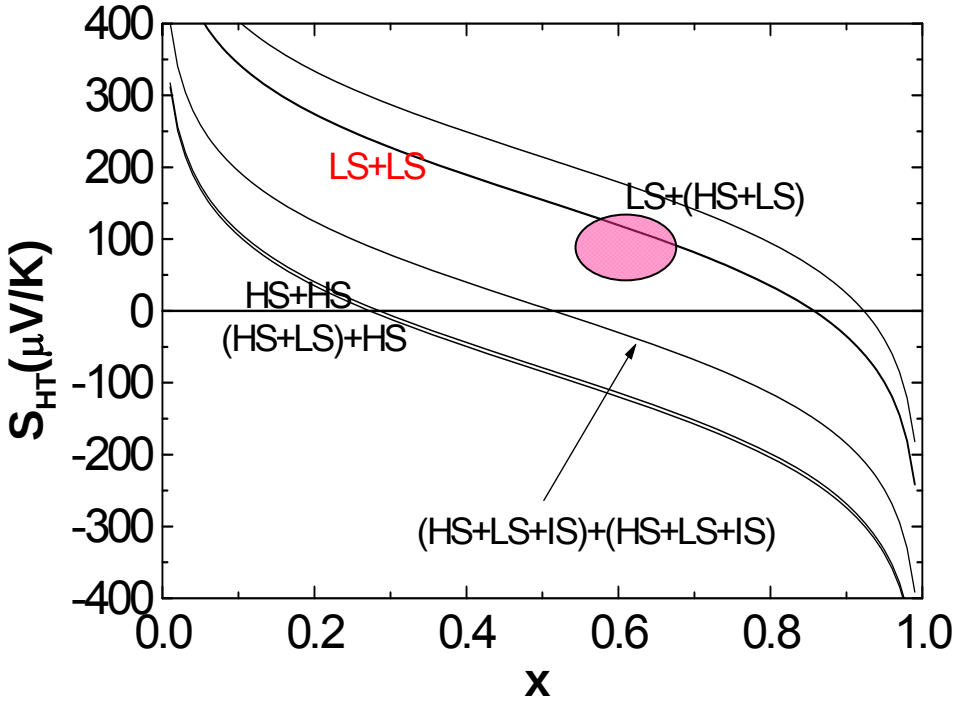

x : Co^{4+} concentration

Large S in Na_xCoO_2

Origin of the metallicity ?

Models

Band structure?

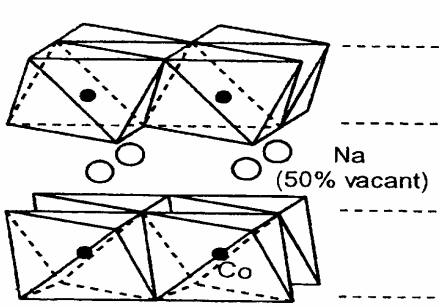

Rhombohedral crystalline field

Lifting of the t_{2g} levels degeneracy

D. J. Singh, Phys. Rev. B 61, 13397 (2000)

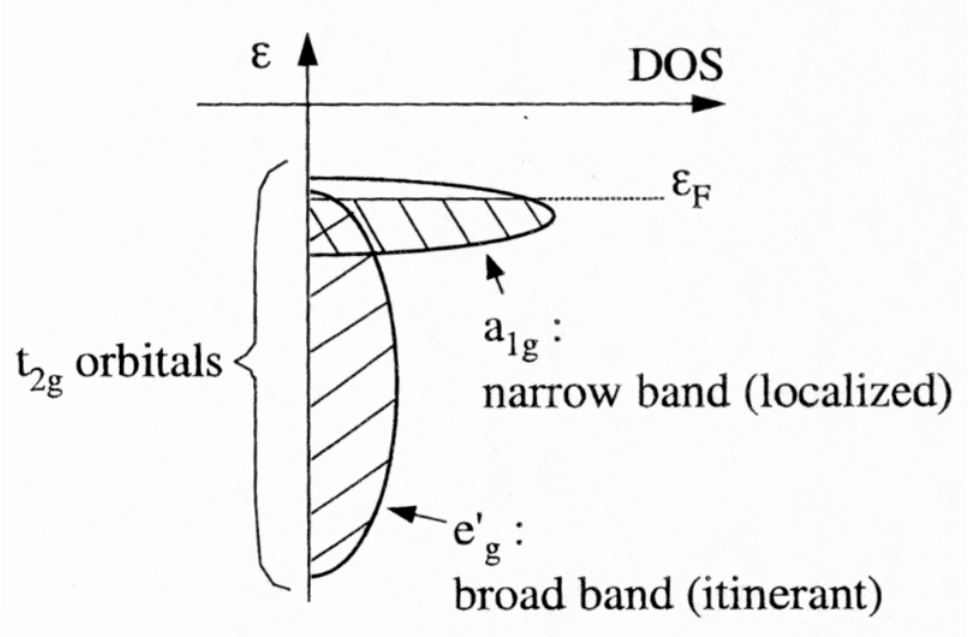

a_{1g} : localized moments / heavy holes

e'_g : mobile carriers / light holes

Peak of $N(E_F)$

$$\frac{S}{T} = \frac{\pi^2 k^2}{3e}\left(\frac{d\ln(\sigma)}{dE}\right)_{E=E_F}$$

avec $\sigma = N(E)\langle v_F(E)^2\rangle$

↳ **S = +110μV/K** at 300K calculated for $NaCo_2O_4$

T. Yamamoto et al., Phys. Rev. B 65, 184434 (2002)

Metallic and large S

'Thermoelectric effects in a strongly correlated model for Na_xCoO_2'

t-J model : t = hopping and J = spin coupling
Kubo formalism
Valid at any T (different from the limit T $\rightarrow\infty$)

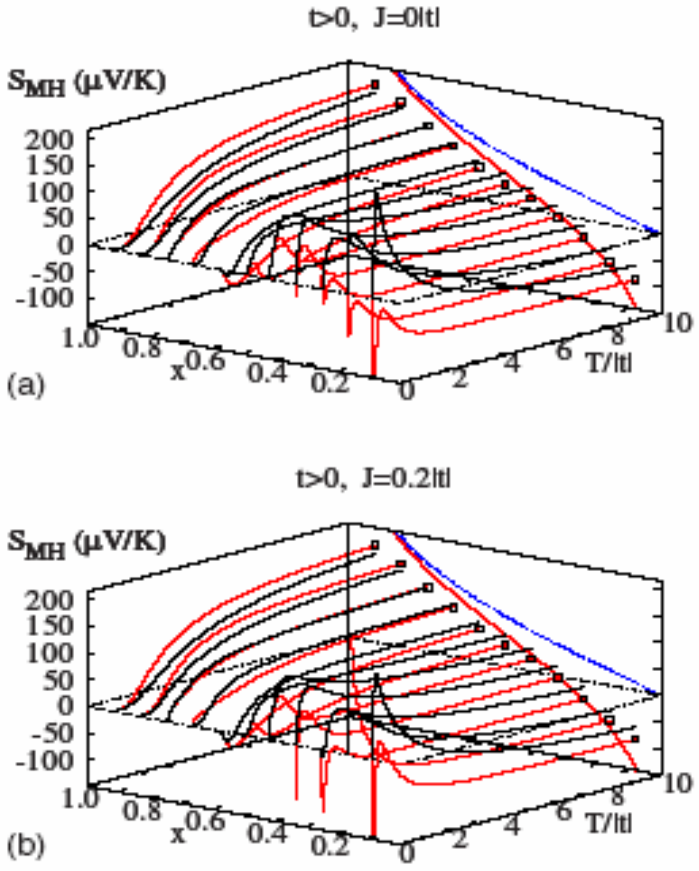

$S = S_{transport} + S_{Heikes}$

Black : Heikes formula
Red : $S = S_{transport} + S_{Heikes}$

In a large part of the phase diagram (x, T, t), the Heikes formula gives a good estimate of S

M. R. Peterson et al., PRB76, 165118 (2007)

The Kelvin formula

M. R. Peterson et al., PRB82, 195105 (2010)

t- J model for
Na_xCoO_2 with x ~ 0.7

Heikes formula valid for T > 6 – 8 t
(blue curve)

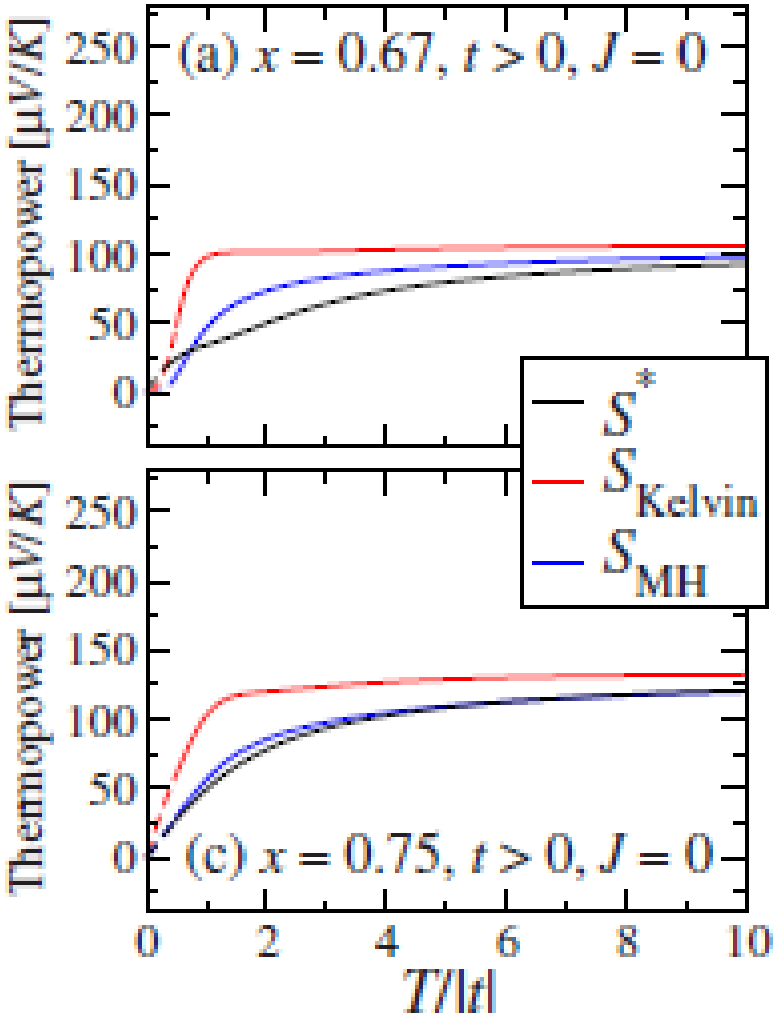

Na_xCoO_2

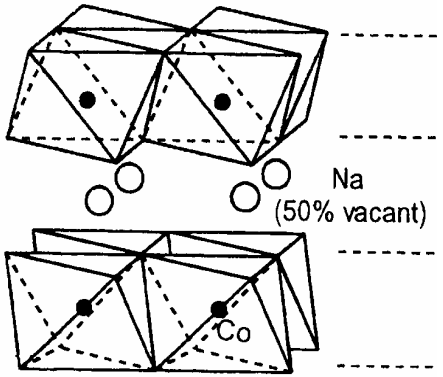

First models : crucial role of the CoO_2 layers

- Lifting of the t_{2g} orbitals : Seebeck calculated from the Mott's formula + metallicity
- High T : the Heikes formula, effect of the spin and orbital degeneracies

↳ Beyond the CoO_2 layers : the impact of the block layer?

Models

Electronic correlations + Disorder effects

Na_xCoO_2

DMFT calculations

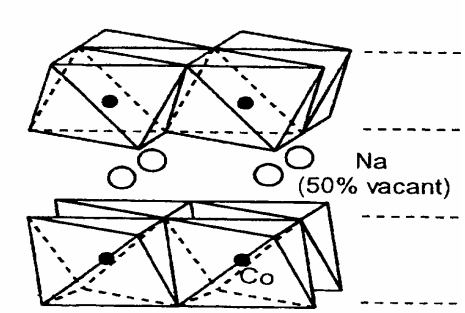

Disorder potential induced by Na^+ cations

Correlations effect

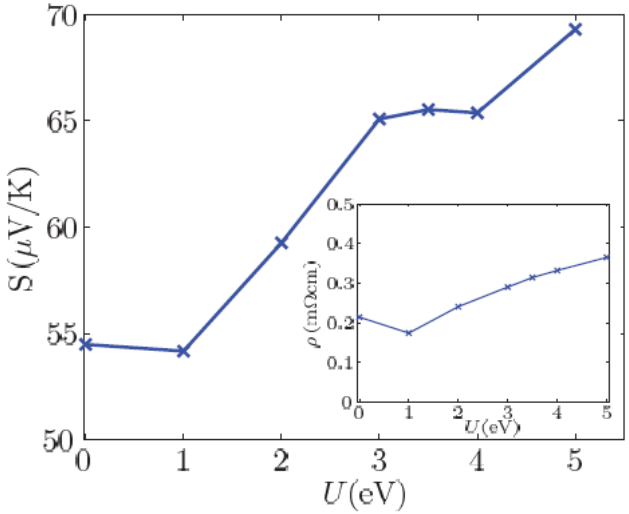

FIG. 18. (Color online) The thermopower S as a function of the correlation U without disorder ($\Delta\varepsilon = 0$) for $T = 290$ K. The inset shows the corresponding values for the resistivity ρ.

Disorder effect

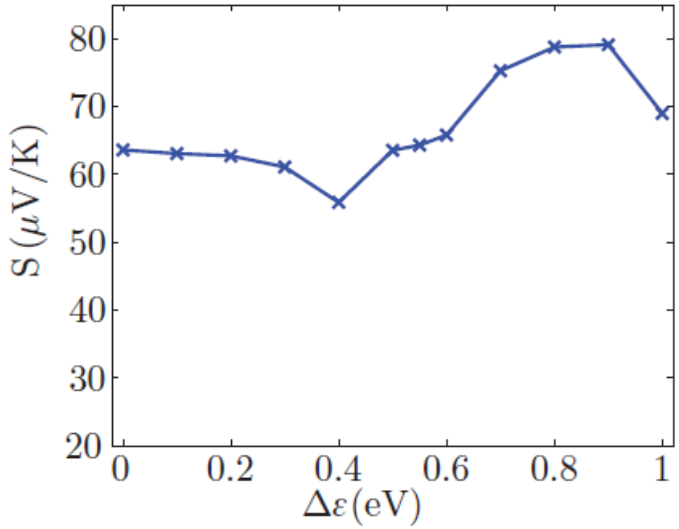

P. Wissgott et al., PRB84, 085129 (2011)

Semi-conducteurs :
The Heikes formula

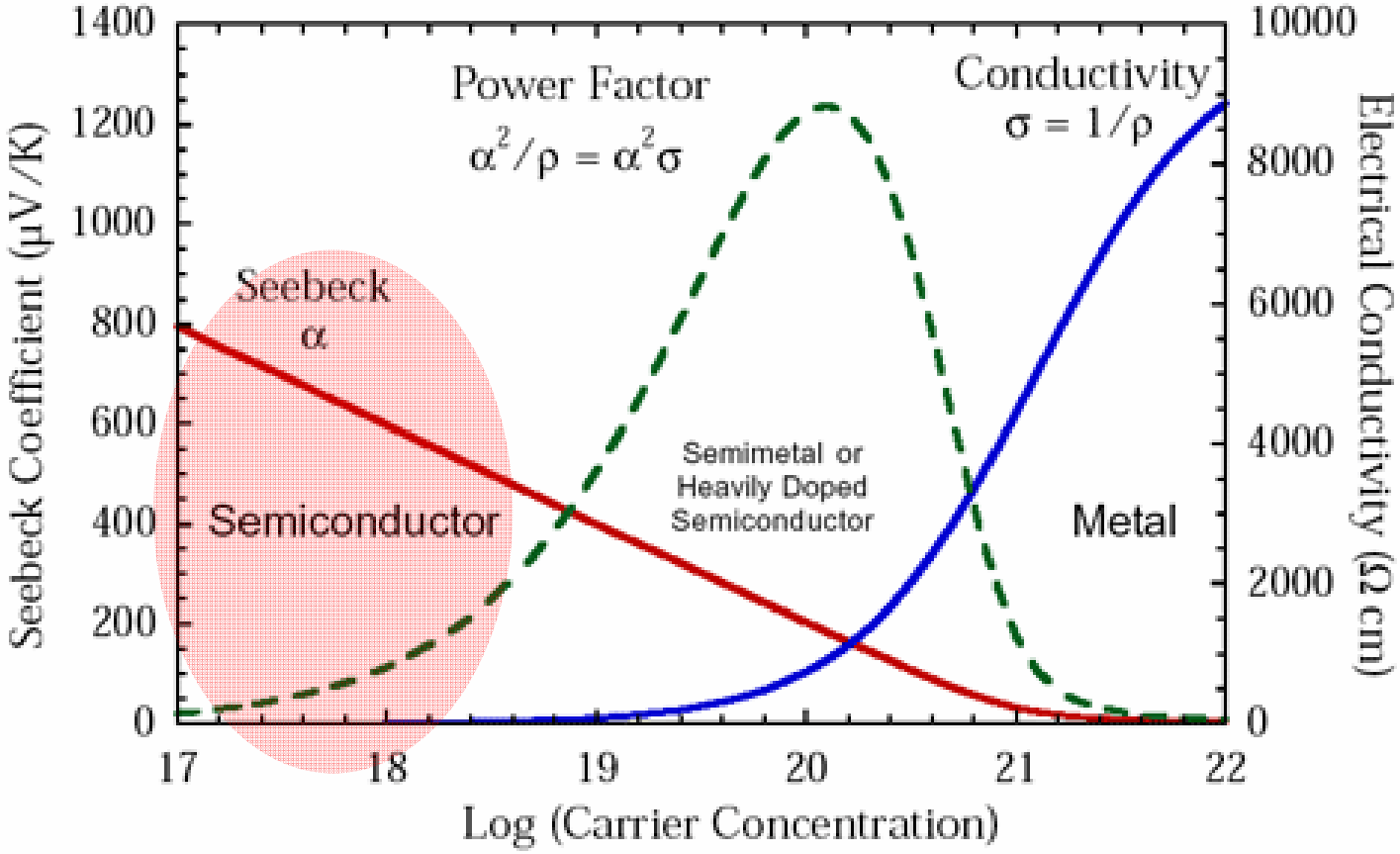

Type p : $Pr_{1-x}Ca_xCrO_3$

Orthochromites

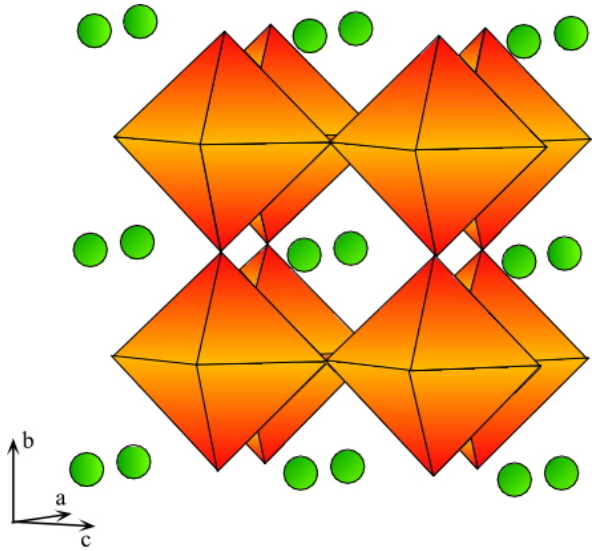

Perovskite structure

$Pr^{3+}_{1-x}Ca^{2+}_{x}Cr^{3+/4+}O_3 : 3d^3/3d^2$

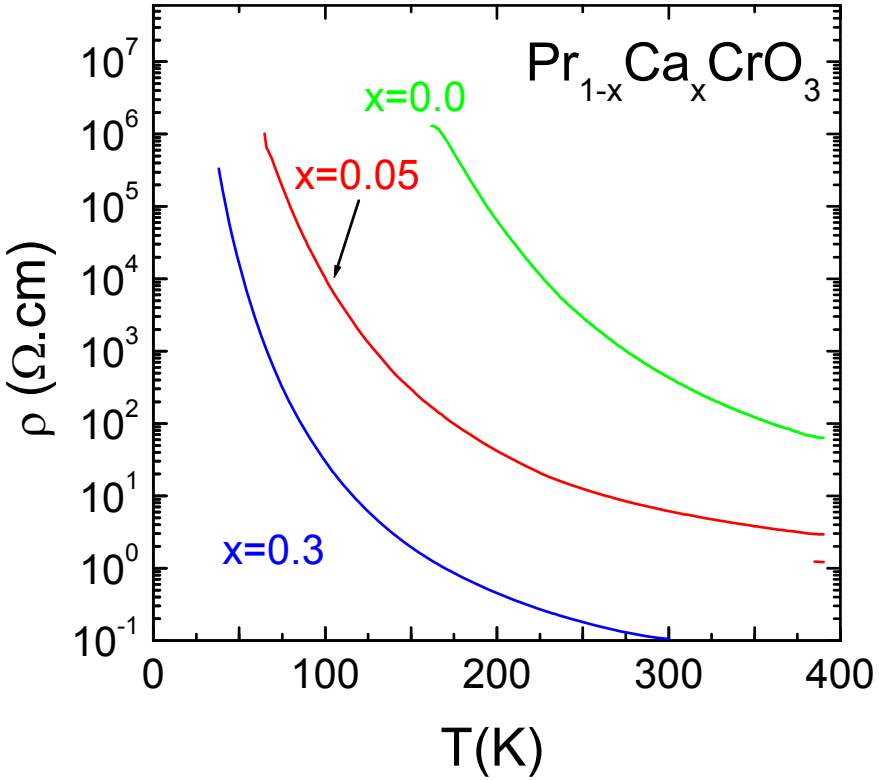

Introduction of holes :
Activated behavior with
a decrease of ρ

S. Pal et al., Eur. Phys. J. B 53, 5 (2006)

Type p : $Pr_{1-x}Ca_xCrO_3$

Orthochromites

$Pr^{3+}_{1-x}Ca^{2+}_xCr^{3+/4+}O_3$: $3d^3/3d^2$

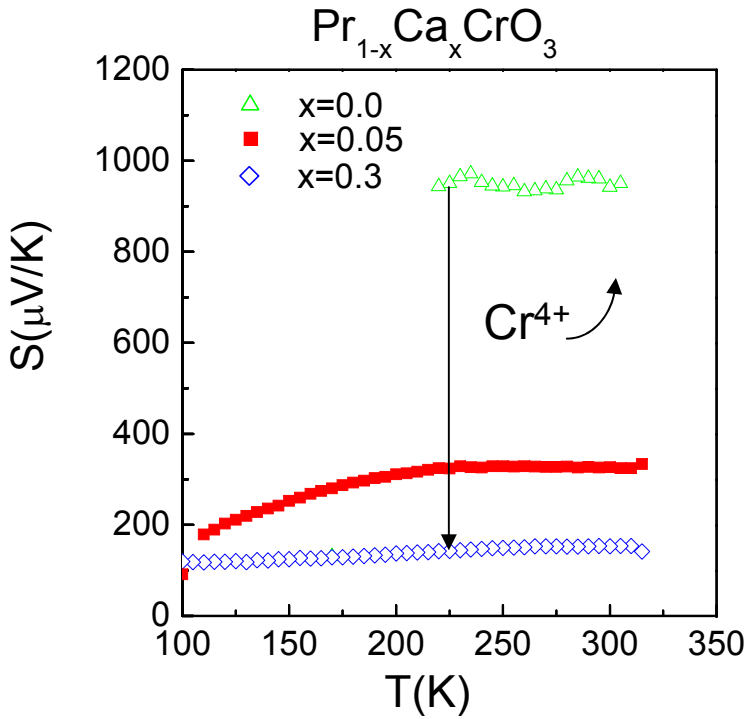

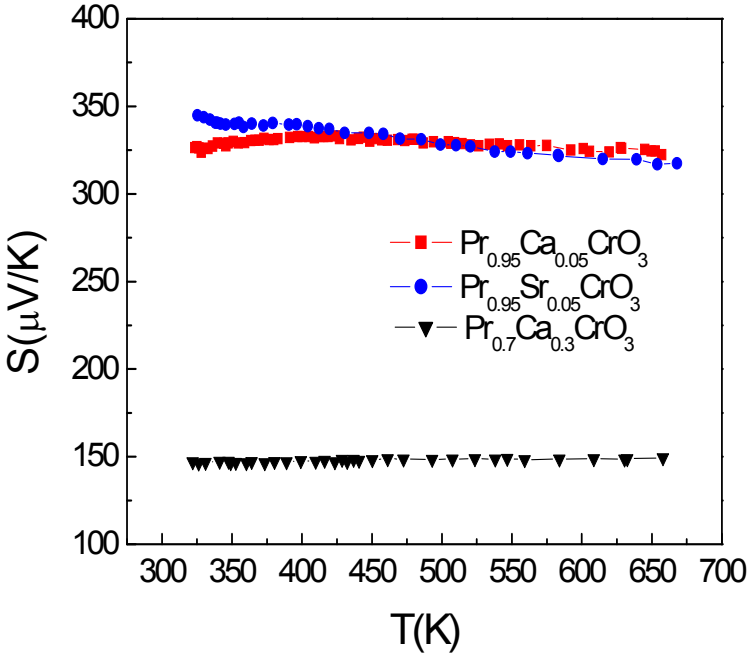

Decrease of S induced by doping

S constant from 200K to high T

S. Pal et al., Eur. Phys. J. B 53, 5 (2006)

Type p : $Pr_{1-x}Ca_xCrO_3$

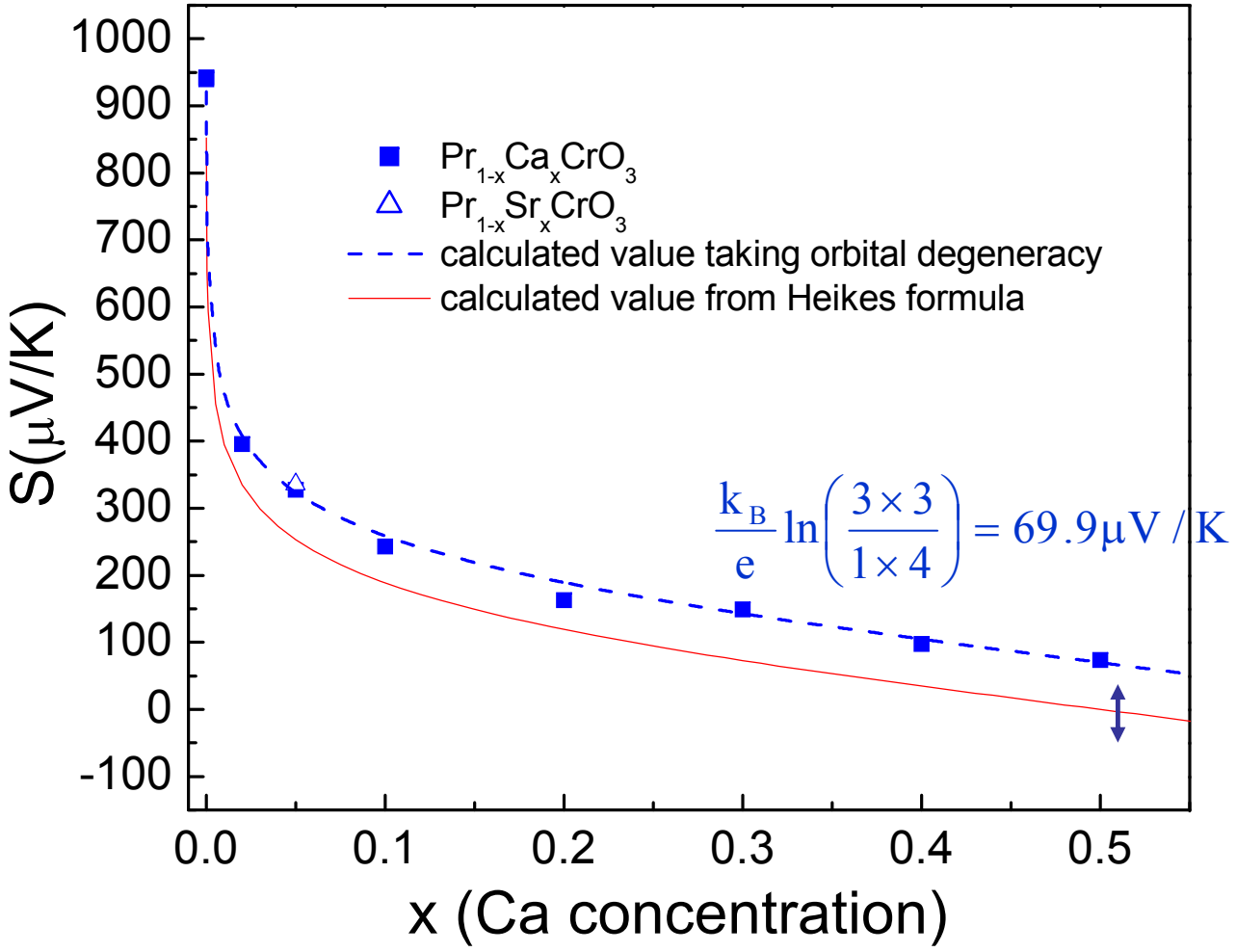

Heikes formula with spin and orbital degeneracies

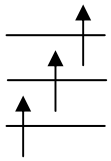

$3d^3$, $S = 3/2$

$\Gamma_{orb}=1$

$\Gamma_{spin} = 4$

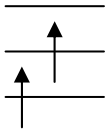

$3d^2$, $S = 1$

$\Gamma_{orb}=3$

$\Gamma_{spin} = 3$

$$S = \frac{-k_B}{|e|}\ln\left(\frac{1-x}{x}\right) + \frac{k_B}{|e|}\ln(\Gamma_{orb}\Gamma_{spin})$$

Marsh and Parris, Phys. Rev. B 54, 7720 (1996)

Type p : $Pr_{1-x}Ca_xCrO_3$

Power factor

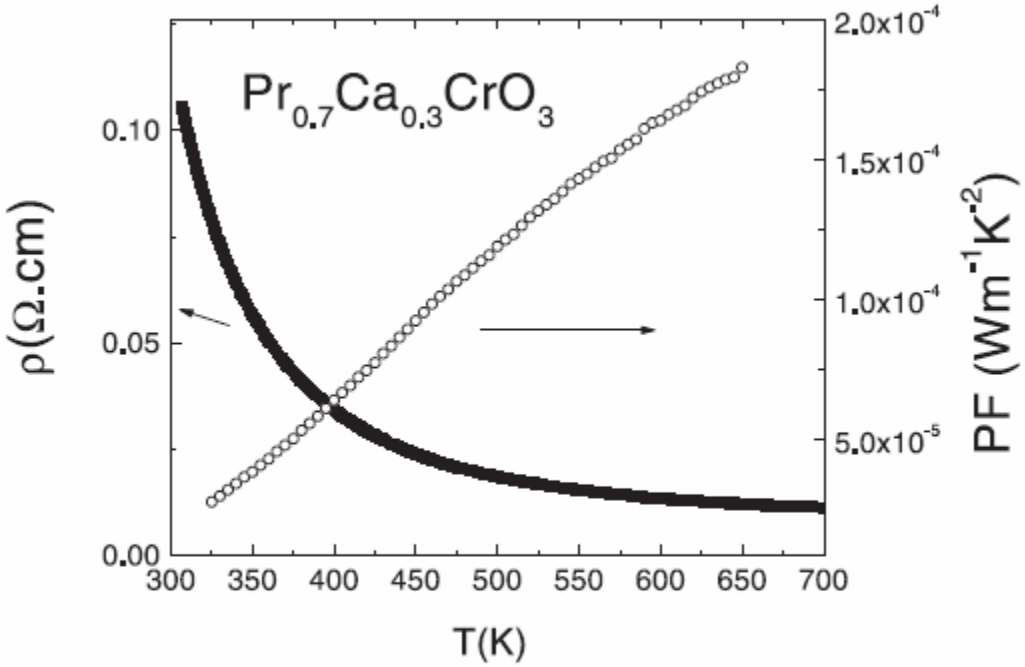

Fig. 6. ρ vs. T (left scale) and Power Factor ($PF = S^2/\rho$) (right scale) of $Pr_{0.7}Ca_{0.3}CrO_3$ measured up to 700 K.

PF ~ 2.10^{-4} $Wm^{-1}K^{-1}$
Typical for oxides

Change of sign in $LaCoO_3$

$LaCoO_3$

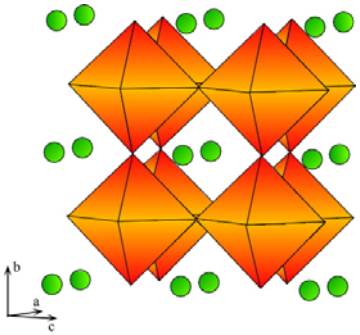

Heikes formula : possible change of sign

$$S = -\frac{k_B}{e}\ln\left(\frac{1-x}{x}\right)$$

x = carrier concentration

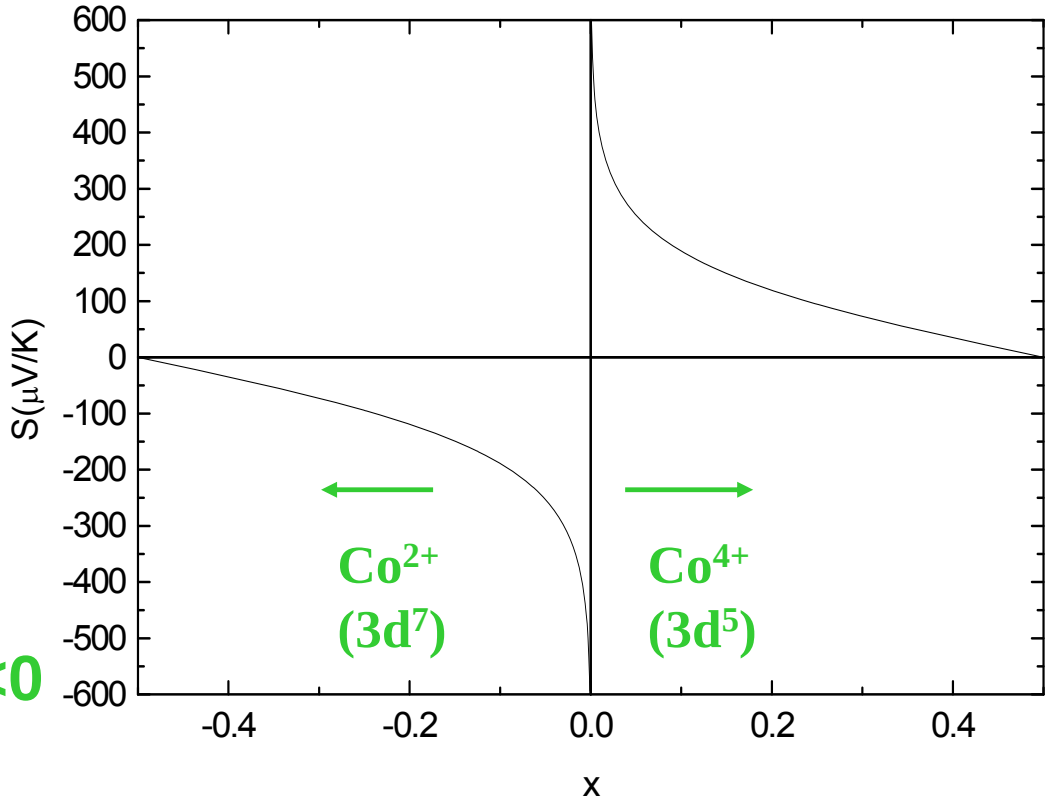

Depending on x, S>0 or S<0

Small x ➡ |S| very large

Change of sign in $LaCoO_3$

$LaCoO_3$: A site substitution

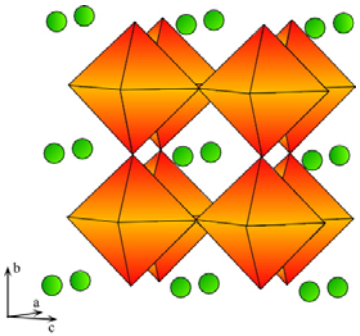

$LaCoO_3$ x~0 : $La^{3+}Co^{3+}O_3$

Sr^{2+} x>0 : $La_{1-x}Sr_xCo^{3+}Co^{4+}O_3$

Ce^{4+} x<0 : $La_{1-x}Ce_xCo^{3+}Co^{2+}O_3$

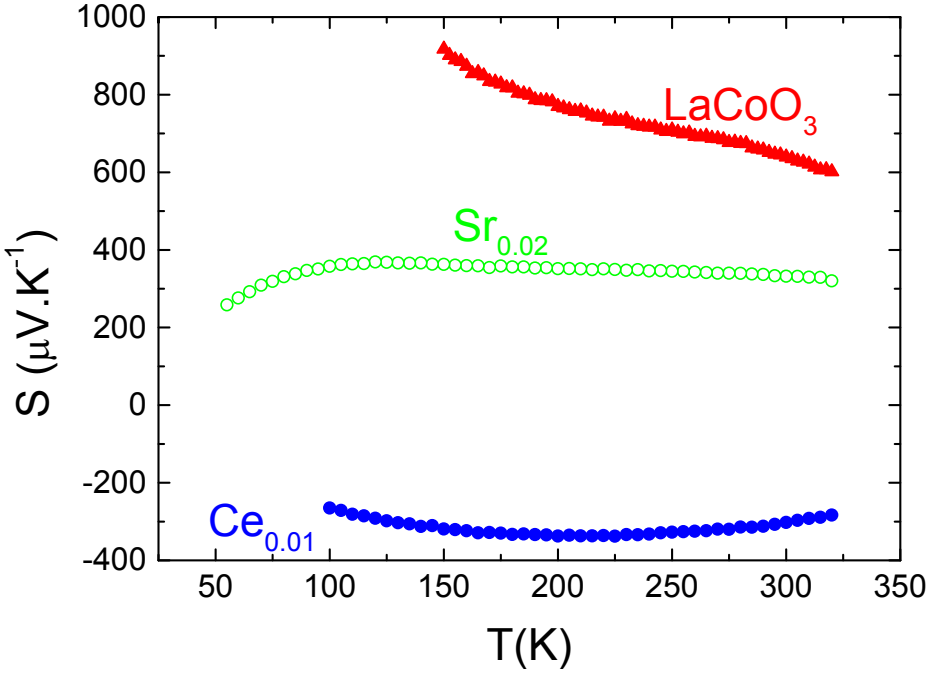

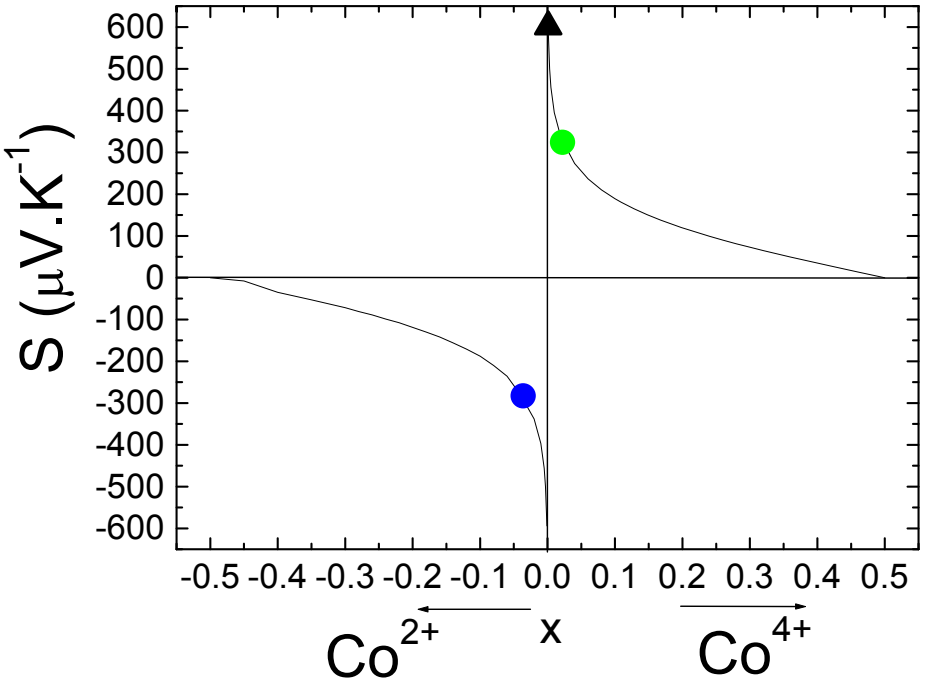

A. Maignan et al., EPJB 39, 145 (2004)

Change of sign in $LaCoO_3$

$LaCoO_3$: B site substitution

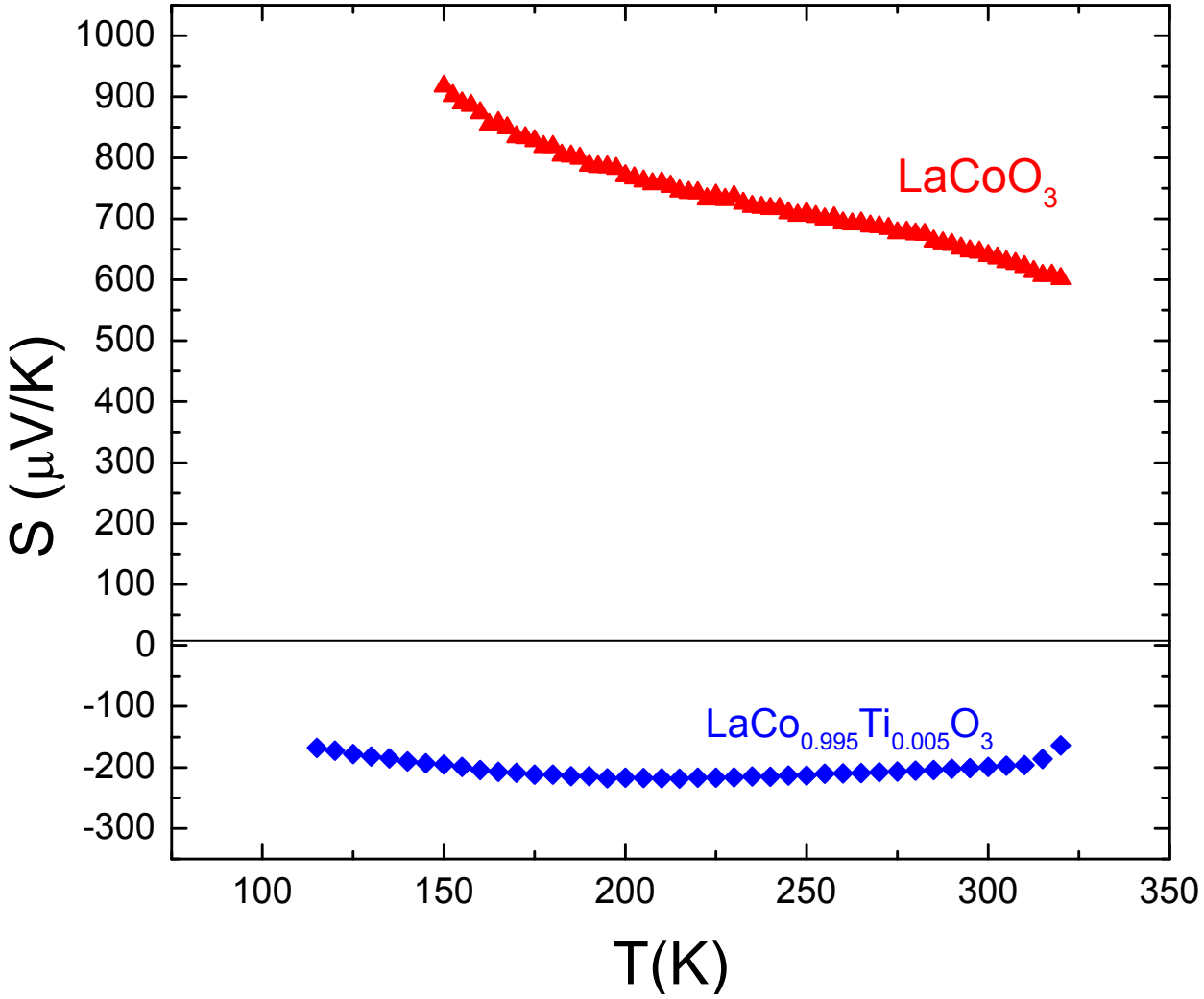

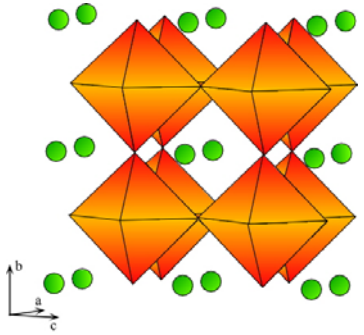

$LaCoO_3$ x~0 : $La^{3+}Co^{3+}O_3$

Ti^{4+} x<0 :

$La(Co^{3+}Co^{2+})_{1-x}Ti^{4+}{}_xO_3$

Type p : $LaCoO_3$

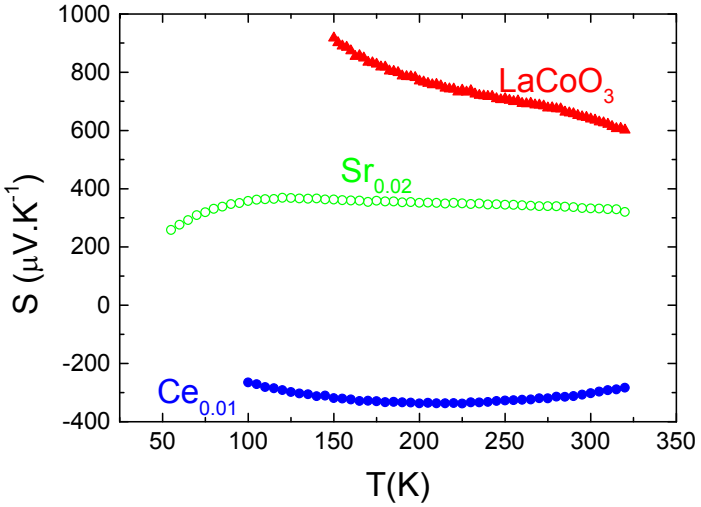

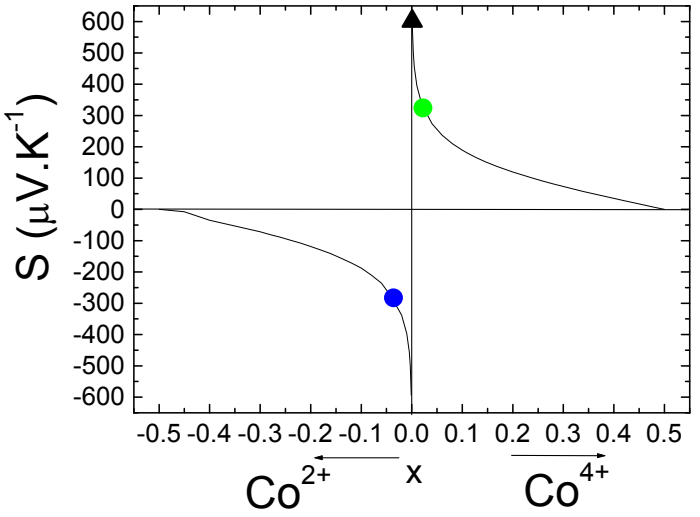

A. Maignan et al., EPJB 39, 145 (2004)

Formule de Heikes pour S, avec

$$S = -\frac{k_B}{e}\ln\left(\frac{g_3}{g_4}\frac{x}{1-x}\right)$$

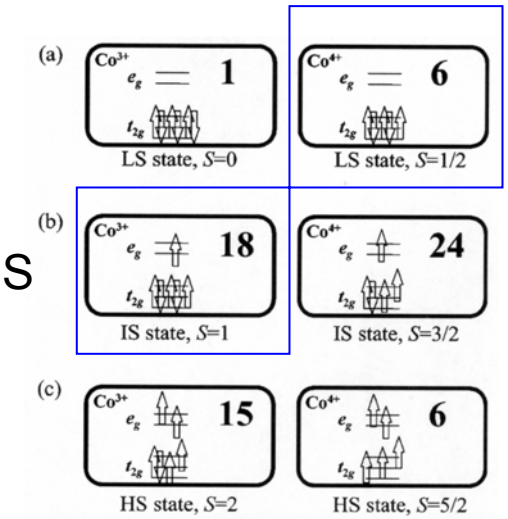

Co^{4+} LS

Co^{3+} IS

Spin only degeneracy

$g_3 = 3$ / $g_4 = 2$

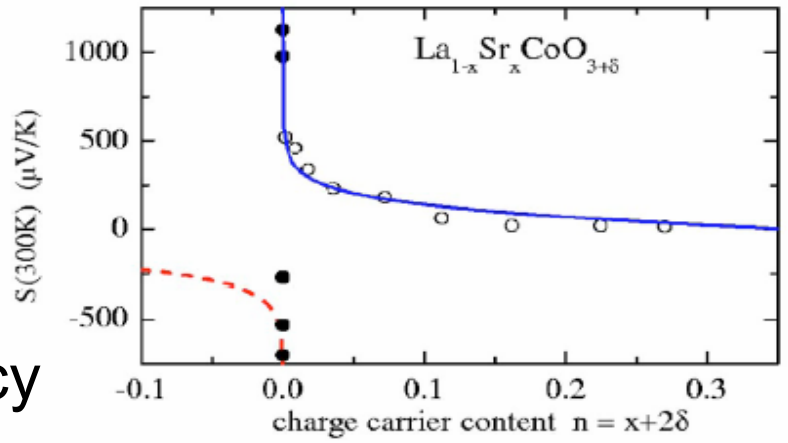

K. Berggold et al., PRB72, 155116 (2005)

Change of sign in $LaCoO_3$

$LaCoO_3$

Single crystals measurements

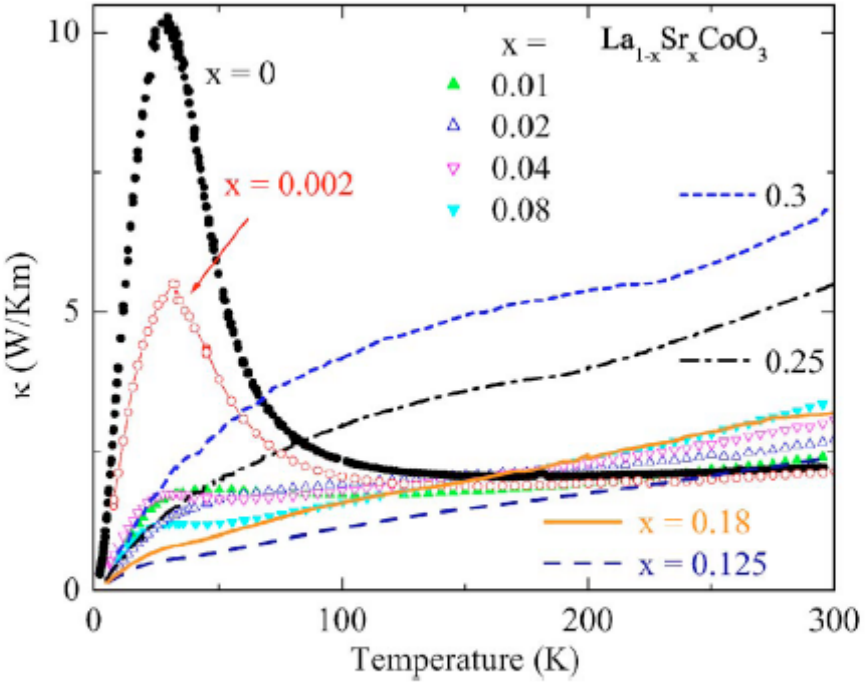

FIG. 1. (Color online) Thermal conductivity of $La_{1-x}Sr_xCoO_3$ a function of temperature for different doping x.

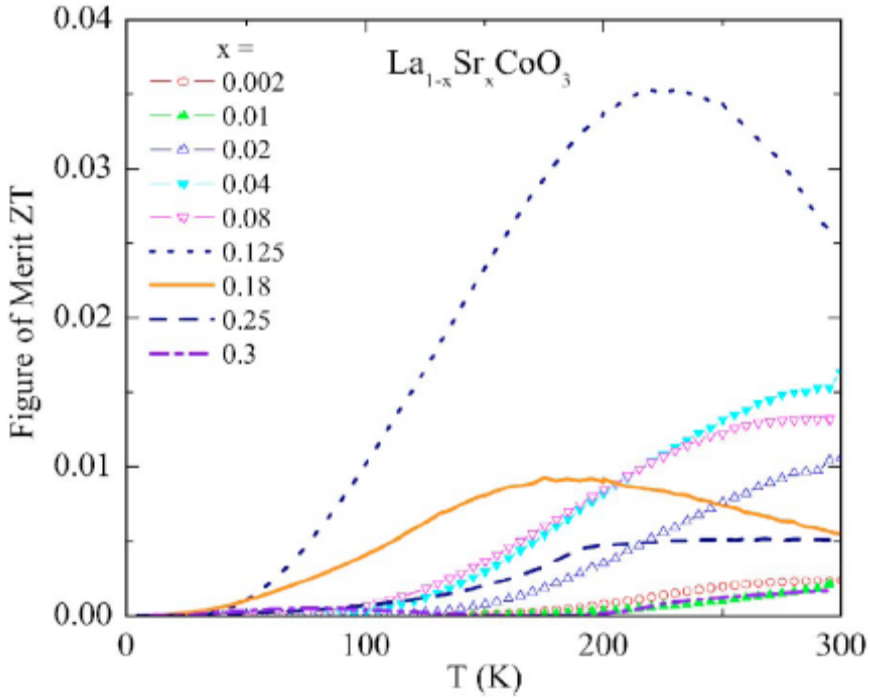

FIG. 5. (Color online) Figure of merit of $La_{1-x}Sr_xCoO_3$ as a function of temperature for different doping x.

K. Berggold et al., PRB72, 155116 (2005)

Type p : $LaCoO_3$

$LaCoO_3$ perovskites

$La_{1-x}Sr_xCo^{3+}{}_{1-x}Co^{4+}{}_xO_3$

ZT = 0.18 at 300K

J. Androulakis et al., APL84, 1099 (2004)

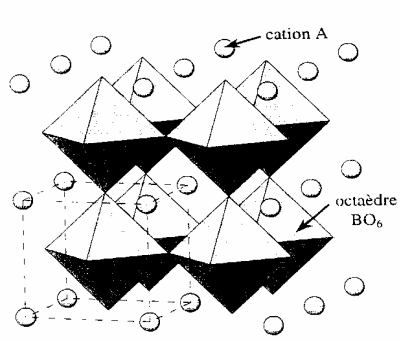

Semi-conducting with 5% hole doping

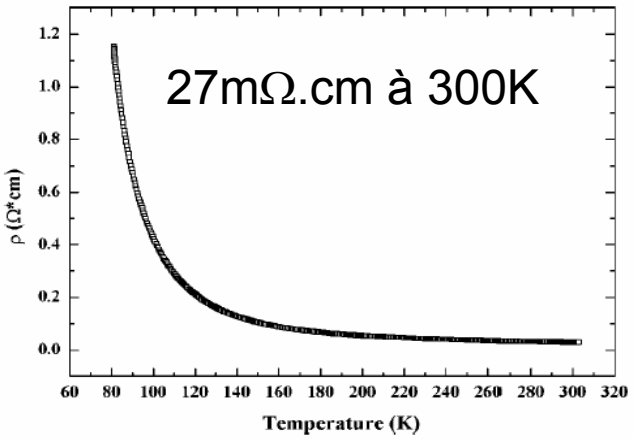

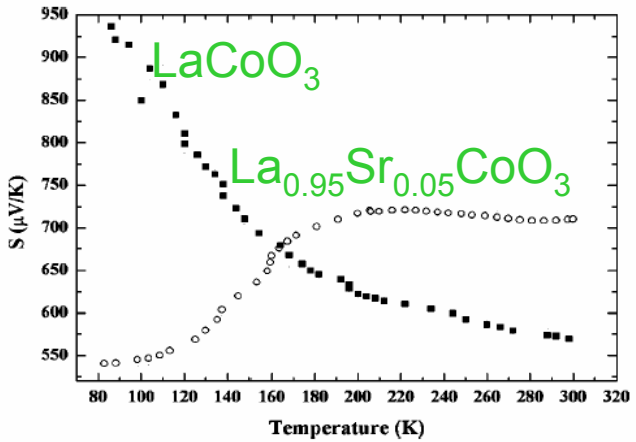

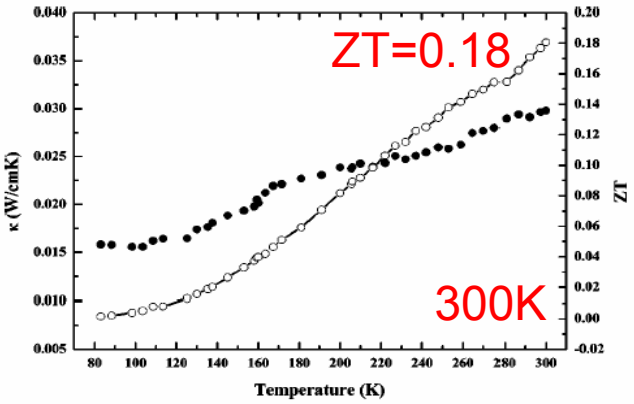

Eg decreases from 250 meV from $LaCoO_3$ to 36meV for $La_{0.95}Sr_{0.05}CoO_3$

Similar κ as Berggold et al., but much larger S
Oxygen stoechiometry?

Resistivity of $La_{1-x}M_xCoO_3$

Asymmetry between hole and electron doping

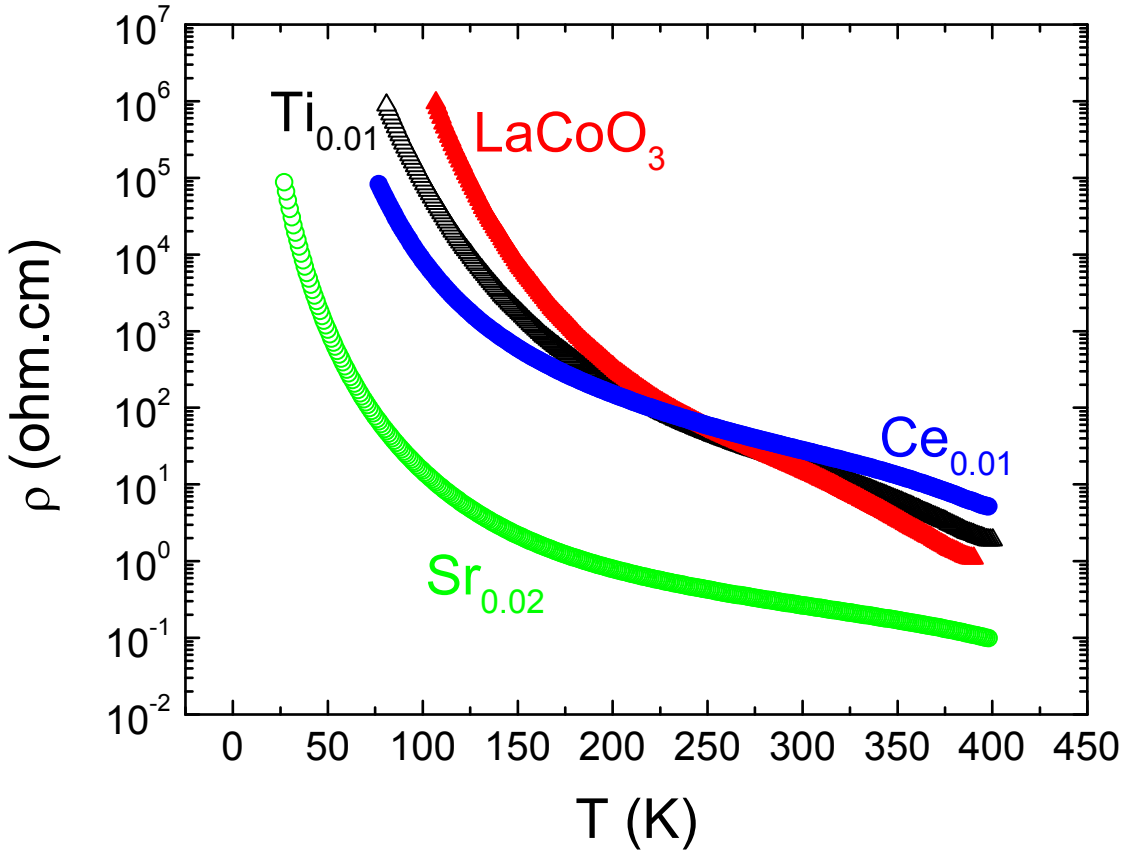

ρ(n type) > ρ (p type)

Typical of many oxides

Change of sign in $LaCoO_3$

Spin blockade mechanism

A t_{2g} hole Co^{4+} can hop in a background of LS Co^{3+}

$3d^5 / 3d^6$

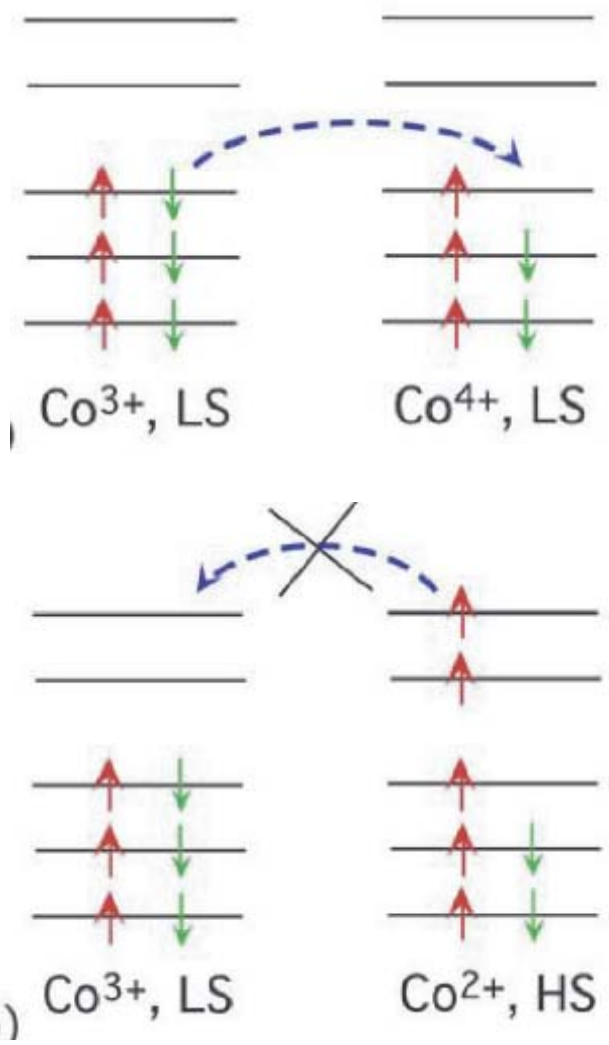

An e_g electron Co^{2+} cannot move in a background of LS Co^{3+} , requires to flip other spins, wrong spin-states LS Co^{2+} and IS Co^{3+} instead of LS

$3d^6 / 3d^7$

A. Maignan et al, Phys. Rev. Lett. 93, 026401 (2004)

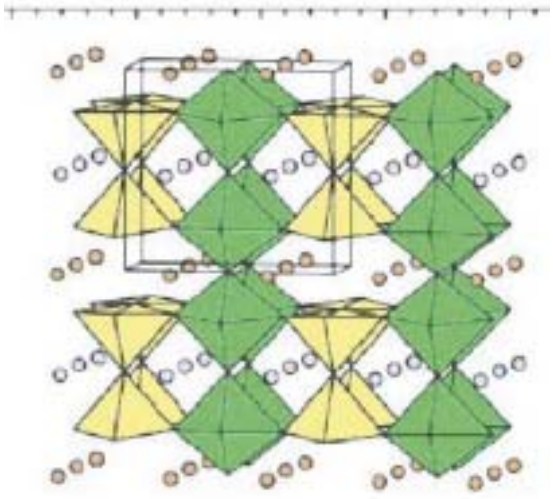

The 112- family

Co^{3+}/Co^{4+} or Co^{2+}/Co^{3+}

Pyramidal and octahedral sites
Possible spin state transitions

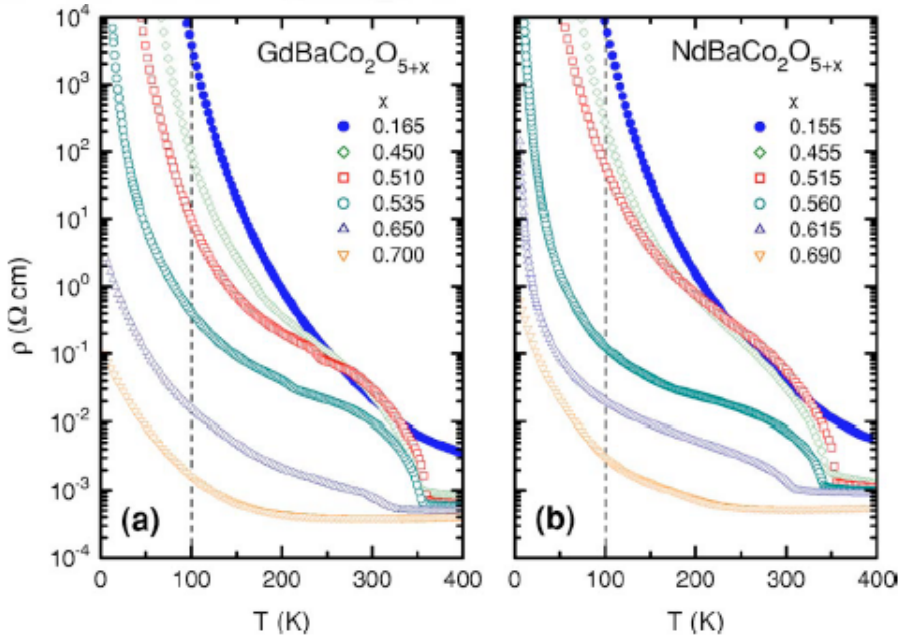

FIG. 2. (Color online) Temperature dependences of the in-plane resistivity $\rho(T)$ of (a) $GdBaCo_2O_{5+x}$ and (b) $NdBaCo_2O_{5+x}$ crystals.

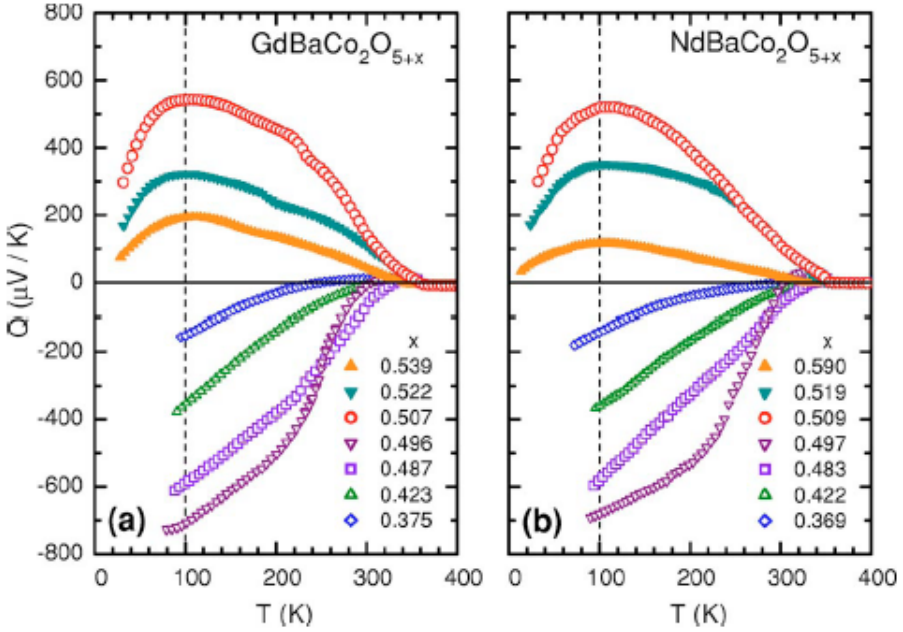

FIG. 3. (Color online) Temperature dependences of the Seebeck coefficient $Q(T)$ of (a) $GdBaCo_2O_{5+x}$ and (b) $NdBaCo_2O_{5+x}$ crystals.

A. A. Taskin et al., PRB73, 121101 (2006)

Quantitative analysis of S

Calculations of spin/orbital degeneracies taking into account the different sites (octahedral / pyramidal)

Explains the larger values for n type (HS Co^{2+}) compared to p type (LS Co^{4+})

Differences in orbital degeneracies for octahedra / pyramids

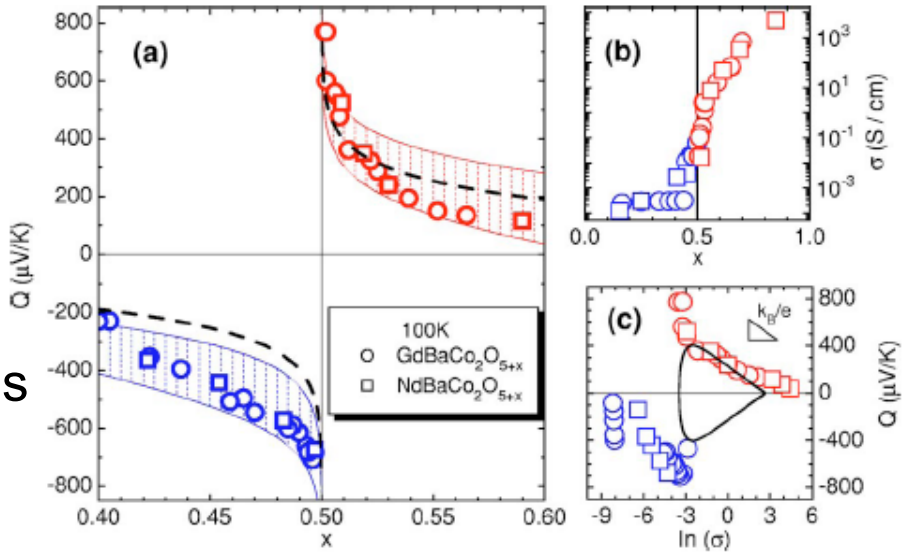

FIG. 4. (Color online) (a) The doping dependence of the Seebeck coefficient $Q(x)$ of $GdBaCo_2O_{5+x}$ (circles) and $NdBaCo_2O_{5+x}$ (squares) crystals at $T=100$ K. The hatched area represents the entire available range of the entropy contribution to the thermopower $\Delta Q_n(x)$ and $\Delta Q_p(x)$. (b) The doping dependence of the conductivity $\sigma(x)$ of $GdBaCo_2O_{5+x}$ (circles) and $NdBaCo_2O_{5+x}$ (squares) crystals at $T=100$ K. (c) Jonker plot for $RBaCo_2O_{5+x}$ (see text).

A. A. Taskin et al., PRB73, 121101 (2006)

High Temperature properties of manganites

S independent on x in a large range of x

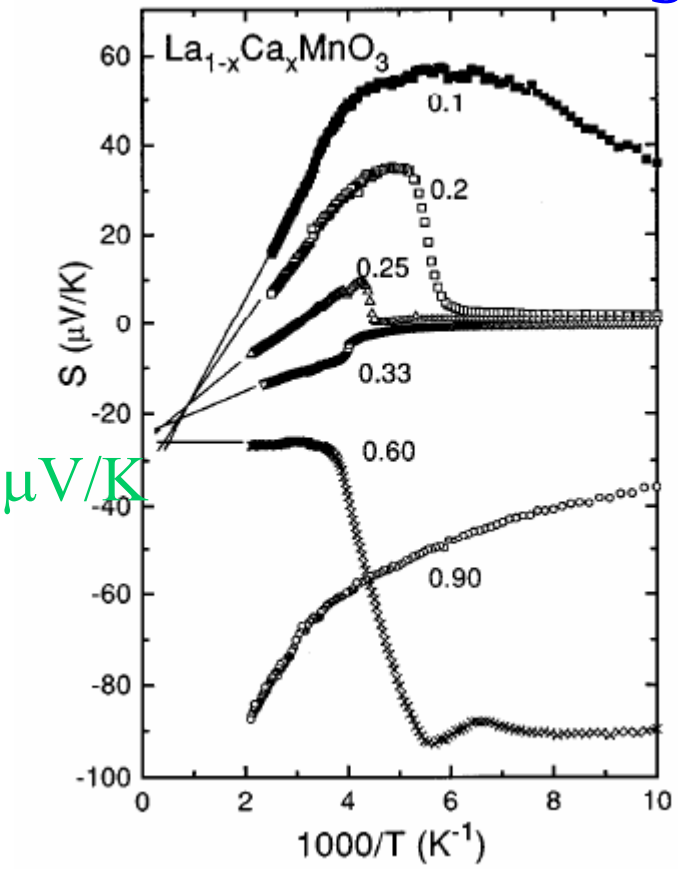

-20μV/K

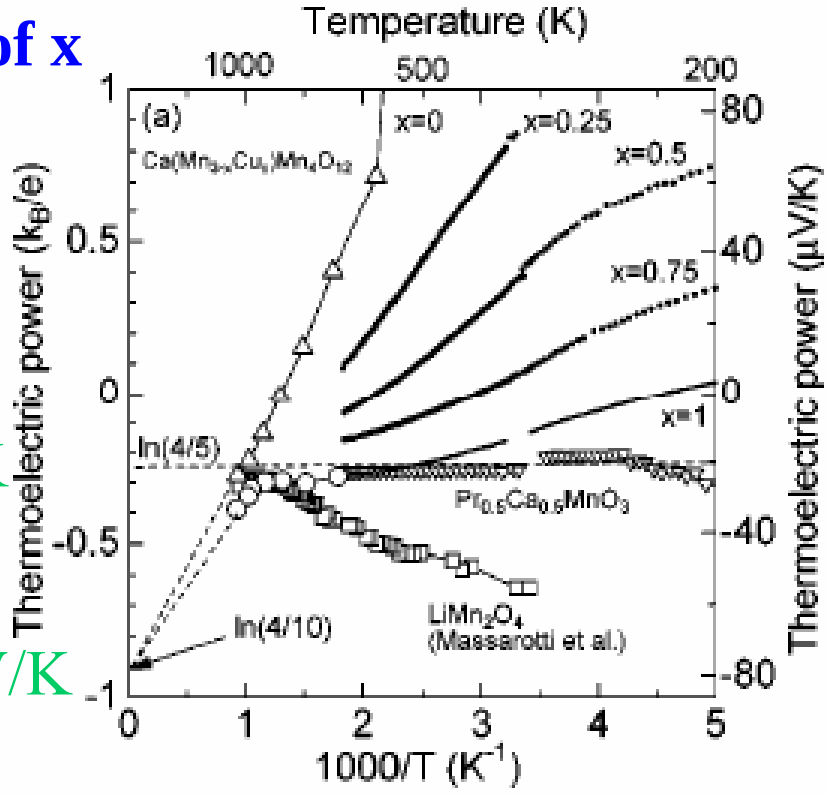

-20μV/K

-80μV/K

T. T. M. Palstra et al., Phys. Rev. B 56, 5104 (1997)

Spin degeneracy + Orbital degeneracy

$$S = -\frac{k_B}{e}\ln\left(\frac{2S_0+1}{2S_1+1}\right) \qquad S_0 = 3/2\ (Mn^{4+}) \qquad S_1 = 2\ (Mn^{3+})$$

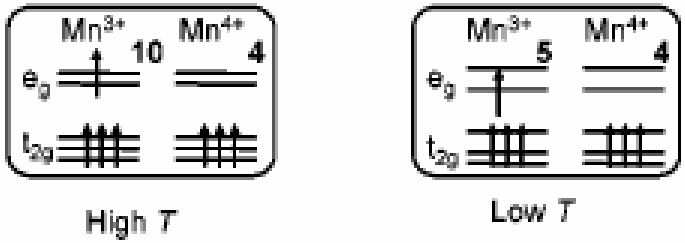

'Probe' of Jahn Teller effect

W. Kobayashi et al., J. Appl. Phys. 95, 6825 (2004)

Semi – conducting oxides

The Heikes formula

→ Possibility to get p and n type oxides

→Spin and/or orbital degeneracies have to be taken into account for a quantitative analysis

→Explains the asymmetry between n and p type

But too large resistivity !

Degenerate semi-conductors : Best n type oxides

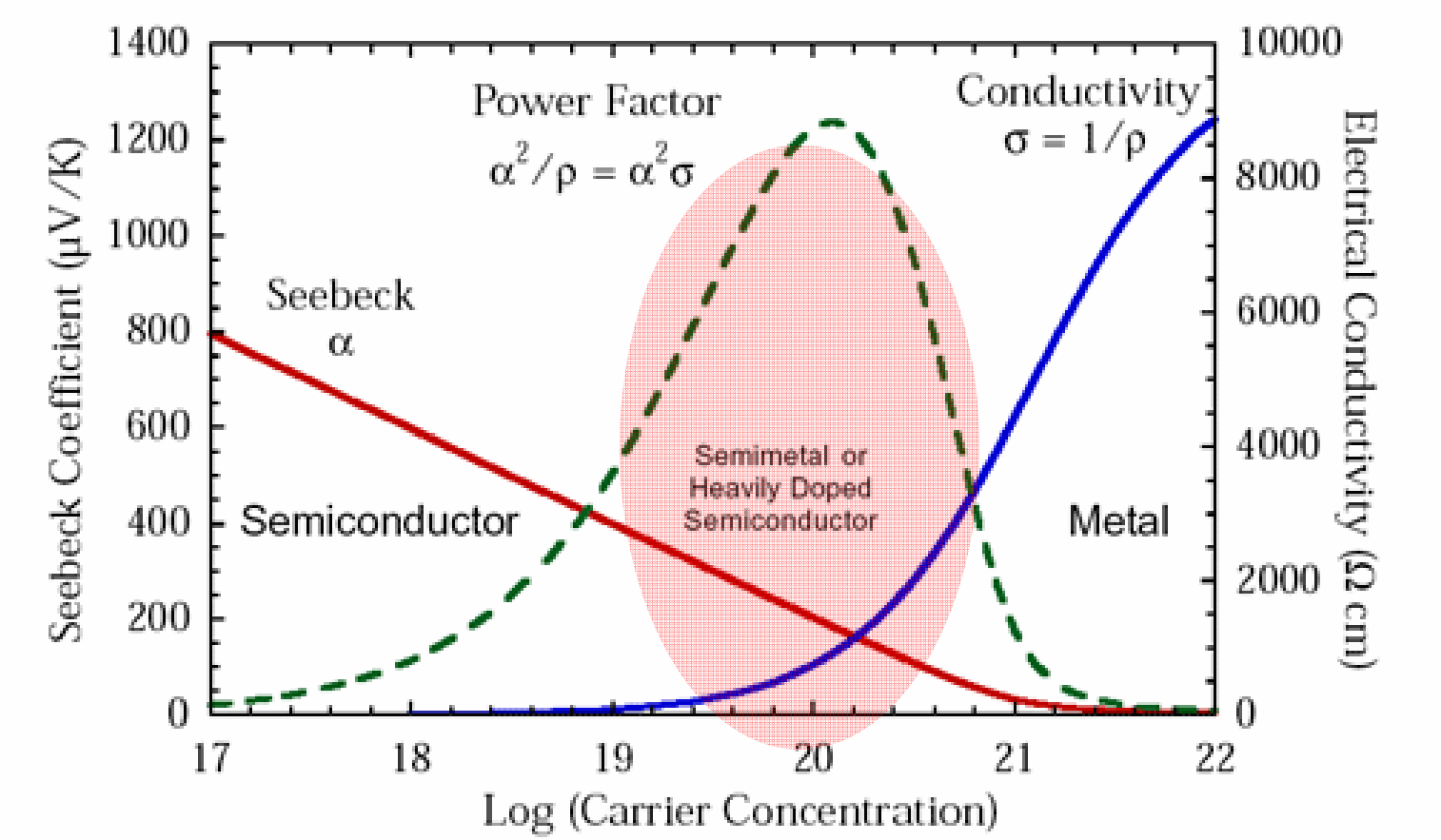

Type n : ZnO

$Zn_{1-x}Al_xO$ (x = 0 – 0.1)

ZT = 0.3

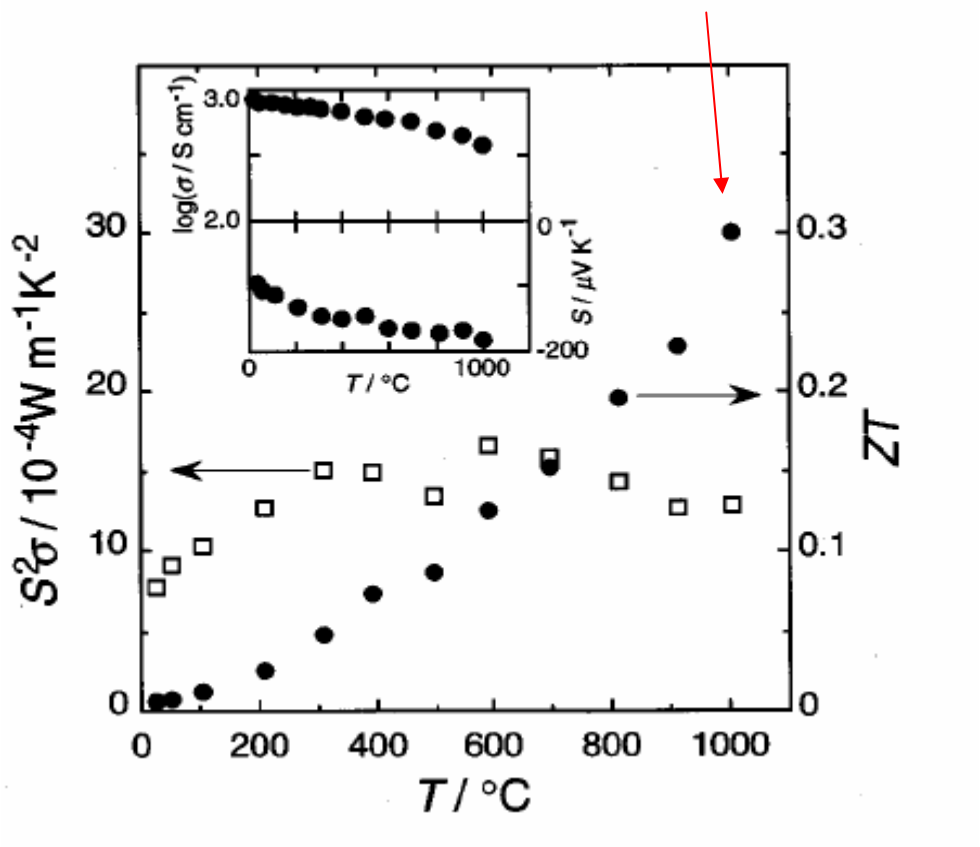

Broadband model for extrinsic n type semiconductor

$$\sigma = n e \mu,$$

$$S = -(k/e)[\ln(N_v/n) + A].$$

Large mobility of the carriers : 3 – 7cm^2/Vs

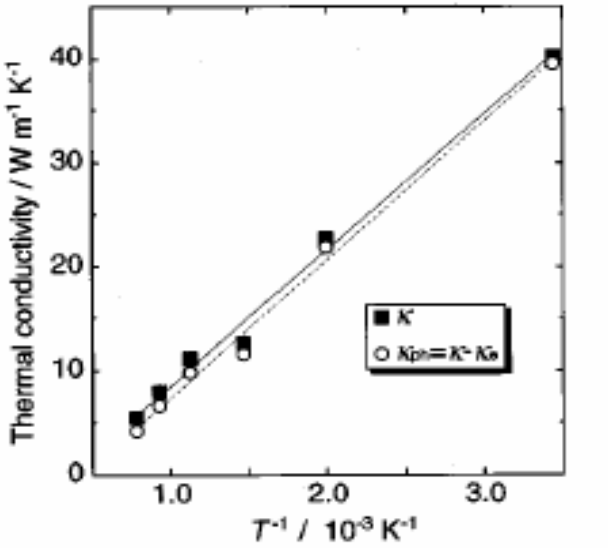

κ too high!

κ = 40Wm^{-1}K^{-1} at 300K

κ=5.4 Wm^{-1}K^{-1} at 1000°C

M. Ohtaki et al., JAP79, 1816 (1996)

Type n : $CaMnO_3$

Partially filled 3d levels

Perovskite $Ca_{1-x}Sm_xMnO_3$

Mn^{3+} $t_{2g}^3e_g^1$, HS JT

V(Mn)=4-x

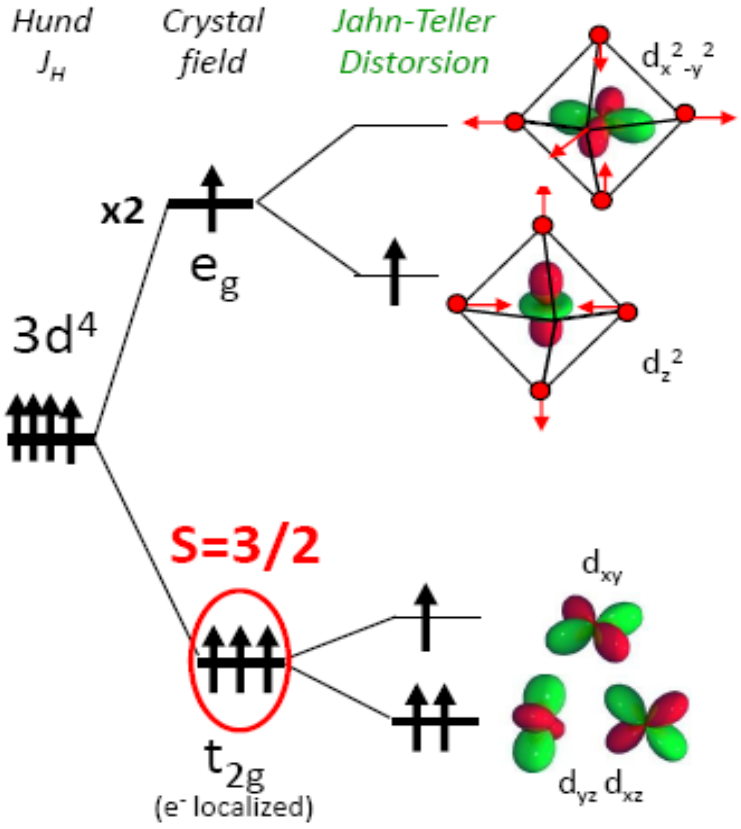

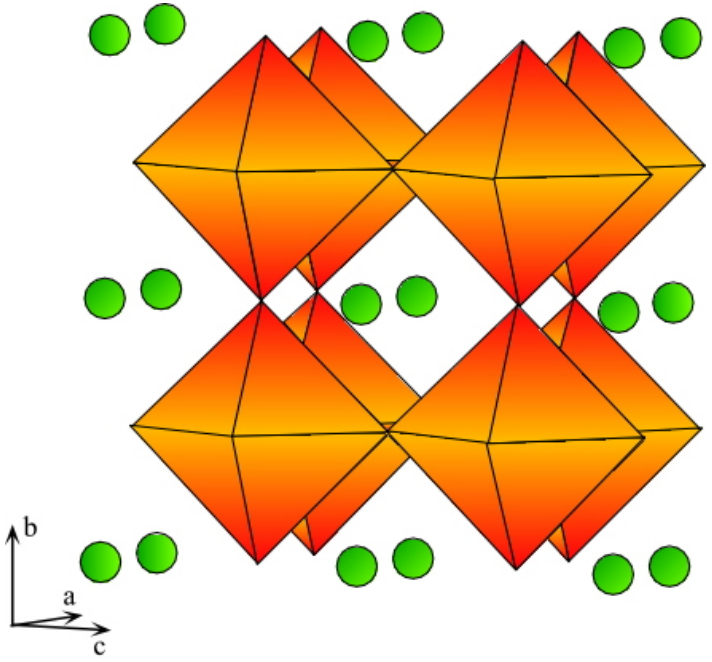

Type n : $CaMnO_3$

V_{Mn} > 3.5 Type n

Perovskite $Ca_{1-x}Sm_xMnO_3$

A-site doping

Partially filled 3d levels

Mn^{3+} $t_{2g}^3e_g^1$, HS JT

Mn^{4+} t_{2g}^3, HS

Polaronic transport

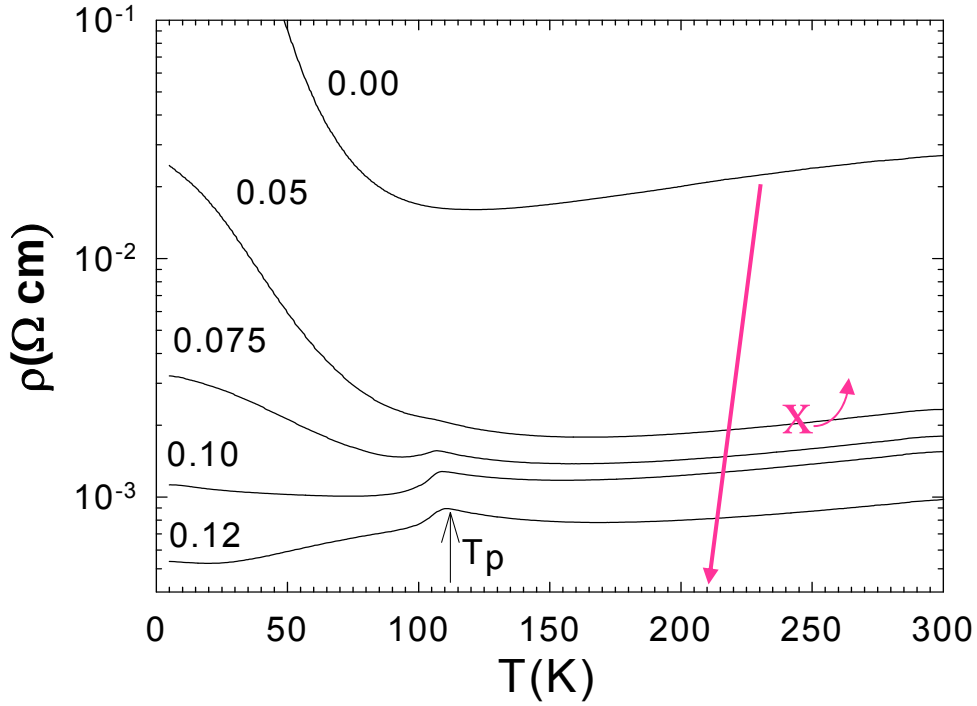

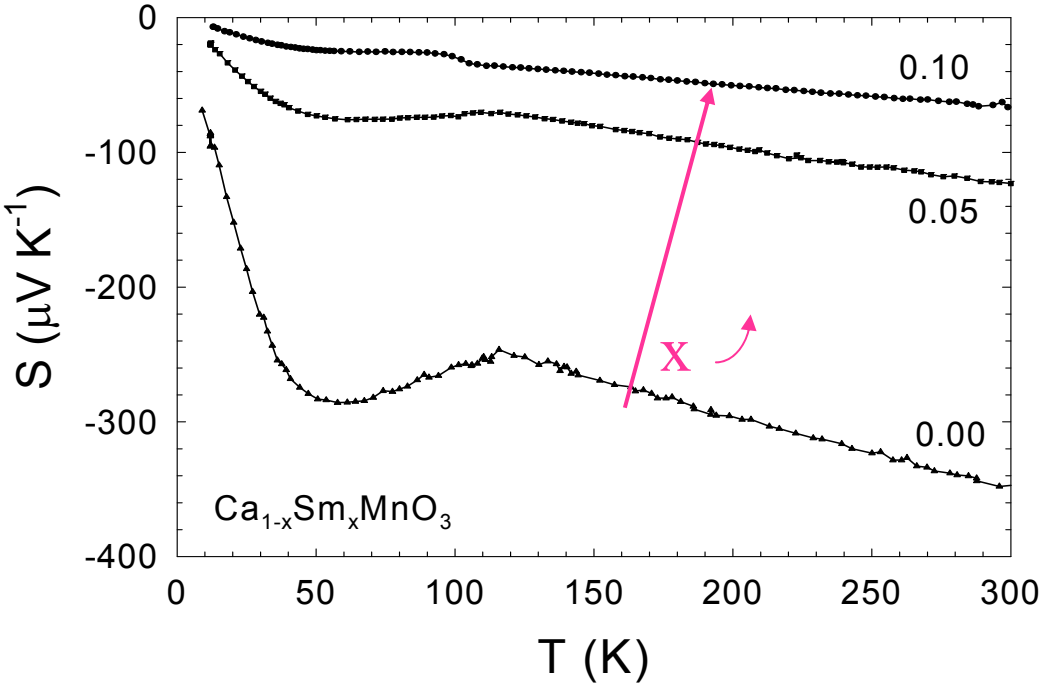

$$-\alpha = \pi^2 * k_B^2/(3e) * T * \{N(E)/n + \text{cst.}\}\big|_{E=E_F}$$

J. Hejtmanek et al., PRB60, 14057 (1999)

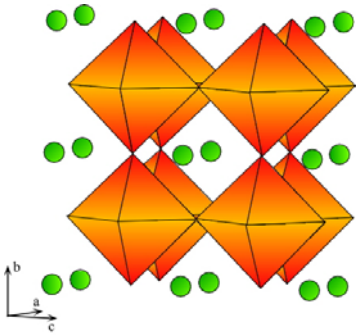

Manganese oxides
n type $SrMn_{1-x}Mo_xO_3$

$3d^3\ t_{2g}^3 / 3d^4\ t_{2g}^3 e_g^1$ $SrMnO_3$: Mn^{4+}

Mo^{6+} ⟲ Mn^{3+}/Mn^{4+}

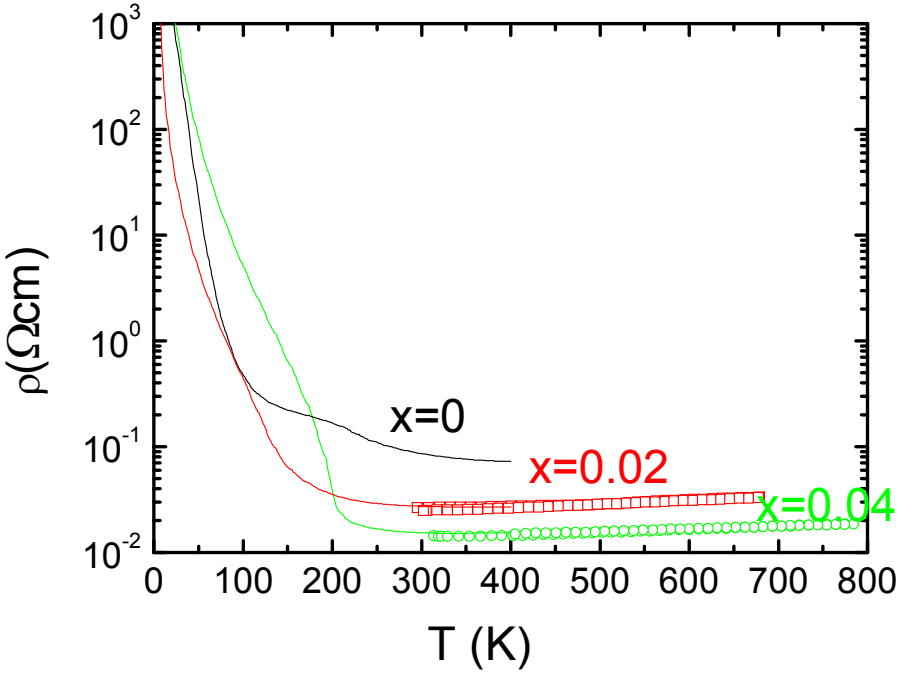

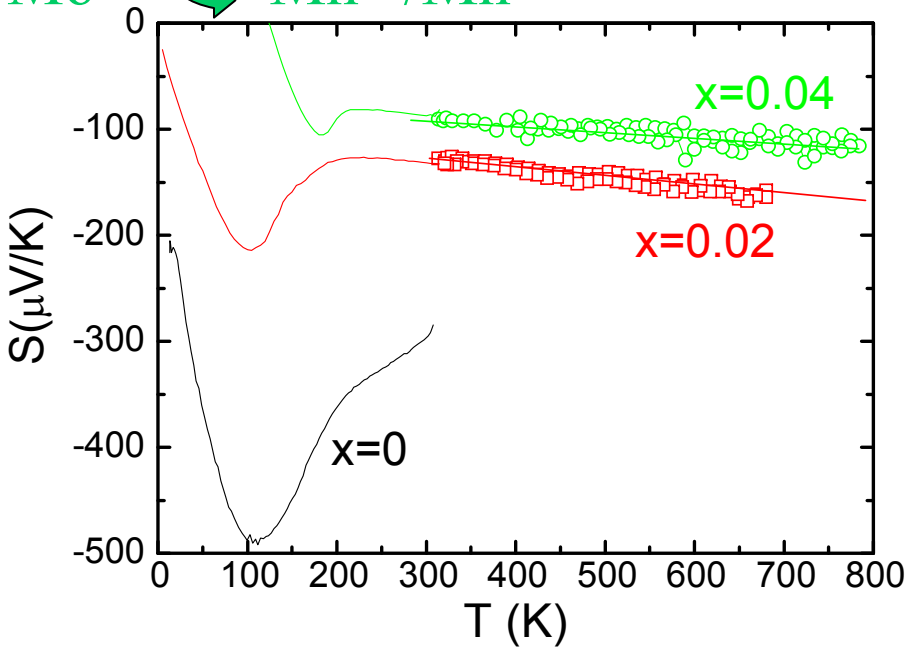

Metallic up to high T / S linear in T

Power factor increases as T increases : PF = $9.10^{-4} Wm^{-1}K^{-2}$ for x=0.02 at 800K

$$S = \pi^2 \times k_B/3e \times k_B T(\partial \ln \sigma(E)/\partial E)$$

Measurements by J. Hejtmanek (Prague)

Type n : $CaMnO_3$

$Ca_{0.9}M_{0.1}MnO_3$

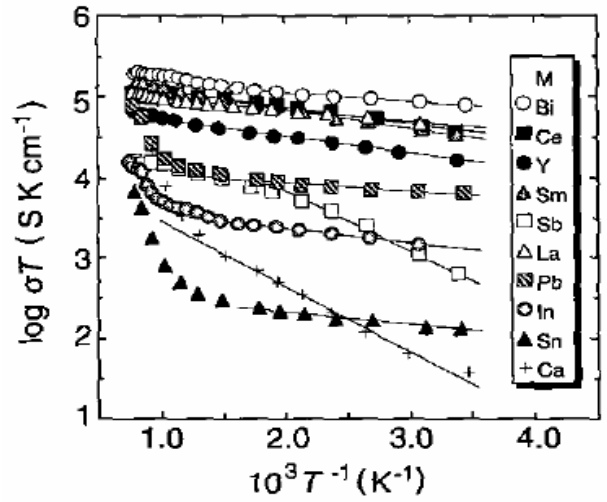

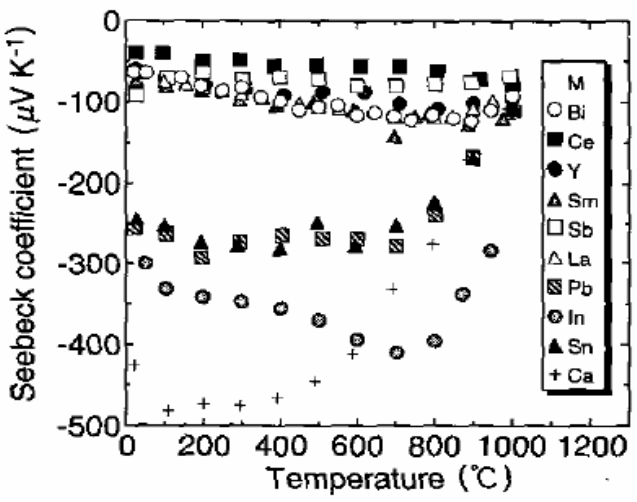

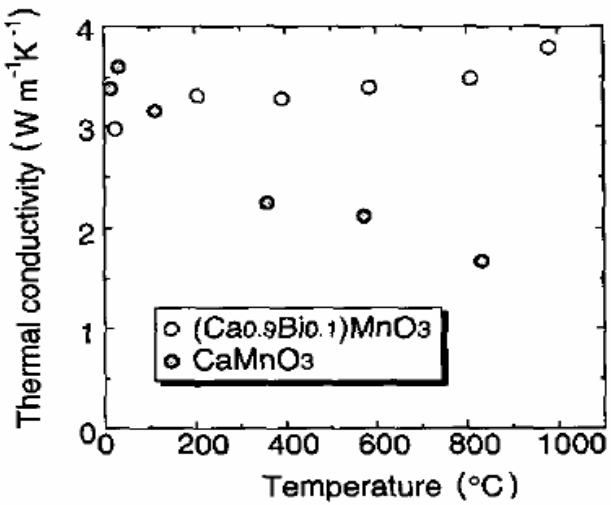

S ~ T

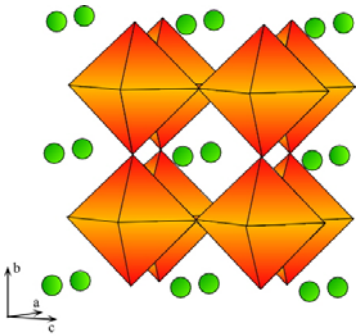

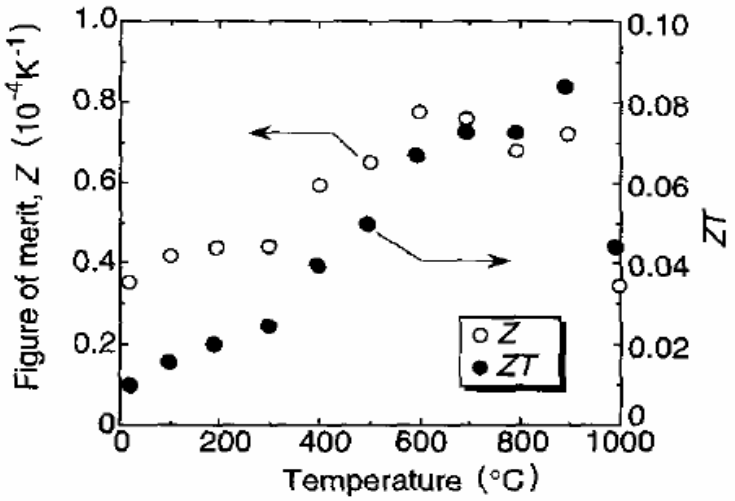

FIG. 7. The temperature dependence of the figures of merit Z and the dimensionless figures of merit ZT for $(Ca_{0.9}Bi_{0.1})MnO_3$.

M. Ohtaki et al., JSSC120, 105 (1995)

ZT ~ 0.1 à 900°C

Carrier concentration
10^{19} -10^{21} cm^{-3}

J. L. Cohn et al.,
PRB72, 024422 (2006)

n type : $SrTiO_3$

$Sr_{1-x}La_xTiO_3$

$SrTiO_3$ = non magnetic insulator
La^{3+} : doping of Ti^{3+} in a matrix of Ti^{4+}

$3d^0$ / $3d^1$

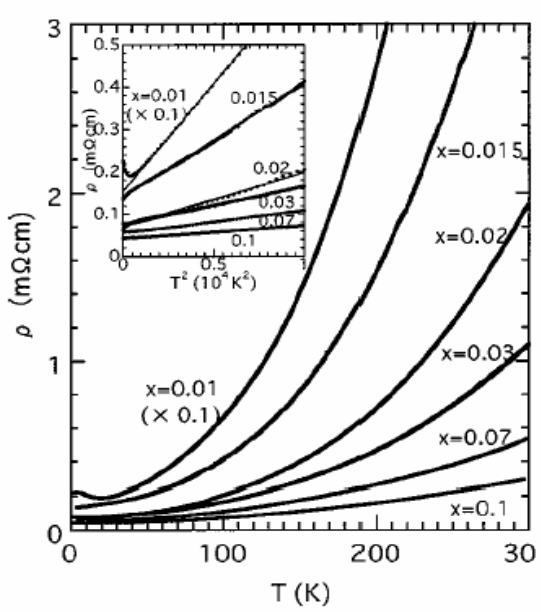

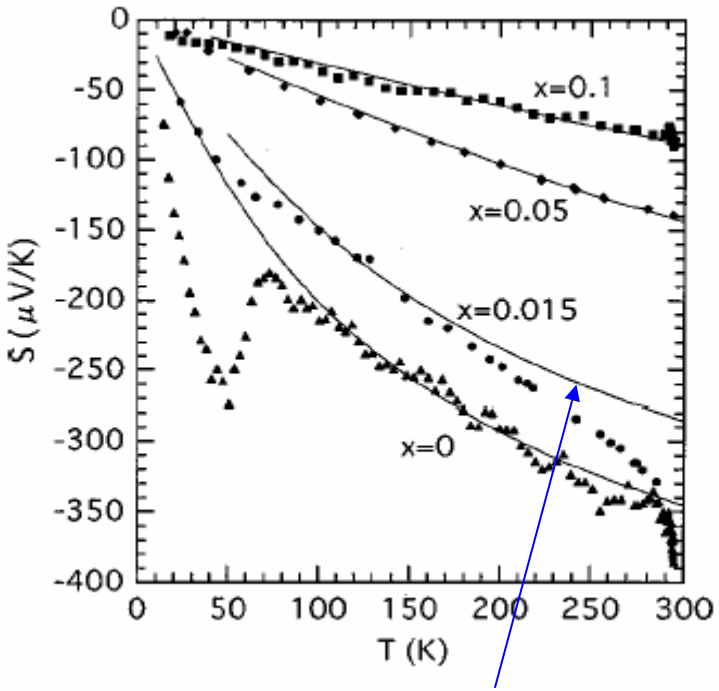

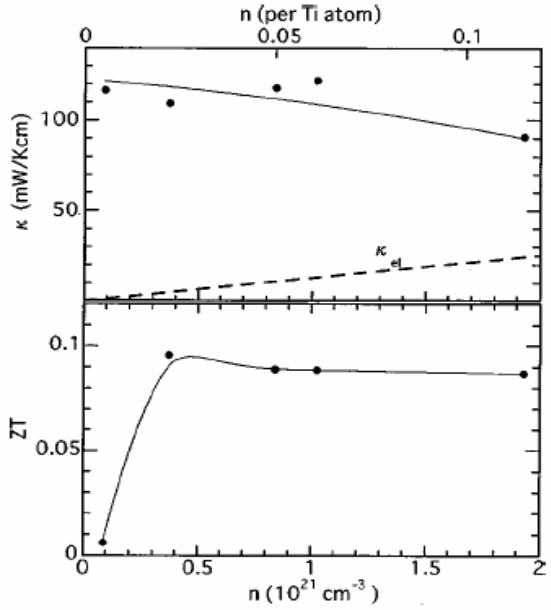

σ~ n
(Constant mobility)

Boltzmann model for a parabolic band
Degenerate semi-conductor

n ~10^{20} – 10^{21} cm^{-3}

PF = 28 -36 10^{-4} $WK^{-2}m^{-1}$
But electrical conductivity too large!!

T. Okuda et al., PRB63, 113104 (2001)

ZT = 0.22 for $Sr_{0.9}Dy_{0.1}TiO_3$ at 573K

H. Muta et al., J. Alloys and Comp.350, 292 (2003)

n type : $SrTiO_3$

$Sr_{1-x}La_xTiO_3$

TABLE I. Various physical quantities derived from measurements of the resistivity, specific heat, Hall, and Seebeck coefficients (S) in $Sr_{1-x}La_xTiO_3$ crystals; n is the carrier (electron) density, A is the T^2 coefficient of resistivity, γ is the electronic specific heat coefficient, m^* is the carrier effective mass, T_F is the Fermi temperature, Θ_D is the Debye temperature, and μ is the chemical potential. S_r represents the calculated Seebeck coefficient with use of the scattering parameter r [see Eq. (1) in the text]. n, μ, S, and S_r are the values at 300 K.

x	n (1/Ti)	n (10^{20} cm^{-3})	A (Ω cm/K^2)	γ (mJ/K^2 mol)	m^*/m_b	T_F (K)	Θ_D (K)	μ (eV)	$-S$ (μV/K)	$-S_0$ (μV/K)	$-S_1$ (μV/K)	$-S_2$ (μV/K)
0	0.0052	0.877	3.68×10^{-7}	0.63	1.17	343	402	0.0061	380	190	268	345
0.015	0.014	2.31	2.58×10^{-8}						350			
0.02	0.022	3.73	1.21×10^{-8}	1.04	1.51	697	378	0.0488	260	150	182	247
0.04	0.05	8.41	6.69×10^{-9}						162			
0.05	0.061	10.23	5.14×10^{-9}	1.96	1.62	1273	380	0.102	147	93	118	168
0.1	0.11	19.31	3.08×10^{-9}						88.7			

Carrier concentration
10^{19} -10^{21} cm^{-3}

γ smaller than for p type oxides
Less sensitive to correlation effects

T. Okuda et al., PRB63, 113104 (2001)

Type p : delafossites

$CuCr_{1-x}Mg_xO_2$ delafossites

CrO_2 layers : edge shared octahedra

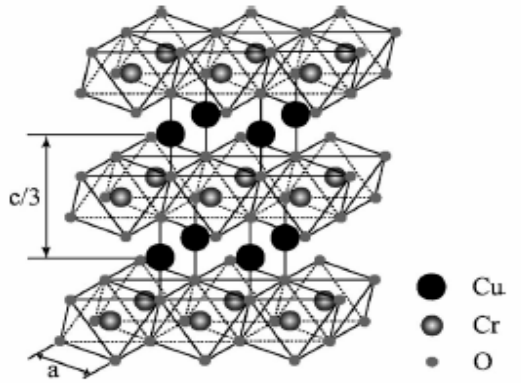

Possibility to get p type oxides

ZT = 0.04 at 950K

$Cu^{+}[Cr^{3+}]_{1-2x}[Cr^{4+}]_x[Mg^{2+}]_x O_2$

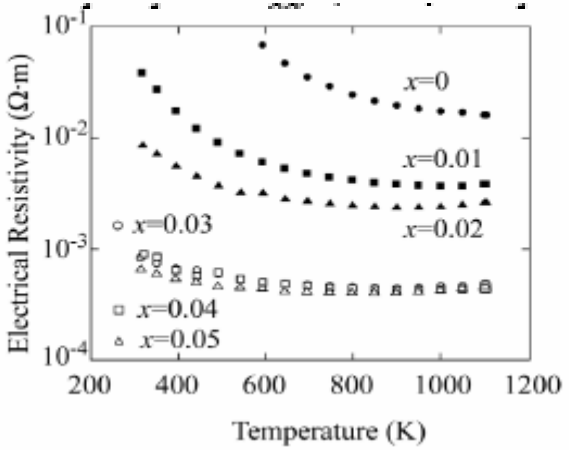

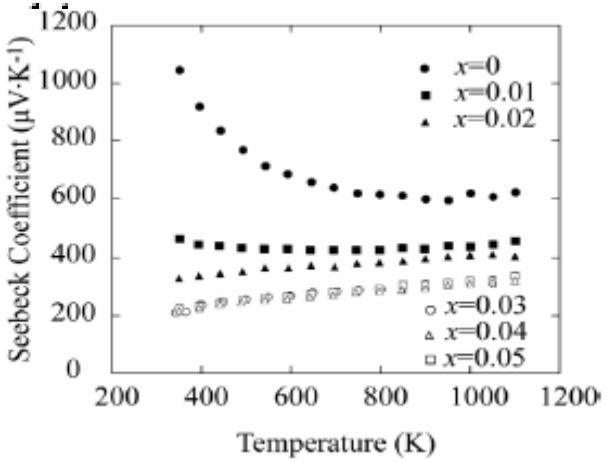

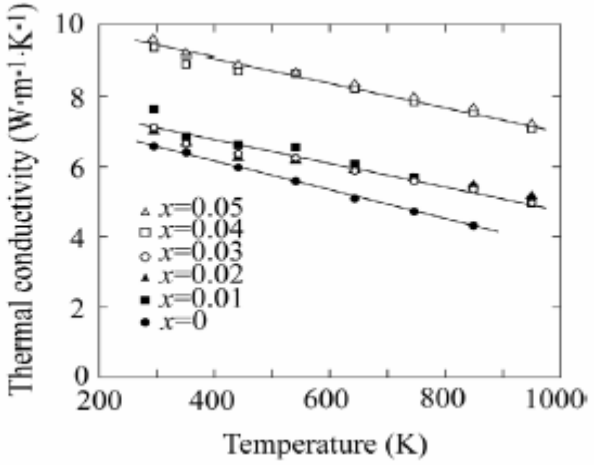

T. Okuda et al., PRB72, 144403 (2005), Y. Ono et al., ICT 2006

$CuRh_{0.9}Mg_{0.1}O_2$: ZT = 0.15 à 1000K

H. Kuriyama et al., ICT2006

C. Marcel et al., Active and Passive Elec. Comp., 1997, Vol. 19, pp. 217-223

$In_{2-x}Ge_xO_3$

XRD

Doping or microstructure effect??

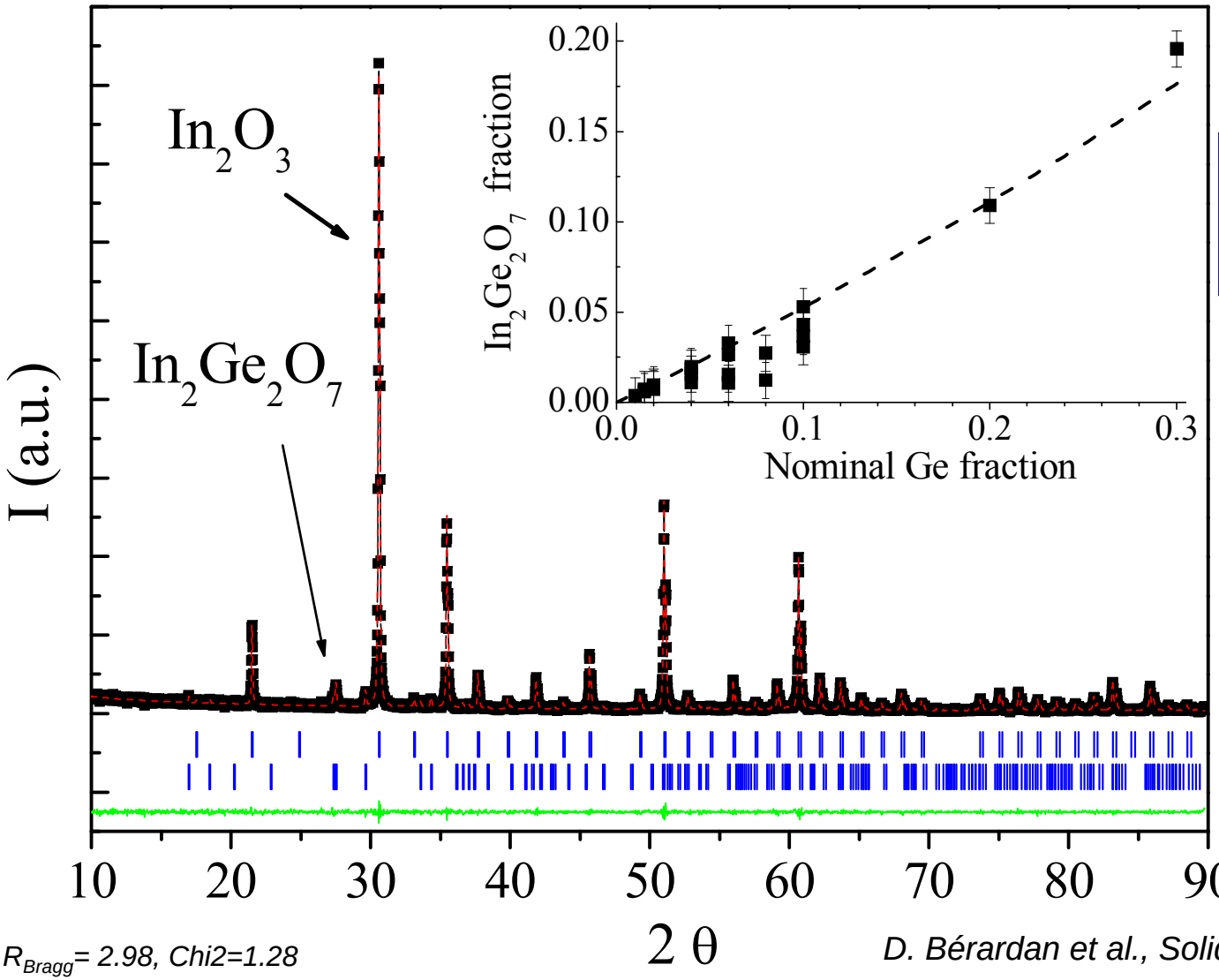

No substitution occurs
or
Small Ge solubility limit

Sample
$In_{1.9}Ge_{0.1}O_3$

R_{Bragg}= 2.98, Chi2=1.28

D. Bérardan et al., Solid Stat. Comm. 146 (2008) 97.

$In_{2-x}Ge_xO_3$

Microstructure

Sample
$In_{1.8}Ge_{0.2}O_3$

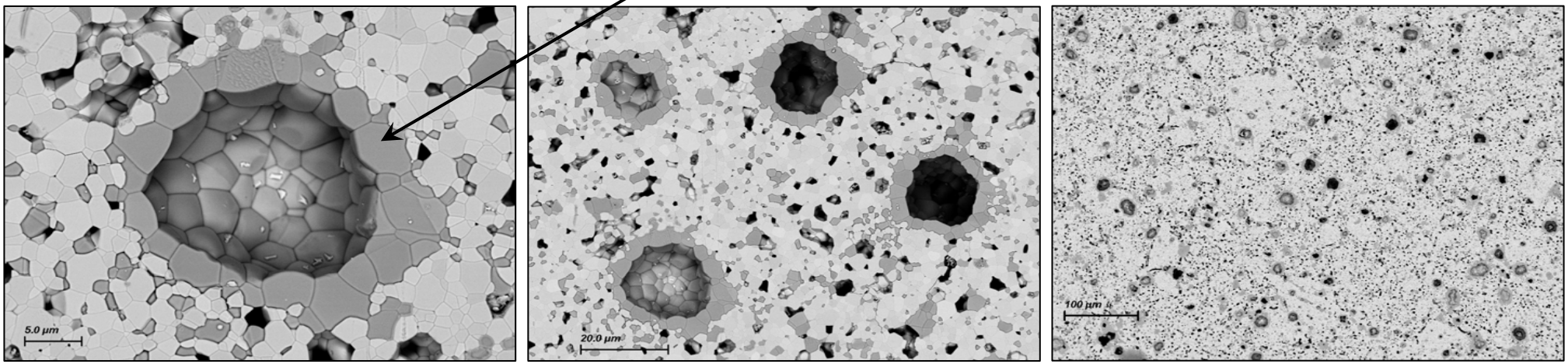

EDS analyses: Ge is not detectable in the grains

No grain size modification

Type n : In_2O_3

In_2O_3 doped with Ge

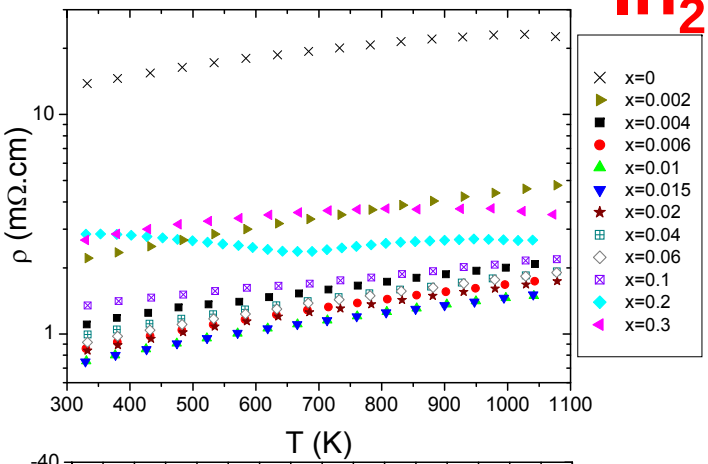

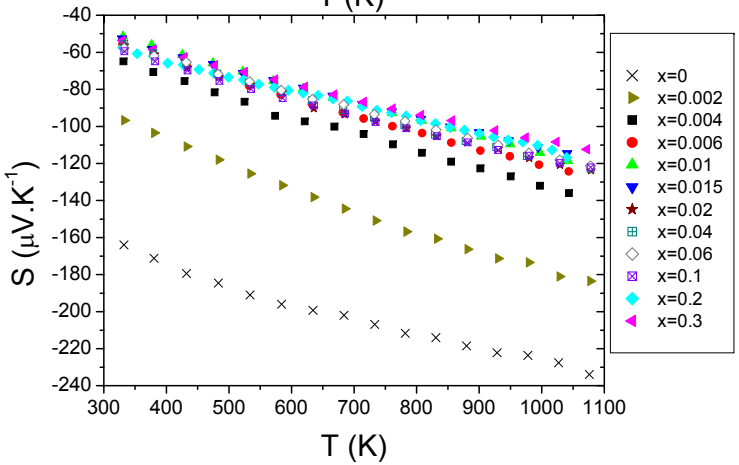

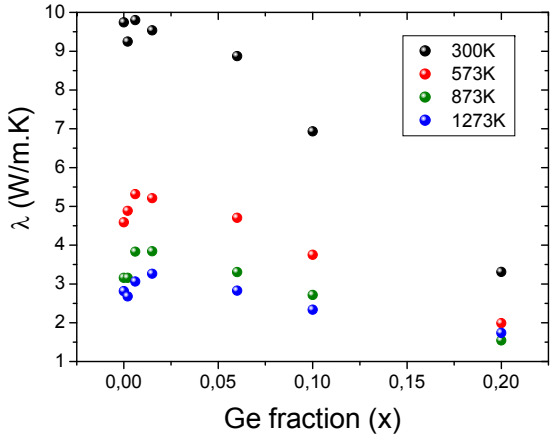

$In_{2-x}Ge_xO_3$

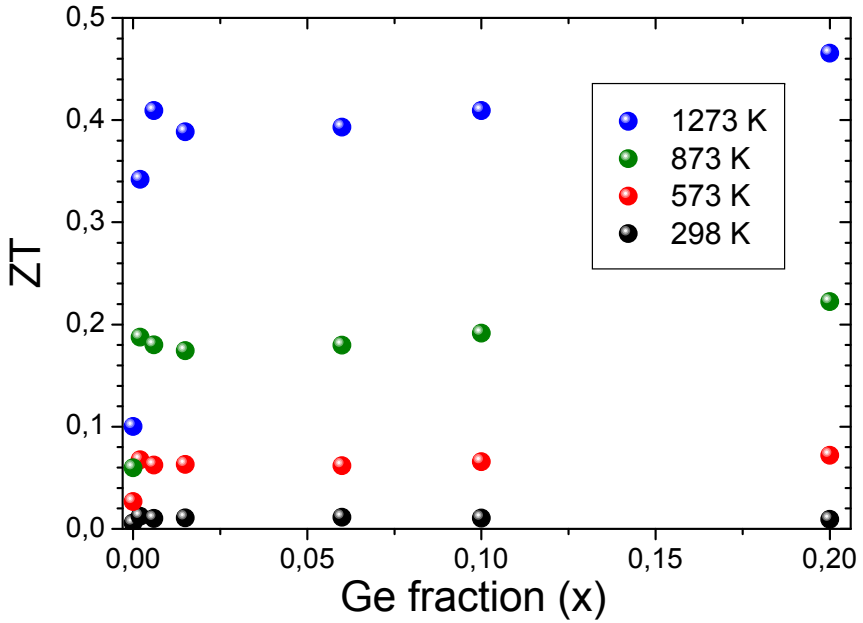

ZT = 0.4 à 1273K

D. Bérardan et al., Solid Stat. Comm. 2008

Doped $CaMnO_3$: New preparation techniques

Soft chemistry techniques

L. Bocher et al., Inorg. Chem. 47, 8077 (2008)

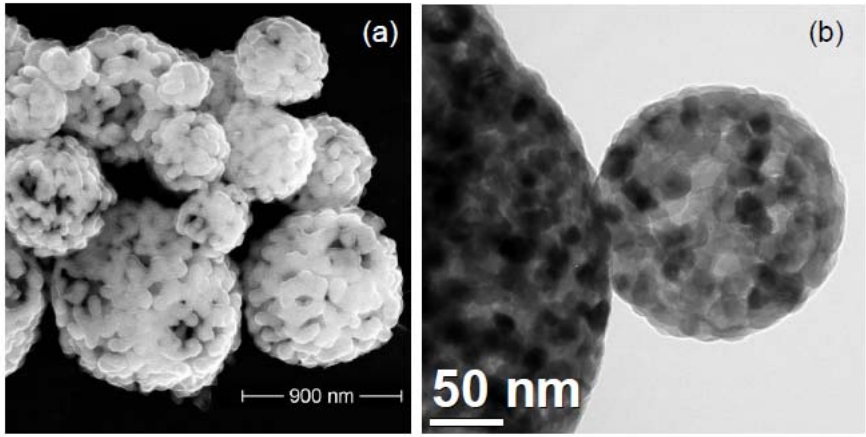

Fig. 1. a) SEM picture and b) low resolution TEM of hollow perovskite spheres

Reduction of κ
Possible size effect?

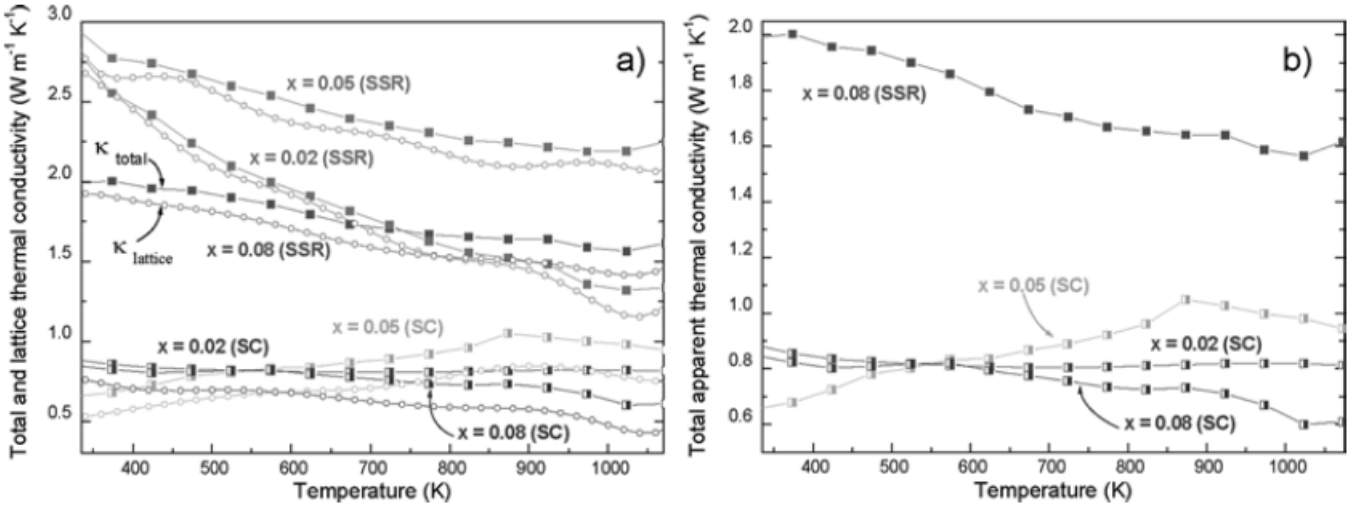

Figure 8. (a) Total thermal conductivity κ_{total} of $CaMn_{1-x}Nb_xO_3$ (x = 0.02, 0.05, and 0.08) synthesized by both SSR (closed symbols) and SC (half-open symbols) methods and lattice contribution κ_l (open symbols) versus T and (b) highlight in the low thermal conductivity range.

Degenerate semi - conductors

- Classical behavior which can be described by the Boltzmann model
  Very small enhancement of the effective mass

- Mostly n type (p tye in delafossites)

- Problem : too large thermal conductivity

Microstructure modification is necessary to enhance ZT

Na_xCoO_2 and related metallic compounds (p type)

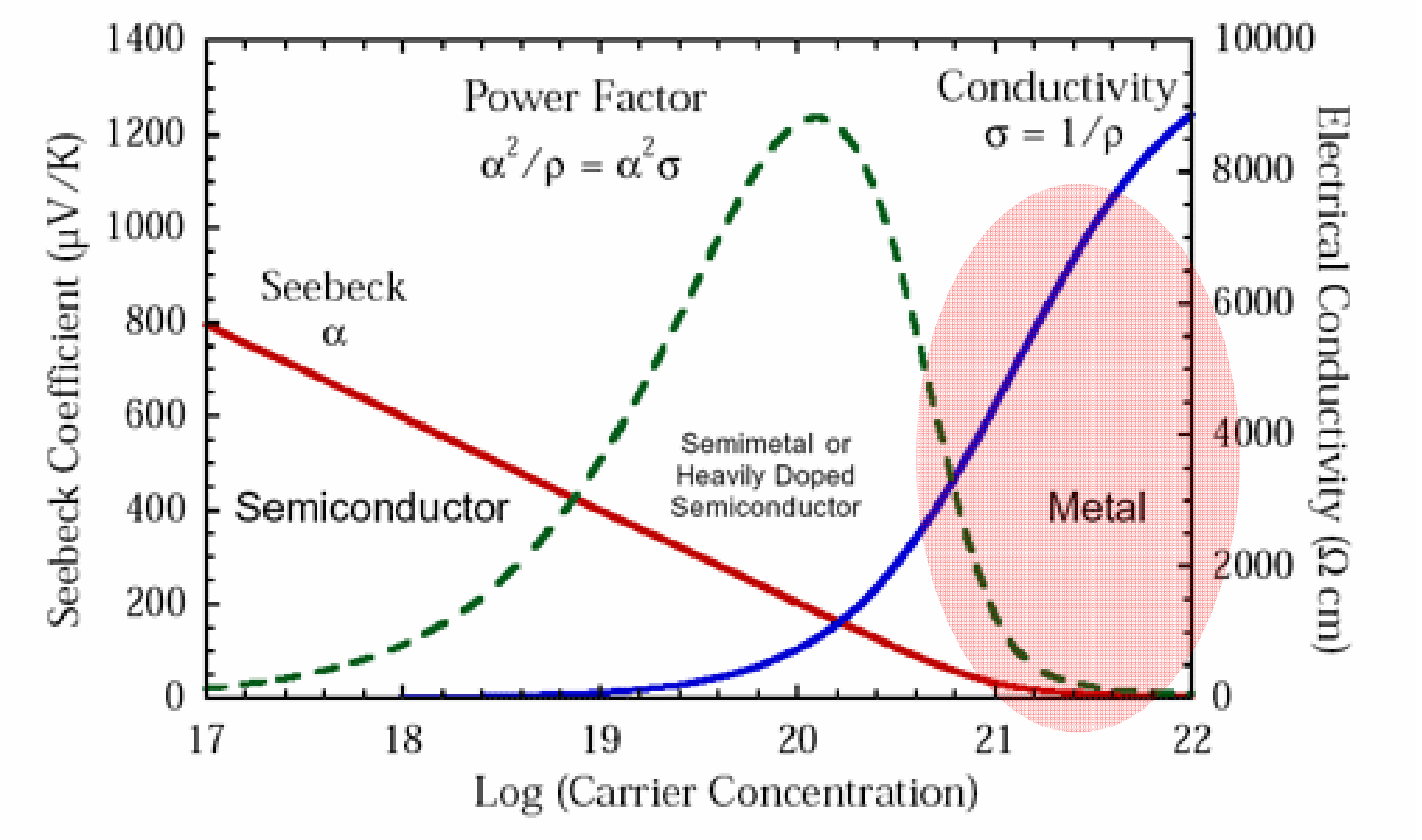

Cobalt bronzes family of Na_xCoO_2

C. Fouassier et al., JSSC6, 532 (1973)

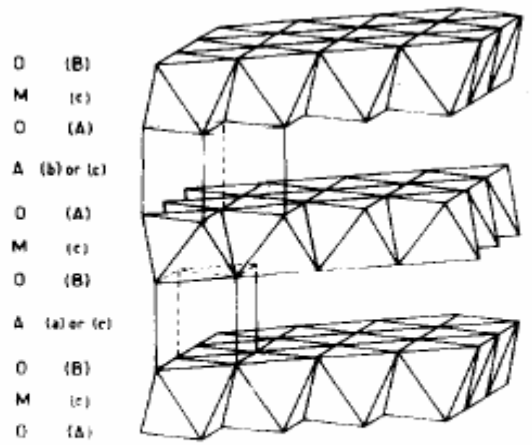

(P2)

Fig. 1. Layer structure of $Na_{0.70}CoO_{2-y}$.

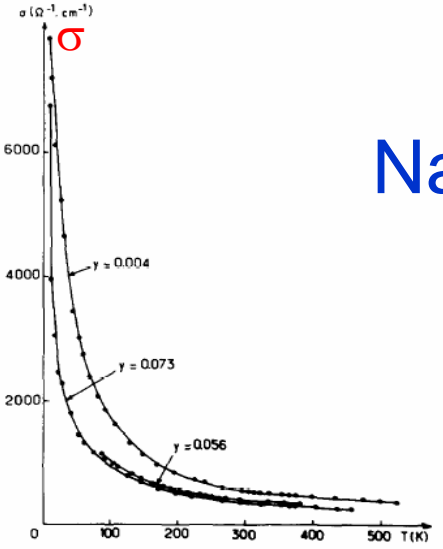

Fig. 6. Temperature dependence of the electrical conductivity of quenched pellets.

T

$Na_{0.7}CoO_{2-\gamma}$

S

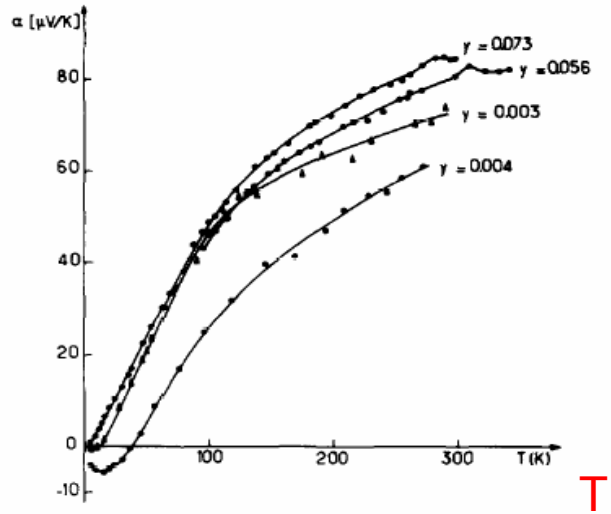

Fig. 7. Temperature dependence of the thermoelectric power of quenched pellets.

T

J. Molenda, C. Delmas, P. Dordor, A. Stoklosa,
Solid Stat. Ionics 12, 473 (1989)

$Na_{0.7}CoO_2$

‘ Phonon Glass / Electron crystal ’

I. Terasaki et al., Phys. Rev. B 56, R12685 (1997)

$Na_xCoO_2 : Na^+_x Co^{3+}_x Co^{4+}_{1-x} O_2$

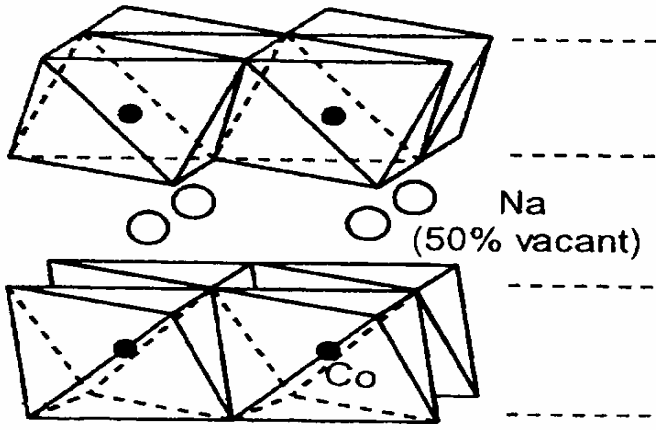

Co^{3+} ($3d^6$) / Co^{4+} ($3d^5$)

Measurements on polycrystals

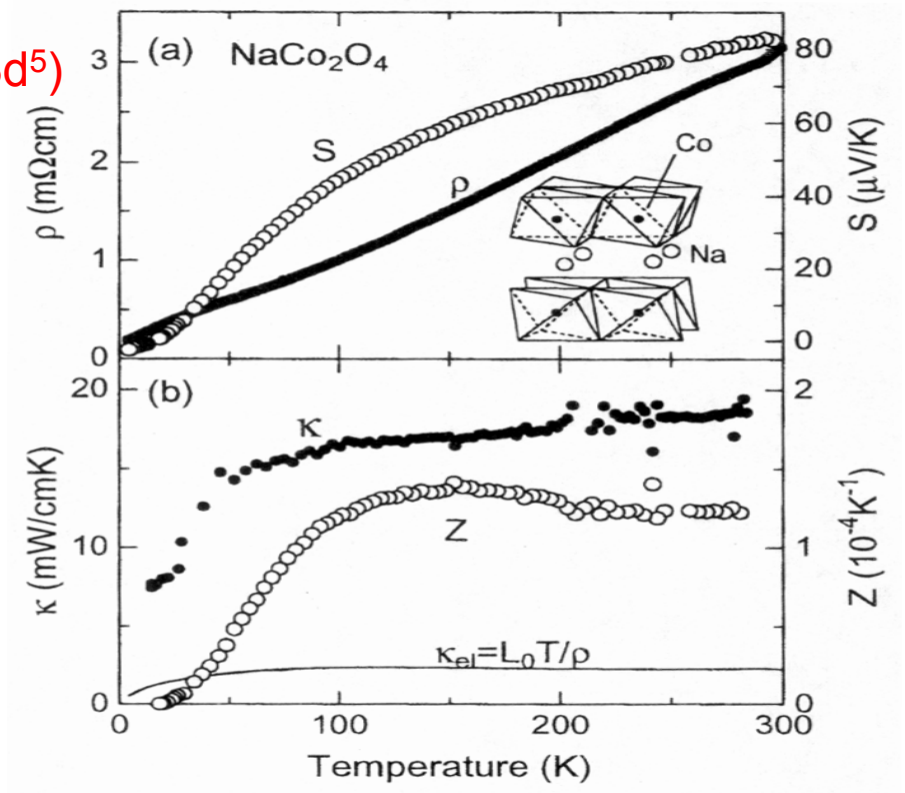

At 300K

Metallicity (crystals) $\rho \sim 0.2\ m\Omega\ cm$

Large S $S \sim +80\ \mu V/K$

Small κ (polycrystals) $\kappa \sim 2 Wm^{-1}K^{-1}$

(crystals) $\kappa \sim 5 Wm^{-1}K^{-1}$

Power factor $P=S^2/\rho$ at 300K

$Na_{0.7}CoO_2$

$P= 50\ 10^{-4}\ WK^{-2}m^{-1}$

Bi_2Te_3

$P= 40\ 10^{-4}\ WK^{-2}m^{-1}$

Na_xCoO_2
Misfits

Lamellar oxides with CoO_2 layers

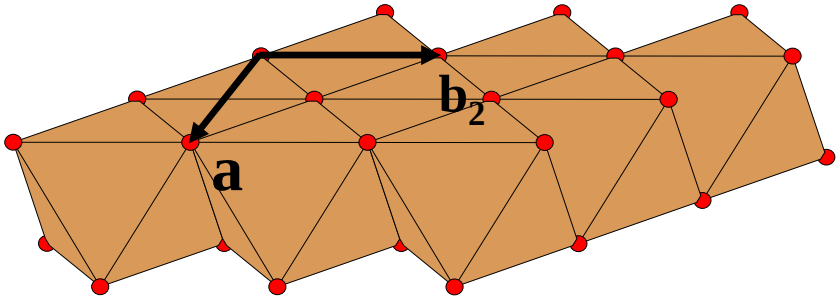

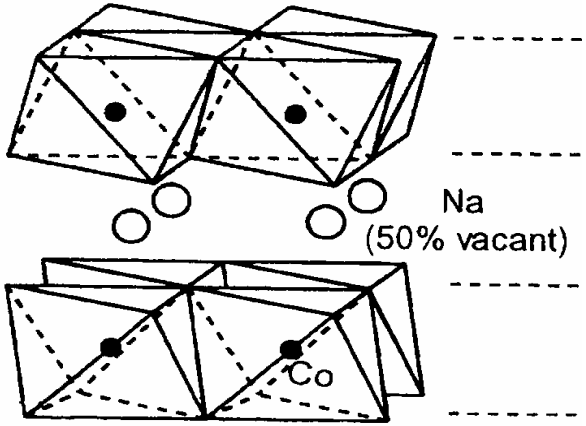

Na_xCoO_2
K_xCoO_2, …

Triple AO layer (NaCl-type)

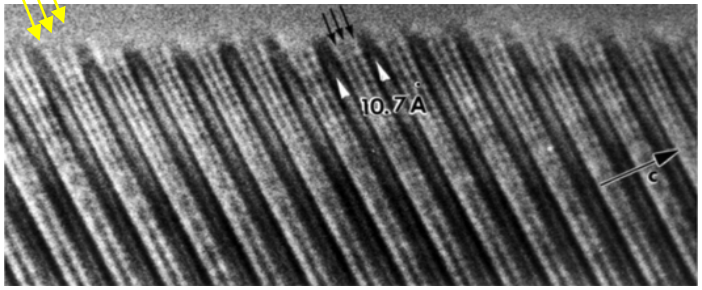

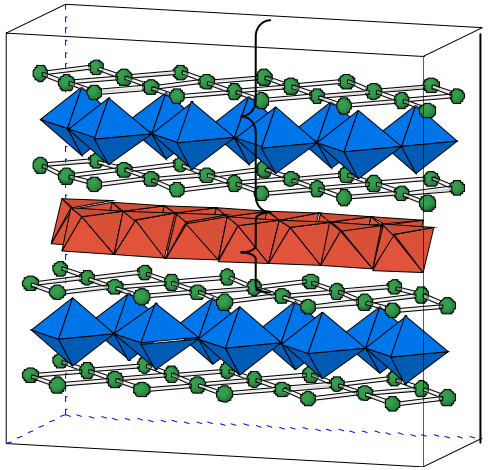

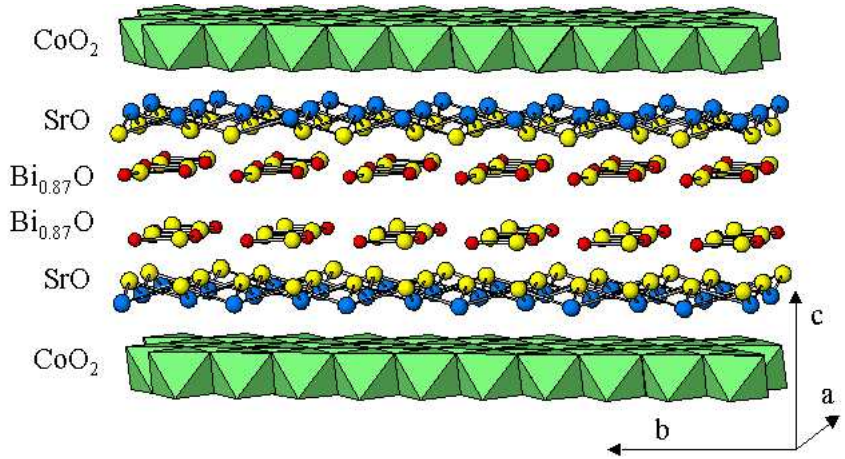

Misfit family : 2, 3 or 4 separating layers

Heikes formula : doping influence?
Band structure influence : peculiarity of CoO_2 layers ?
Role of separating block layers?

Modification of the block layers

K_xCoO_2

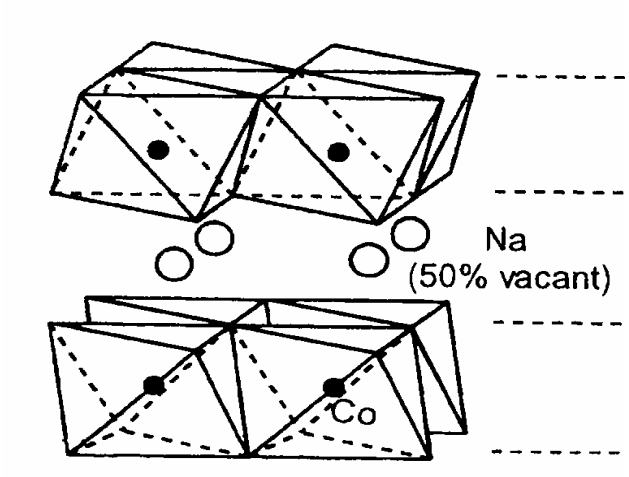

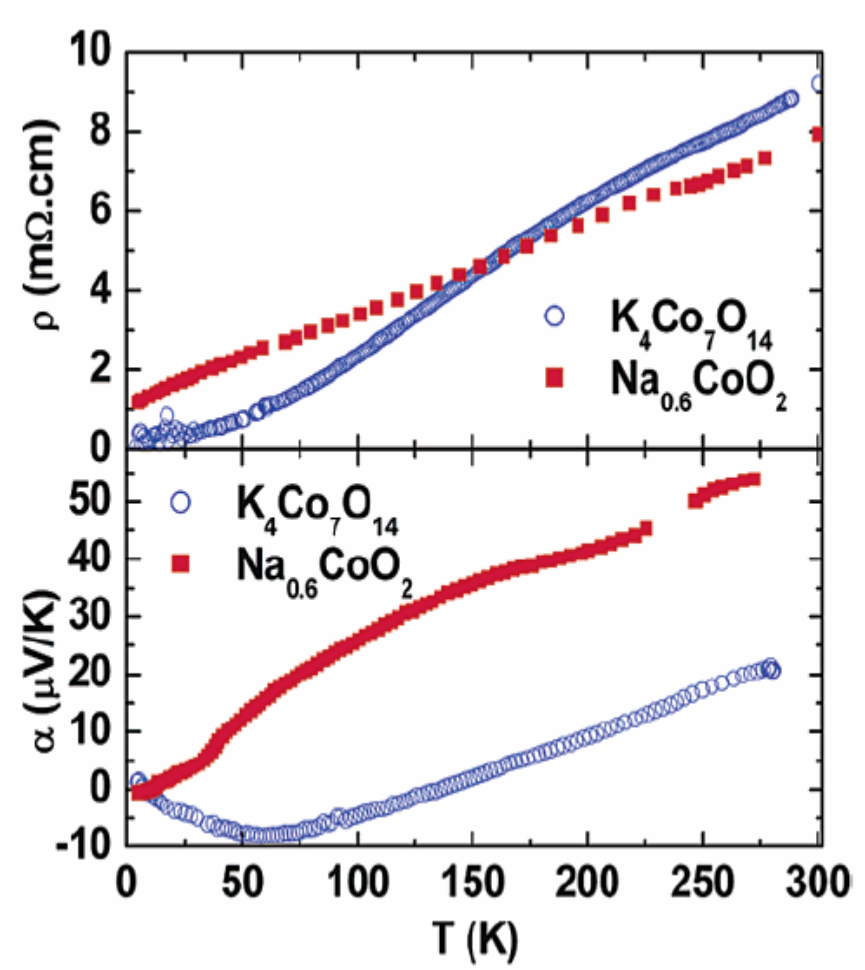

M. Blangero et al., Inorg. Chem. 44, 9299 (2005)

Na_xCoO_2
Misfits

Modification of the block layers

Misfits

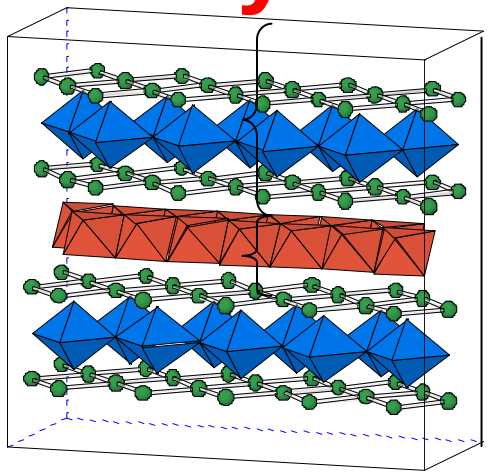

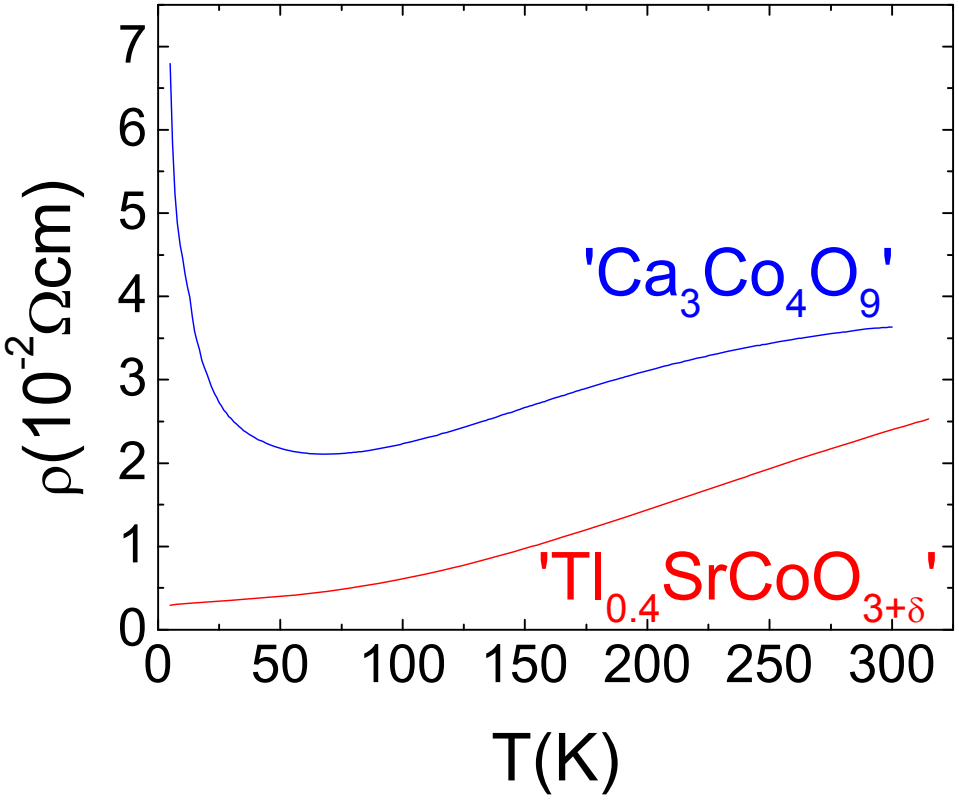

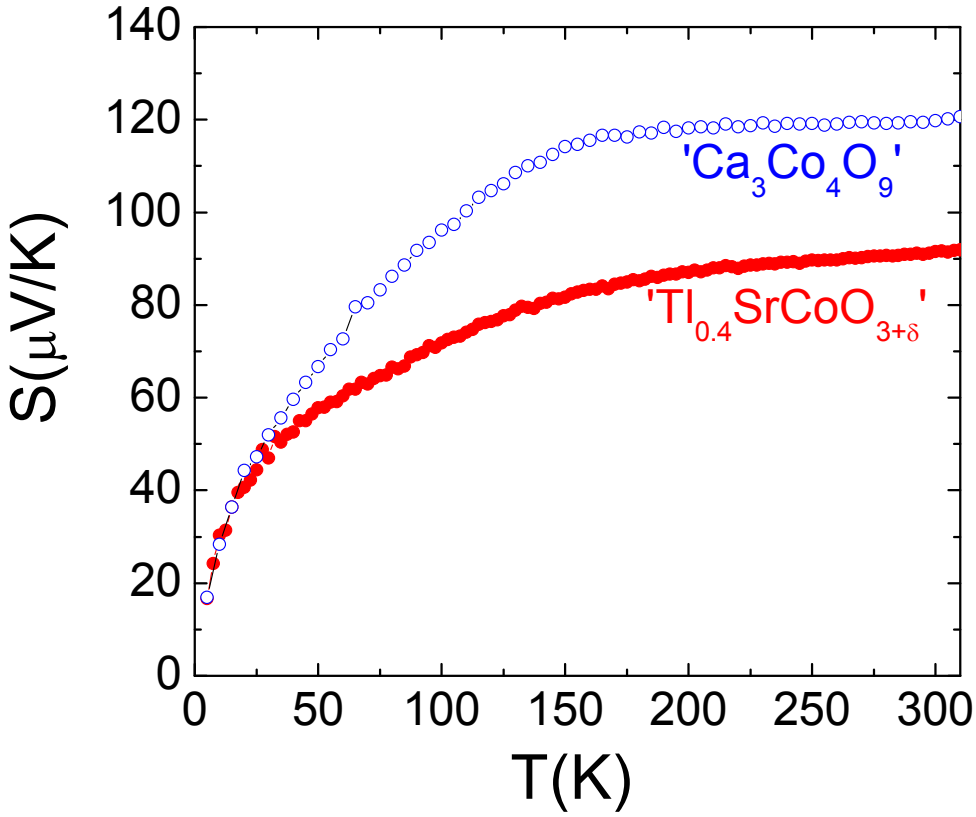

Na_xCoO_2 Misfits

Unique behavior of CdI_2 type layers: Comparison with other oxides

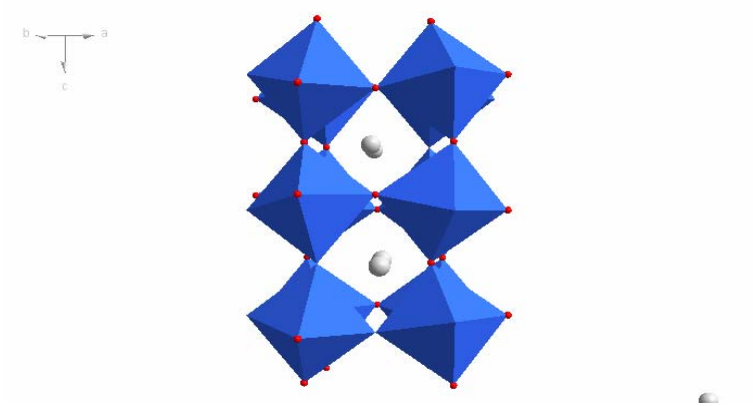

Perovskite $Sr_{2/3}Y_{1/3}CoO_{8/3+\delta}$

Corner shared octahedra

≠ edge shared octahedra

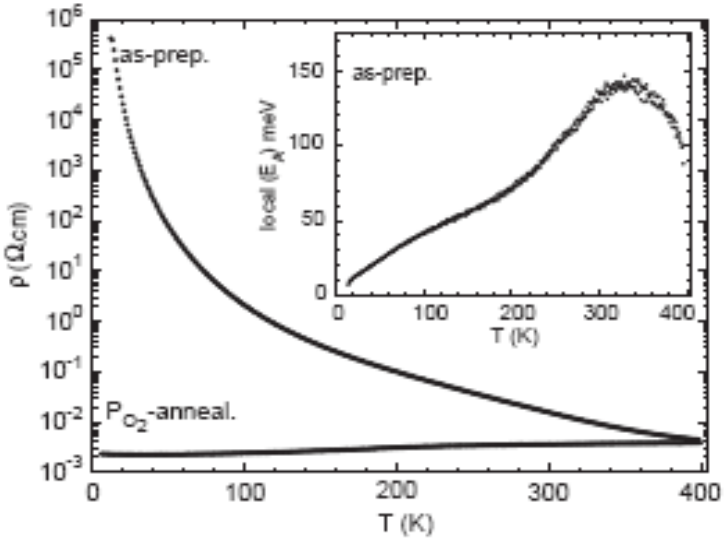

Metallicity

⟶

Seebeck ≈ 0

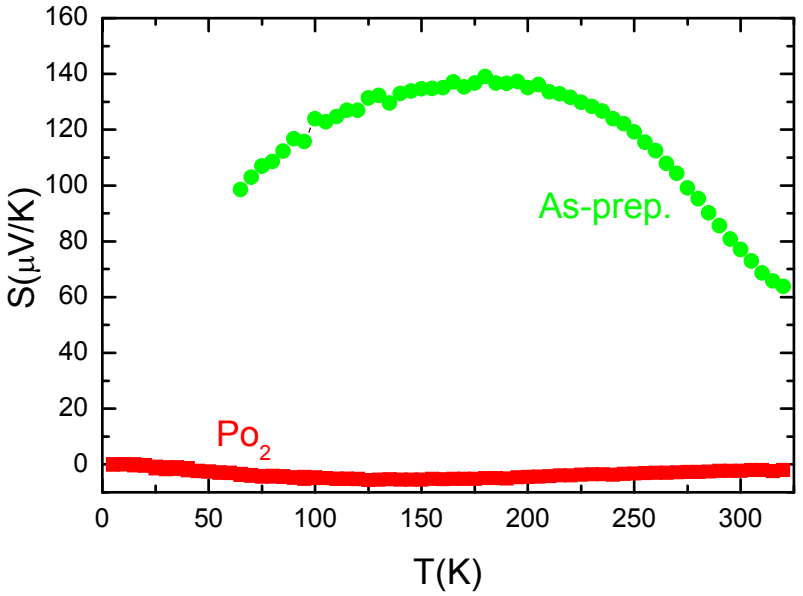

A. Maignan et al., JSSC178, 868 (2005)

Oxygen content influence

$Ca_3Co_4O_{9+\delta}$

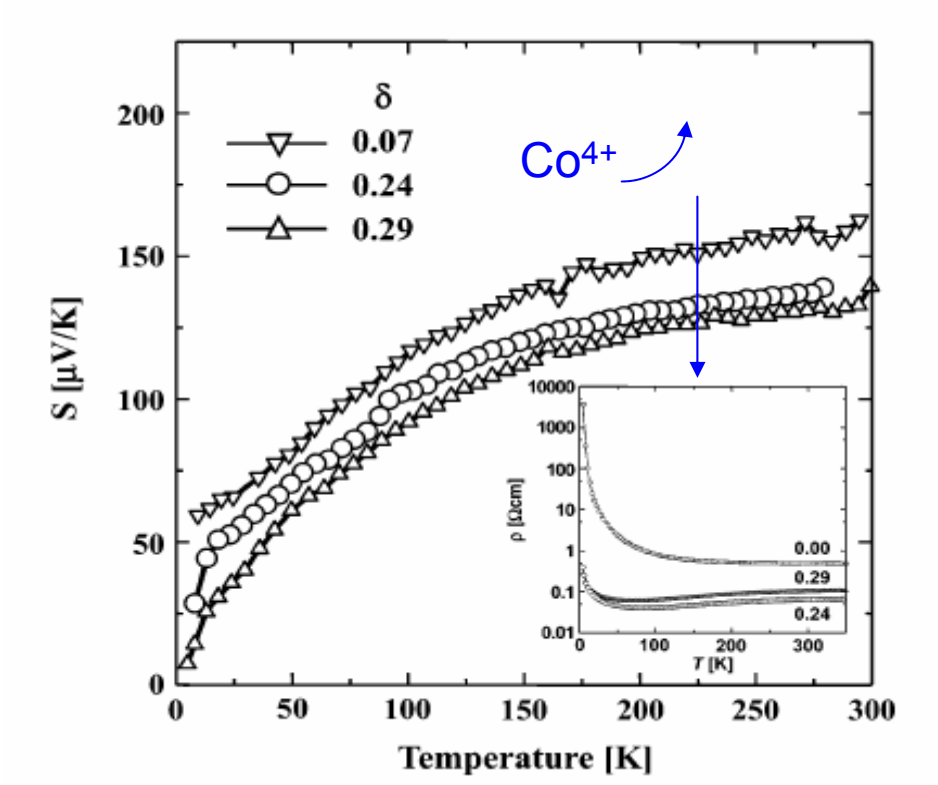

M. Karppinen et al., Chem. Mater. 16, 2790 (2004)

Misfits : S the largest for the smallest 'Co^{4+}' content

Doping effect in the misfit family

$Ca_3Co_4O_9$

Ca_2CoO_3
NaCl-like

CoO_2
CdI_2-like

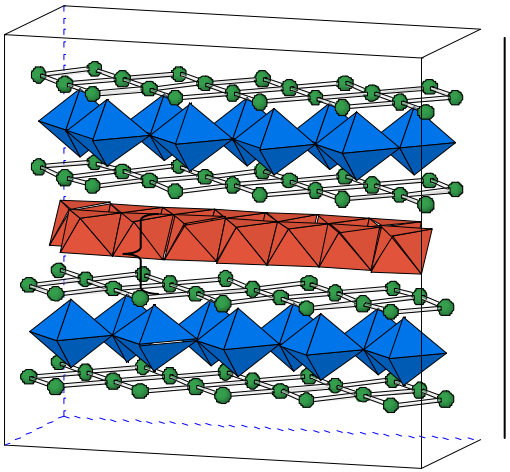

Electronic neutrality :

$[Ca_2CoO_{3\pm\delta}]^{RS}[CoO_2]_{b1/b2}$

2+ 3+ 2- ν_{Co} 2-

$\alpha > 0$

$$\nu_{Co} = 4 - \frac{\alpha}{b_1 / b_2}$$

Modification of ν_{Co} via α and b_1/b_2

Link between ν_{Co} and S?

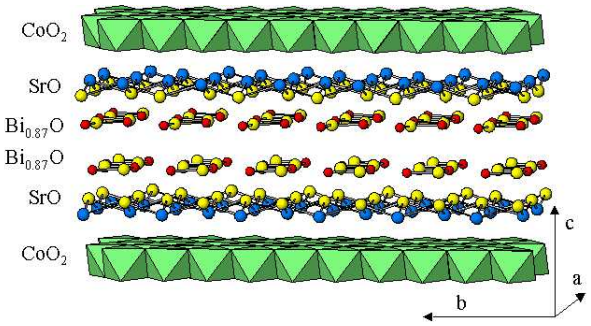

$$v_{Co} = 4 - \frac{\alpha}{b_1 / b_2}$$

BiSrPbCoO single crystals : modification of α

$[Bi_{1.74}Sr_2O_4][CoO_2]_{1.82}$ $[Bi_{1.5}Pb_{0.5}Sr_2O_{4-\delta}][CoO_2]_{1.86}$

Substitution of Bi^{3+} by Pb^{2+} : decrease of α

Increase of v_{Co}

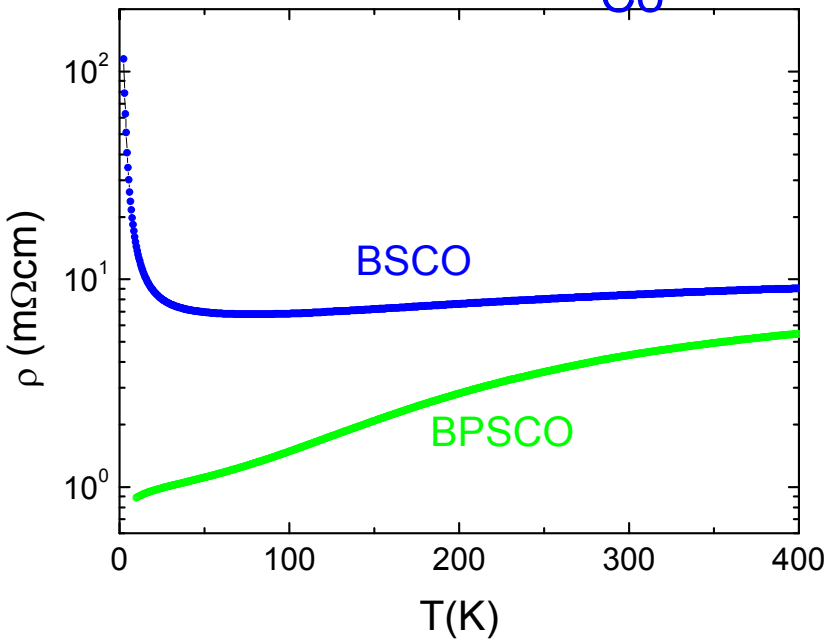

Metallic behavior down to 5K with $\rho = AT^2$

Characteristic of electronic correlations

Na_xCoO_2 Misfits

BiSrPbCoO single crystals : modification of α

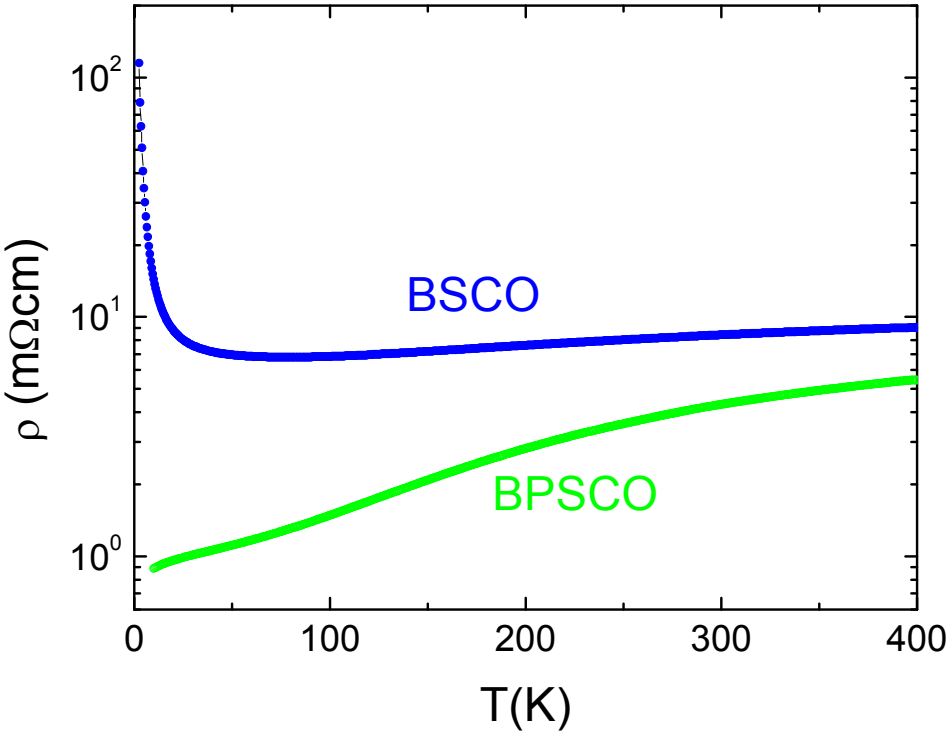

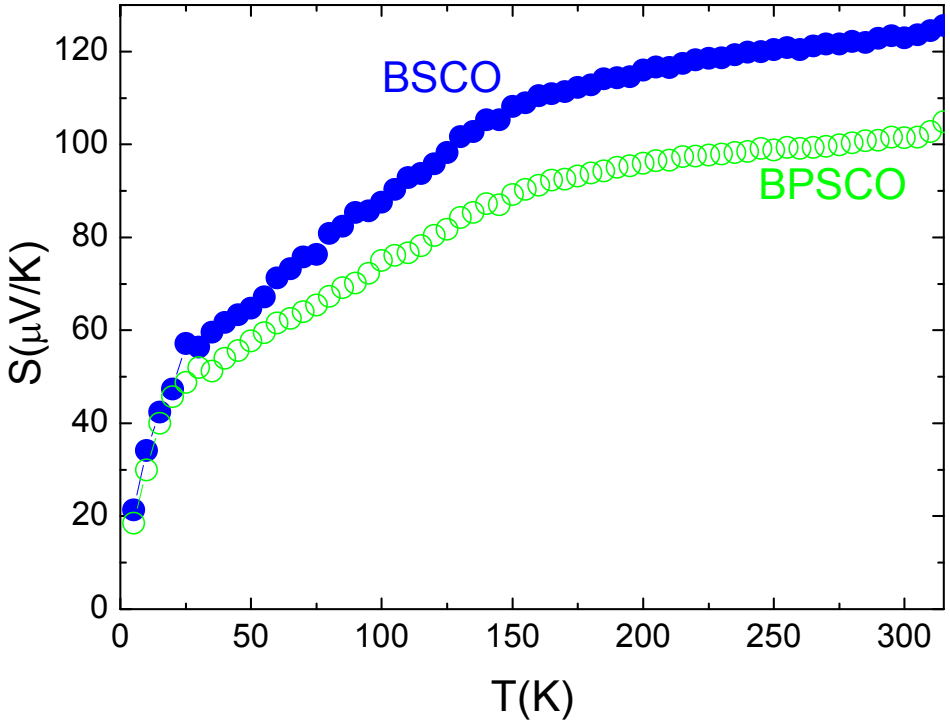

$$S = -\frac{k_B}{e}\ln\left(\frac{g_3}{g_4}\frac{x}{1-x}\right)$$

Increase of ‘Co^{4+}’ associated to a decrease of S

Generalized Heikes formula : increase of v_{Co}

3.59 for BSCO and 3.65 for BPSCO

Na_xCoO_2
Misfits

BiSrPbCoO single crystals : modification of α

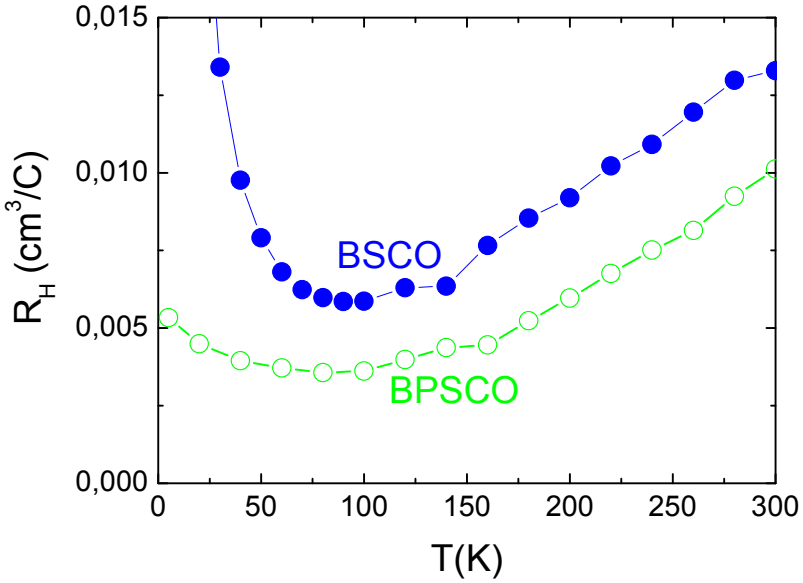

At 100K
1.06×10^{21} cm^{-3} for BSCO
1.73×10^{21} cm^{-3} for BPSCO

Increase of v_{Co}
3.11
3.18

t- J model : Linear T dependence of R_H
t ~10 – 40K
Justifies the Heikes formula

B. Kumar et al., PRB68, 104508 (2003)
Y. Wang et al., cond-mat/0305455
G. Leon et al. , PRB78, 085105 (2008)

W. Kobayashi et al., JPCM21, 235404 (2009)

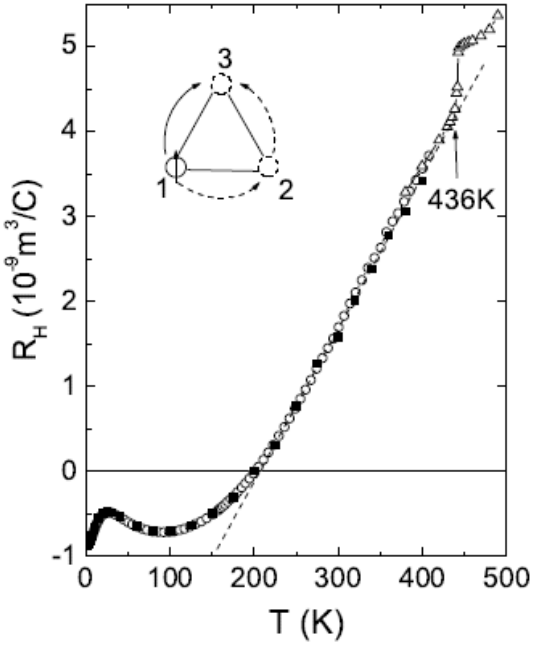

Na_xCoO_2
Misfits

Influence of b_1/b_2

b_1 : NaCl layers / b_2 : CoO_2 layers

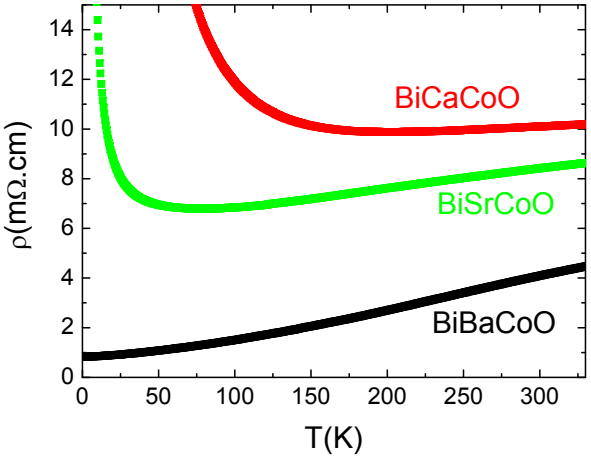

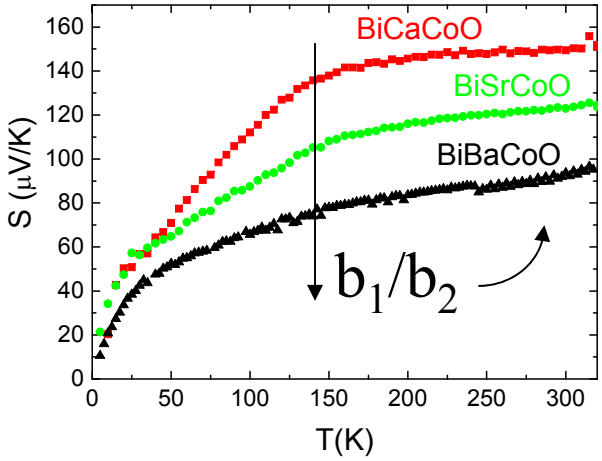

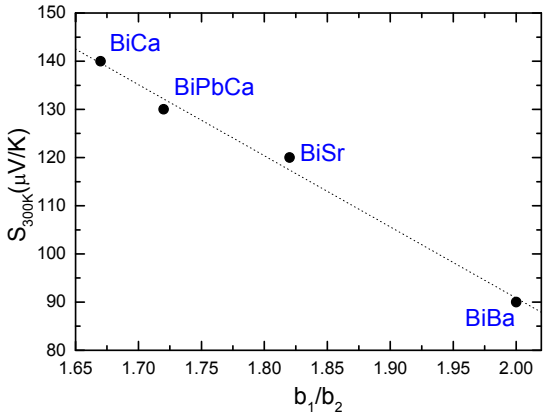

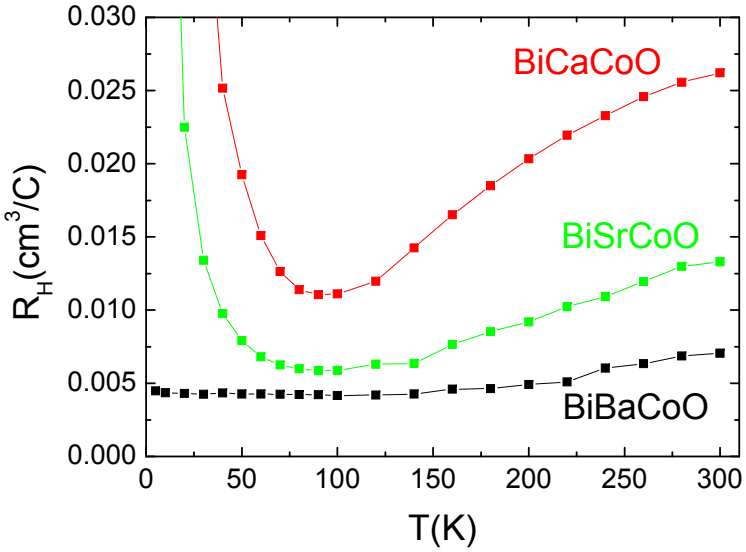

W. Kobayashi et al.

If b_1/b_2 ↗ , concentration of Co^{4+} ↗

$$v_{Co} = 4 - \frac{\alpha}{b_1 / b_2}$$

⇘S at 300K depends on Co^{4+} modified through b_1/b_2

Carrier concentration ~ 10^{22} cm^{-3},
larger than for conventional thermoelectrics

Na_xCoO_2
Misfits

Heikes formula

$$S = -\frac{k_B}{|e|}\ln\left(\frac{g_4}{g_3}\frac{1-x}{x}\right)$$

Co valency in BiCaCoO/ BiSrCoO / BiBaCoO?

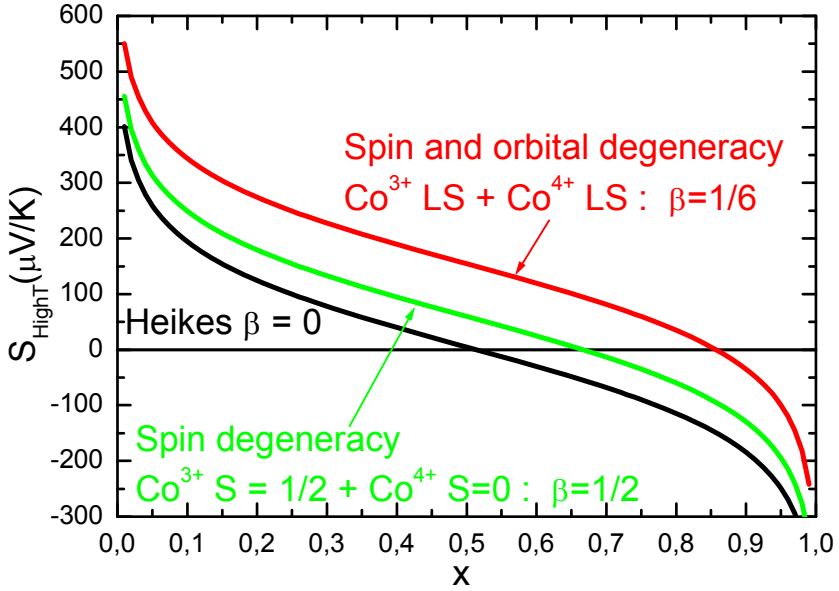

Heikes (S at 300K)	Hall effect
3.5 -3.7 for g_4 / g_3 = 6	3.05 -3.15

Carrier concentration

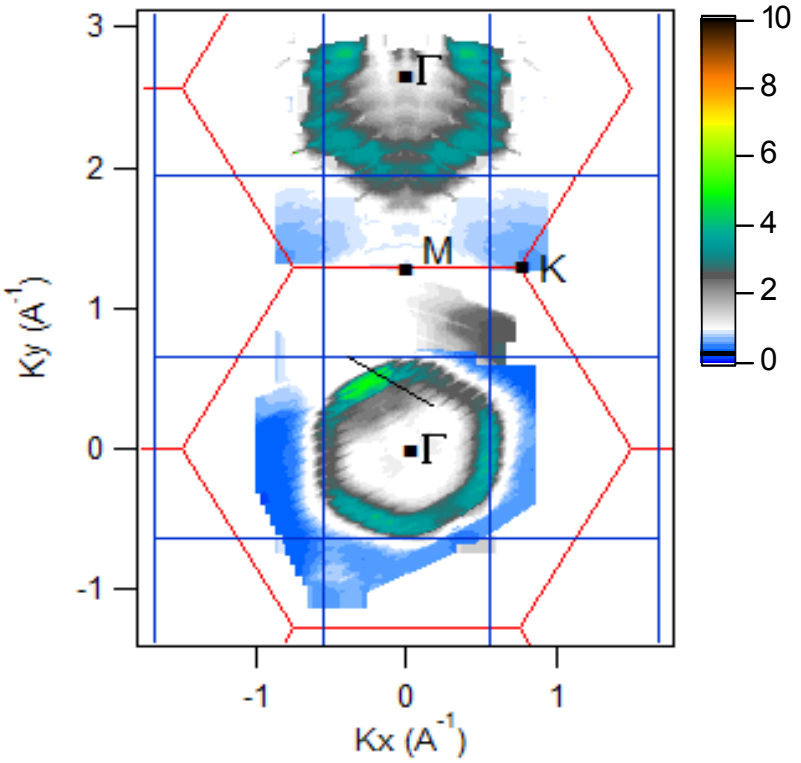

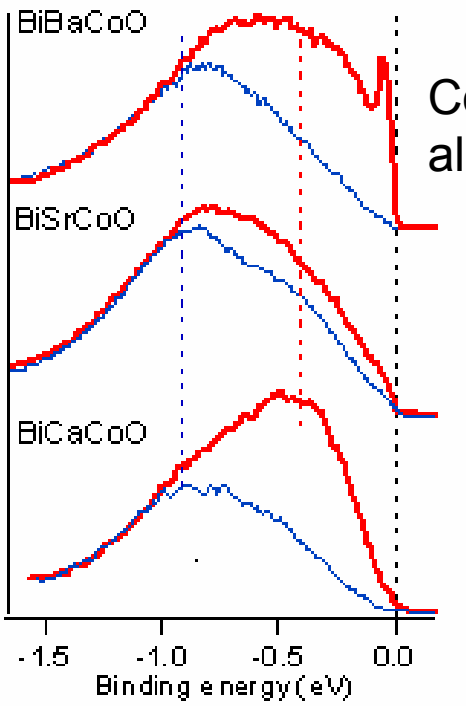

ARPES

Collaboration with V. Brouet et al., LPS Orsay

Reliable data for v_{Co} are obtained for BiBaCoO

$$v_{Co} = 4 - \frac{\alpha}{b_1 / b_2} \quad (\alpha=\text{const})$$

single hole-like fermi surface (a_{1g} character)

$k_F = 0.57 \pm 0.05$ Å^{-1} for BiBaCoO

→ similar to k_F of Na_xCoO_2 (x=0.7)

→ $Co^{3.3+}$ for BiBaCoO

V. Brouet et al., PRB76, 100403 (2007)

$Co^{3.2+}$ for BiSrCoO

$Co^{3.1+}$ for BiCaCoO

Na_xCoO_2
Misfits

Heikes formula

$$S = -\frac{k_B}{e}\ln\left(\frac{g_3}{g_4}\frac{x}{1-x}\right)$$

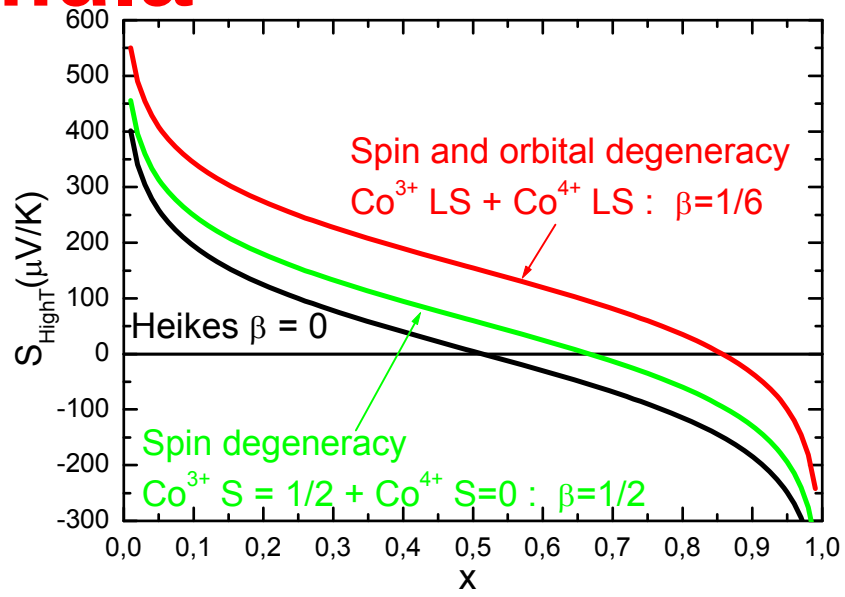

Co valency in BiCaCoO/ BiSrCoO / BiBaCoO

Heikes g_3/g_4 = 1/6 S à 300K	Seebeck avec S(H) g_3/g_4 = 1 BiCaCoO	Effet Hall	ARPES BiBaCoO	RMN	Susceptibilité BiCaCoO
3.5 -3.7	3.33 P. Limelette et al., PRL97, 046601 (2006)	3.05 -3.15 W. Kobayashi et al.	3.3 V. Brouet et al., PRB76, 100403 (2007)	3.1 -3.3 J. Bobroff et al., PRB76, 100407 (2007)	3.24 M. Pollet et al., JAP101, 083708 (2007)

g_3 / g_4 = 1/2 instead of 1/6

Confirms the results in BiCaCoO : v_{Co} = 3.24

M. Pollet et al., JAP101, 083708 (2007)

Na_xCoO_2 Misfits

Orbital filling in Na_xCoO_2 and misfit cobaltites with edge-shared CoO_6

LS Co^{3+}/Co^{4+} mixed-valency

↓

metallicity

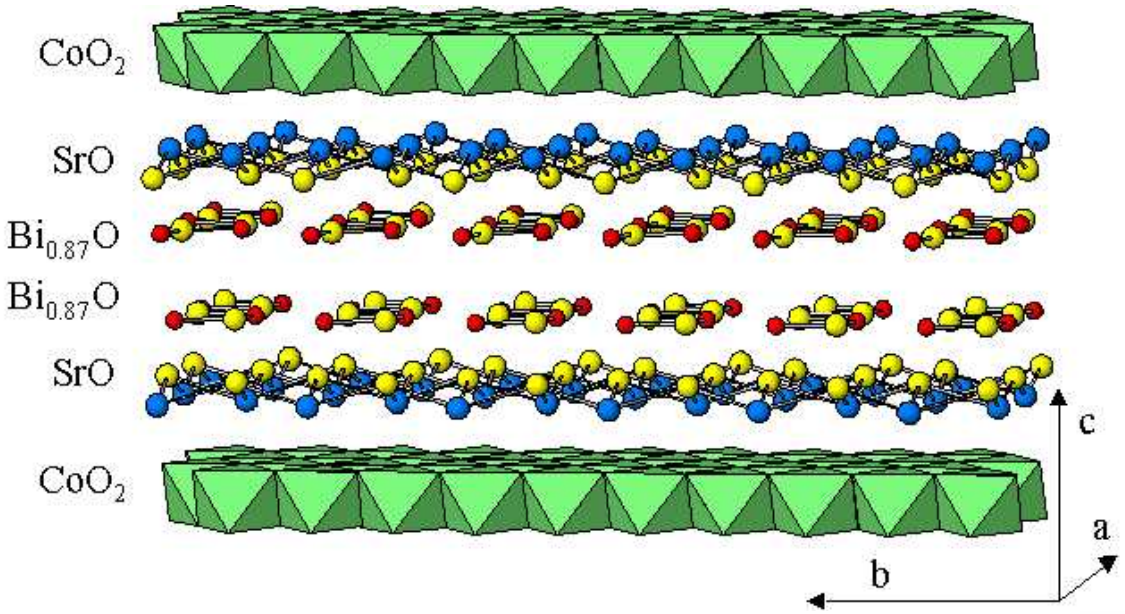

MB Lepetit PHYSICAL REVIEW B 74, 184507 (2006)

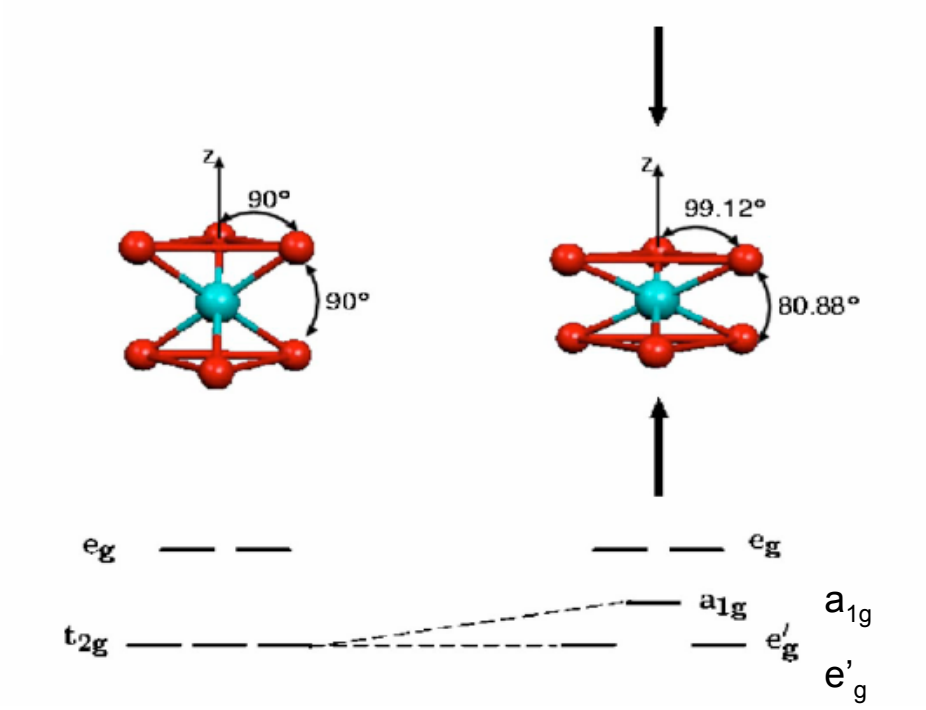

Ligand field splitting : trigonal distortion

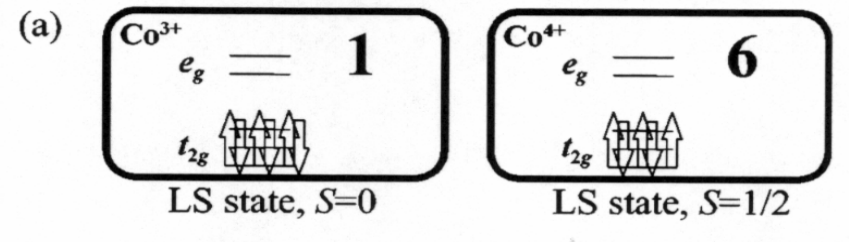

1 for Co^{3+} but 2 instead of 6 for Co^{4+}

$\beta = 1/6$

$\beta = 1/2$

Na_xCoO_2 Misfits

Influence of electronic correlations

For T→0 $$q = \frac{S}{T}\frac{N_{Av}e}{\gamma} = cste$$ S ~ γT

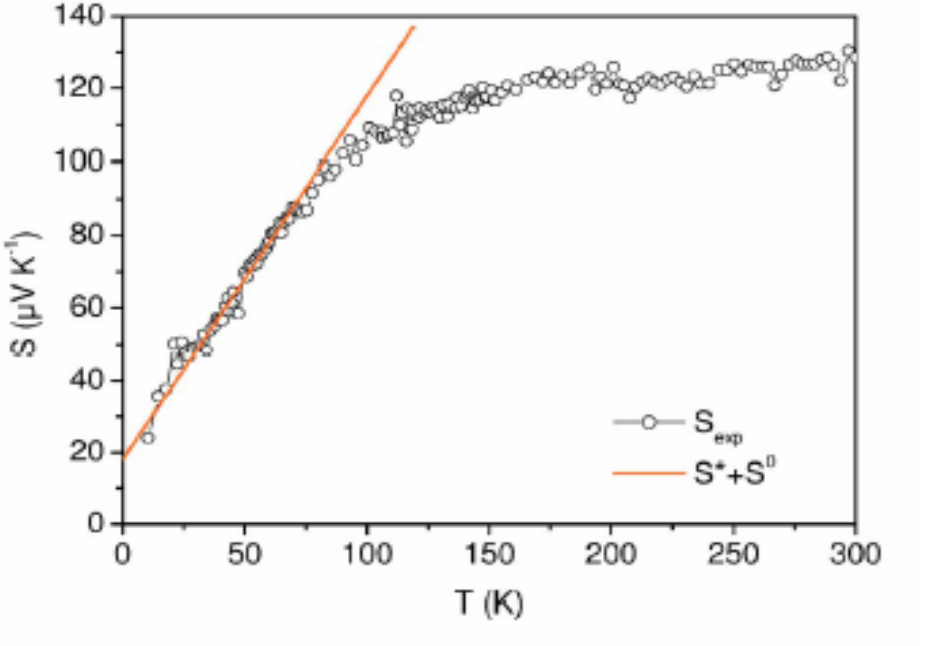

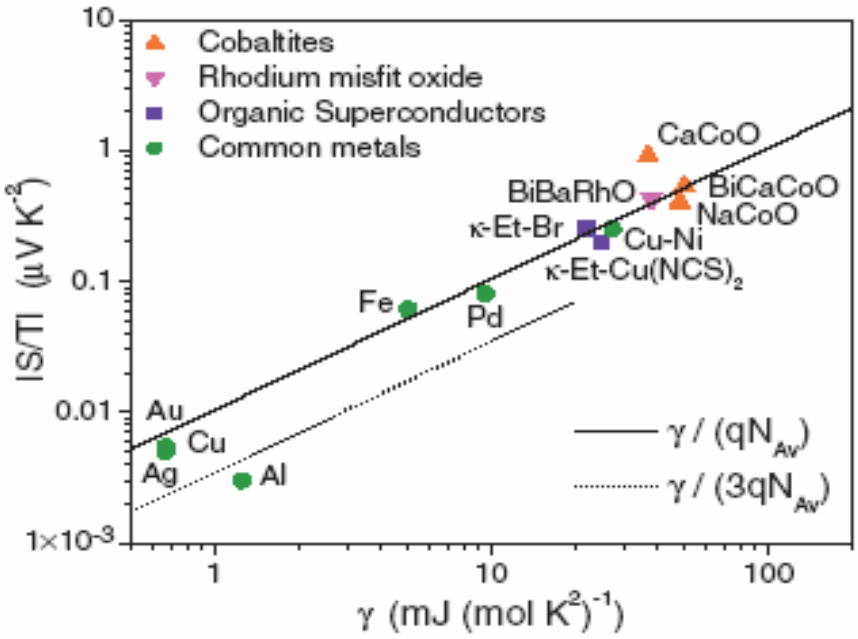

P. Limelette, PRB71, 233108 (2005)

P. Limelette, PRL97, 046601 (2006)

Low T : Spin entropy

BiCaCoO : excess of S at low T

A. Maignan et al., JPCM 15, 2711 (2003)

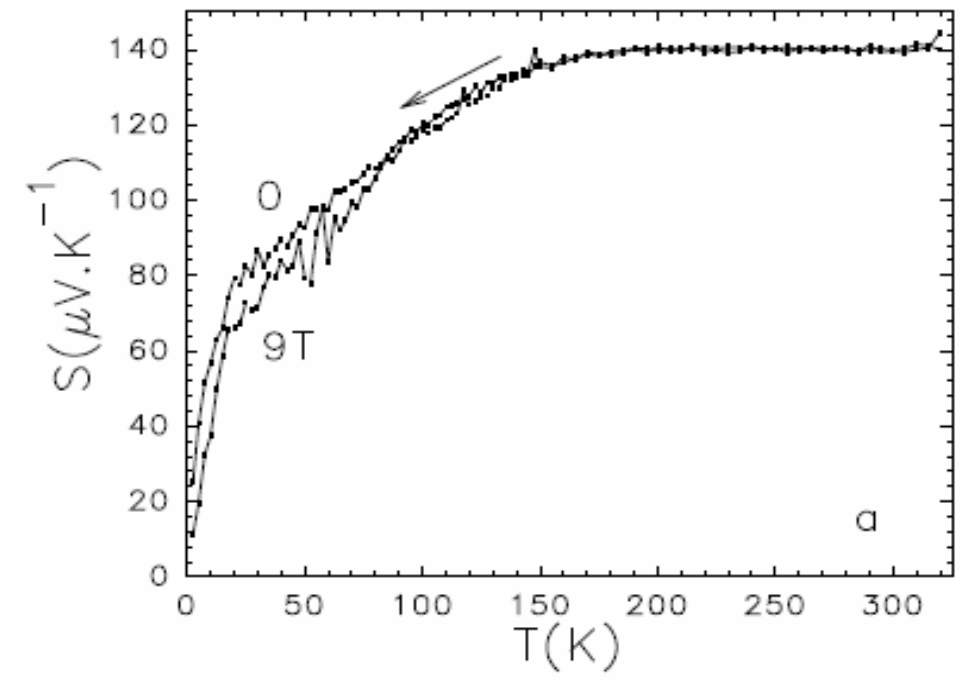

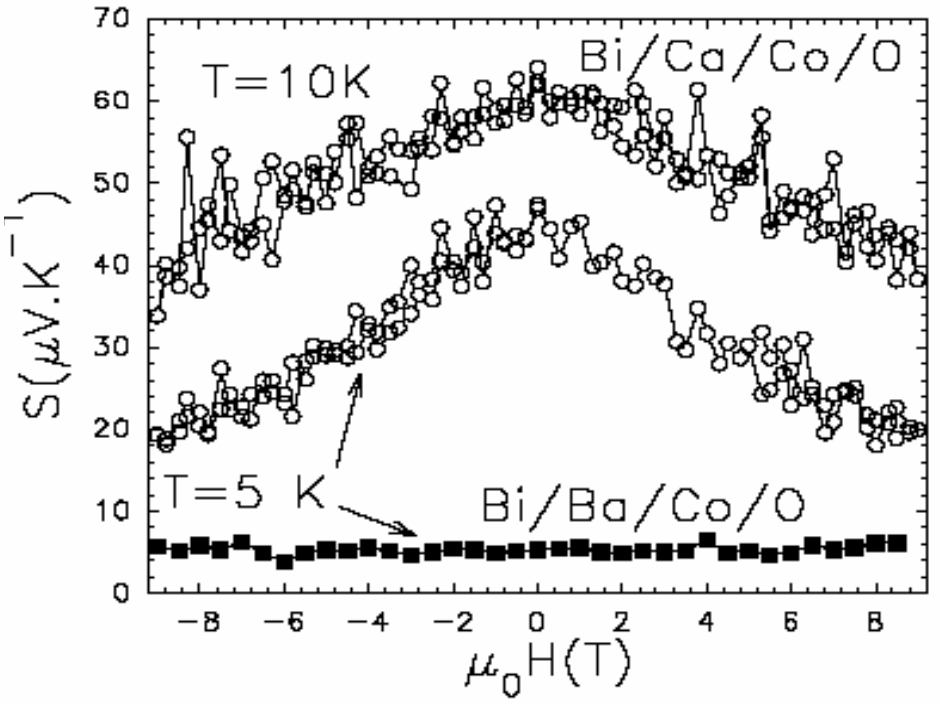

Observed also in Na_xCoO_2

[Wang et al. Nature 423, 425 (2003)]

Spin entropy at low T

Misfit BiCaCoO

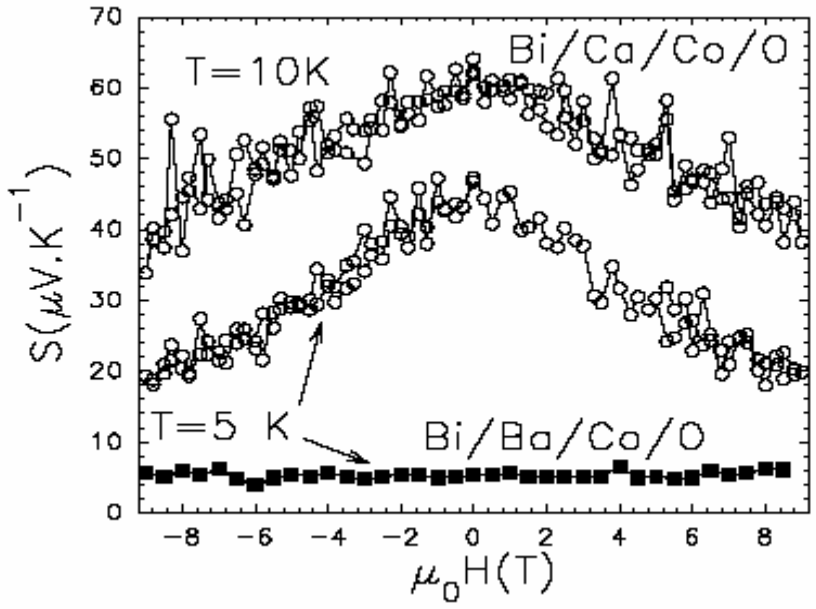

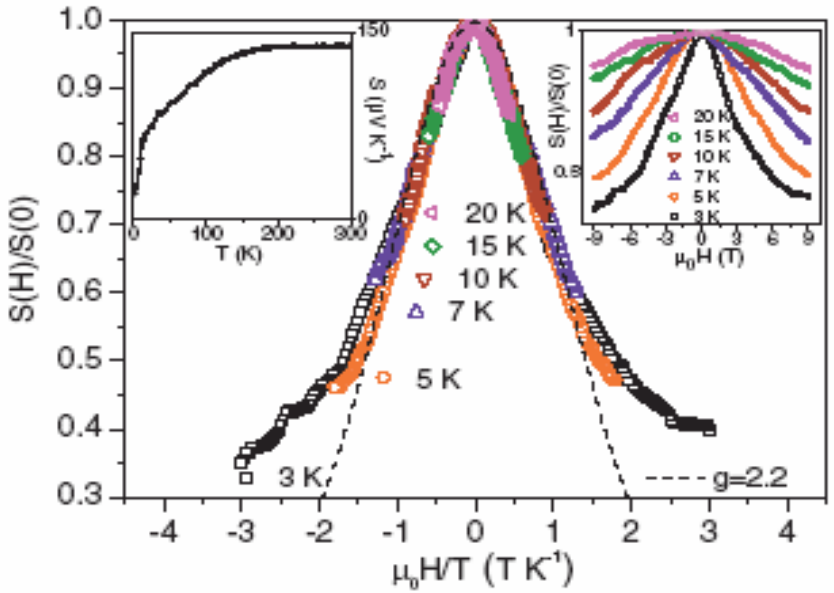

P. Limelette et al., PRL97, 046601 (2006)

Decrease of S under field at low T
Due to the alignement of paramagnetic spins

A. Maignan et al., JPCM15, 2711 (2003)

Peak of susceptibility

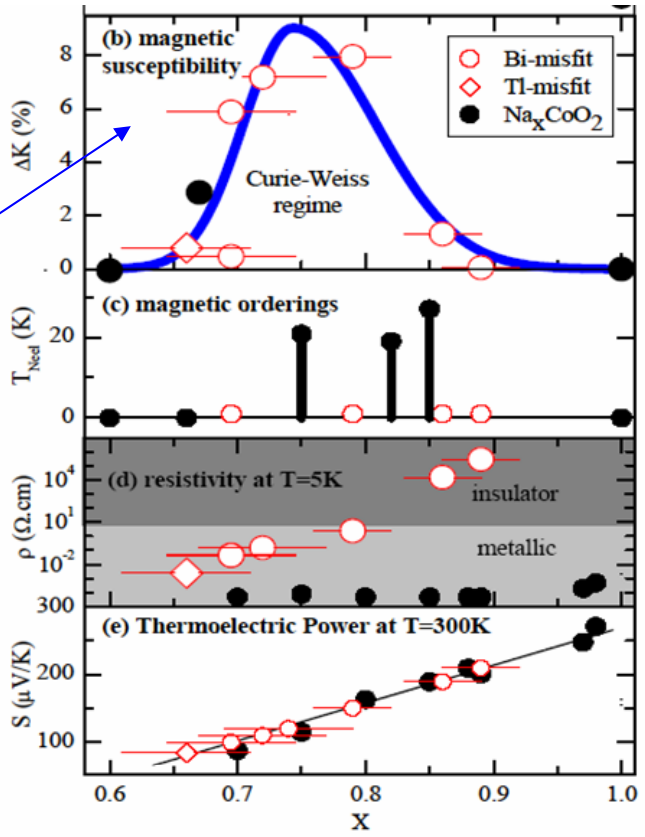

Scaling law for S(H) : paramagnetic spins S=1/2
Brillouin function

$$S(x)/S(0) = (\ln[2\cosh(x)] - x\tanh[x])/\ln(2).$$

$Na_{0.7}CoO_2$

Y. Wang et al., Nature423, 425 (2003)

Na_xCoO_2
Misfits

Misfit oxides

NaCl-like triple layer (RS)

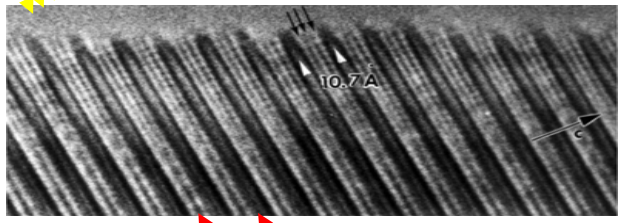

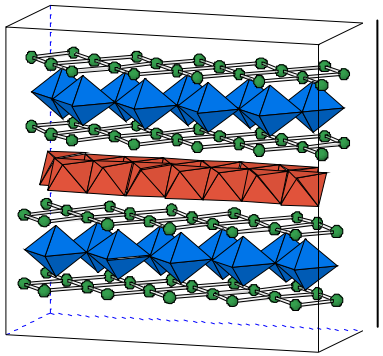

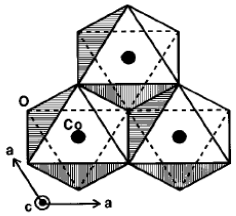

Co^{3+} ($3d^6$) / Co^{4+} ($3d^5$)
Low spin : t_{2g} orbitals
+ triangular network

CoO_2 (type CdI_2)

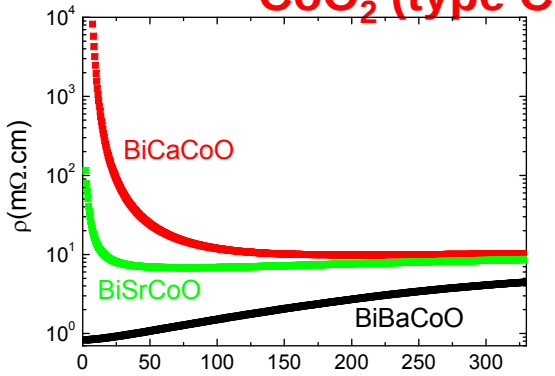

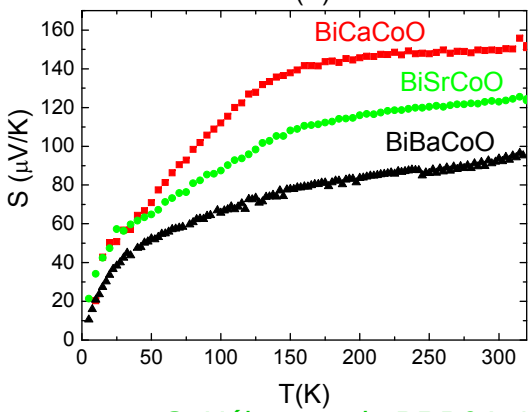

For T > 100K : metallicity + large S

- **High T** : Seebeck depends on Co^{4+}
  Heikes formula with spin / orbital degeneracye)

- **Low T :** electronic correlations : S ~ γT
  + spin entropy depending on doping

- **High T limit** : small t from Hall effect. Justifies the Heikes formula

S. Hébert et al., PRB64, 172101 (2001), P. Limelette et al., PRL97, 046601 (2006), W. Kobayashi et al., JPCM21, 235404 (2009)

Thermoelectric power of misfits

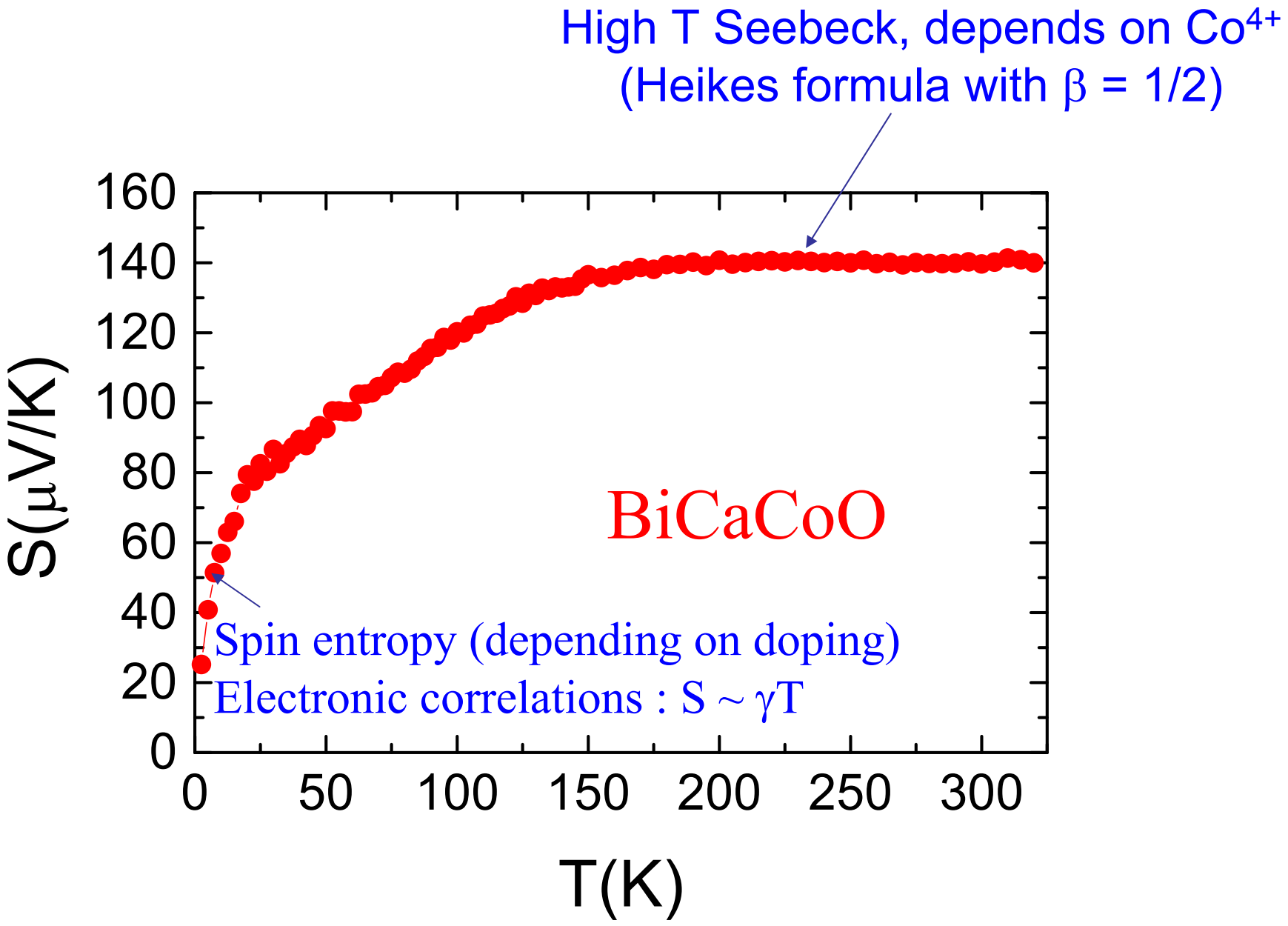

Na_xCoO_2
Misfits

Power factor

enhancement for BiBaCoO and BiPbSrCoO

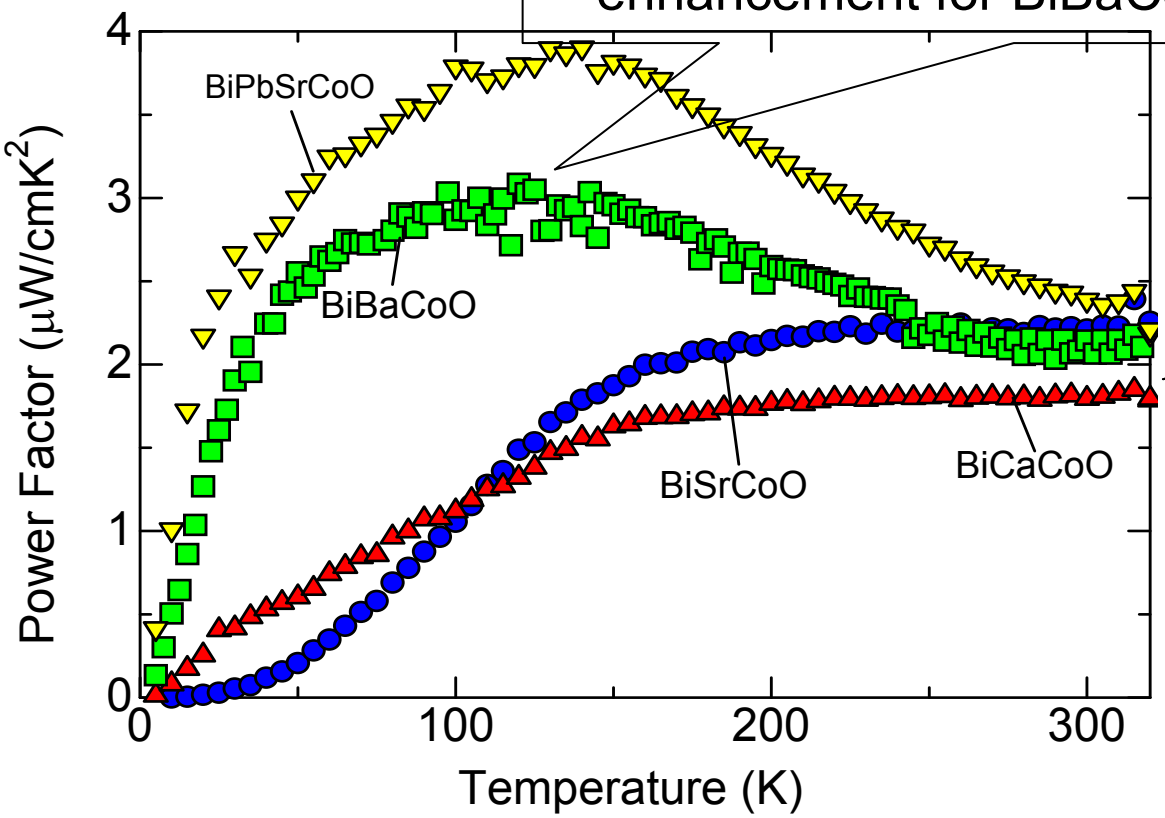

P is almost independent of carrier concentration

2.10^{-4} $Wm^{-1}K^{-2}$ at 300K

In conventional semiconducting thermoelectric material such as Bi_2Te_3, *n* is an important parameter to tune the properties.

How to modify the electronic properties?
Influence of the block layer?

Na_xCoO_2
Misfits

Role of the block layer?

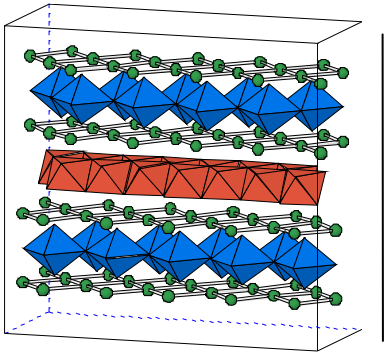

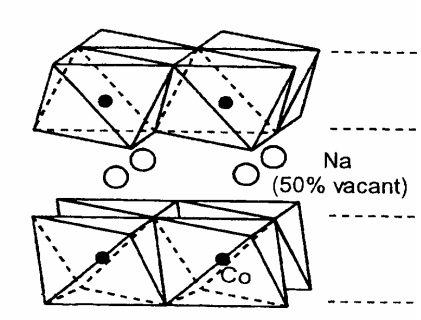

Curie-Weiss

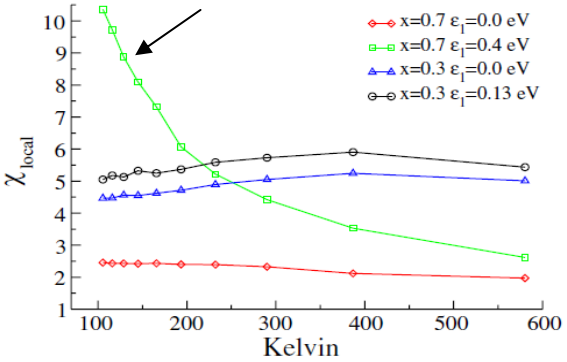

• Role of Na^+ : Curie-Weiss behavior obtained by introducing the electrostatic potential of Na^+ (Co^{3+} S = 0 / Co^{4+} S = 1/2)
C. Marianetti et al., PRL98, 176405 (2007)

•Kagomé lattice in Na_xCoO_2 with x = 2/3 : strong electronic correlations
F. Lechermann et al., PRL107, 236404 (2011)

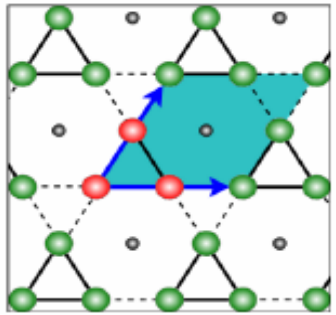

High T measurements in $Ca_3Co_4O_9$

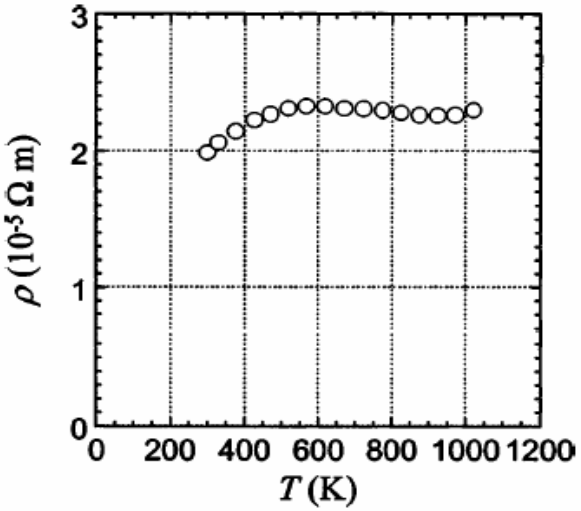

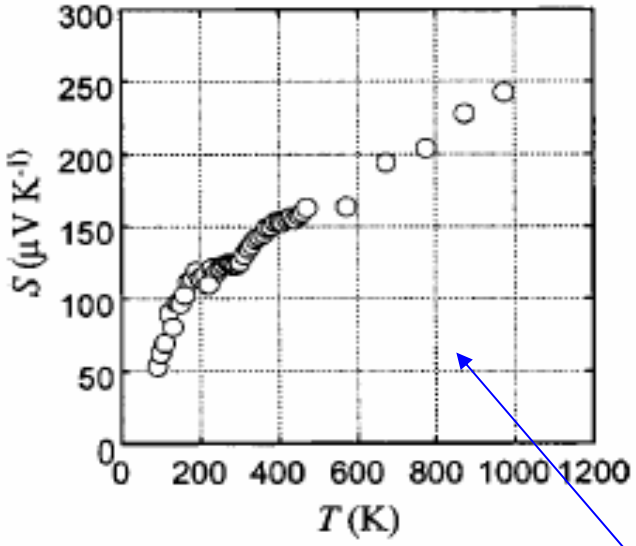

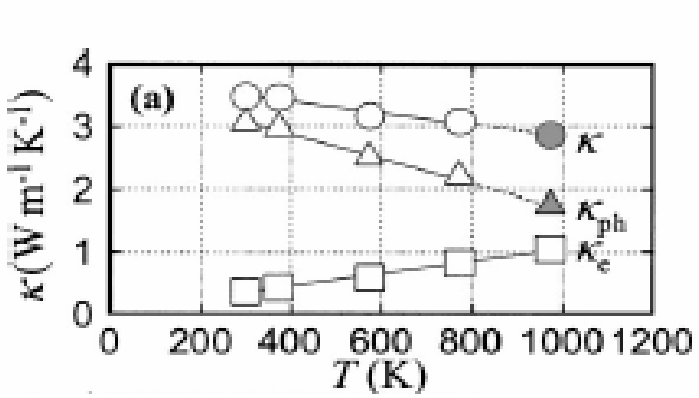

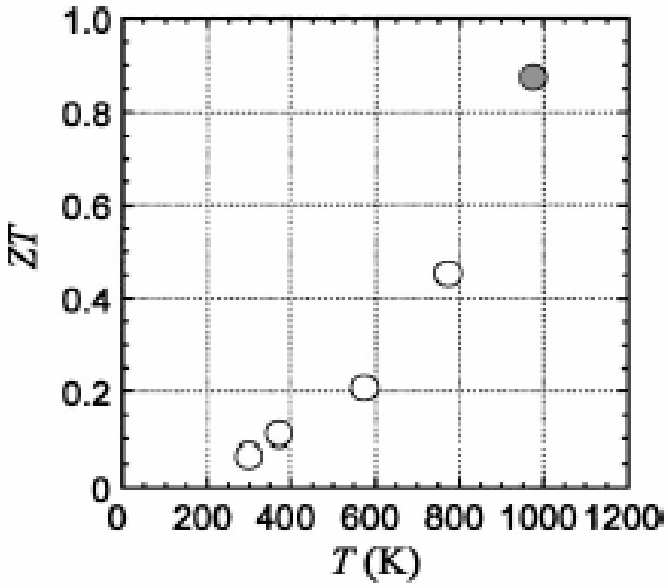

Increase of S at high T

Measurements in air?

M. Shikano et al., APL82, 1851 (2003)

Na_xCoO_2
Misfits

Thermal conductivity

Measurements of single crystals (Harman method)

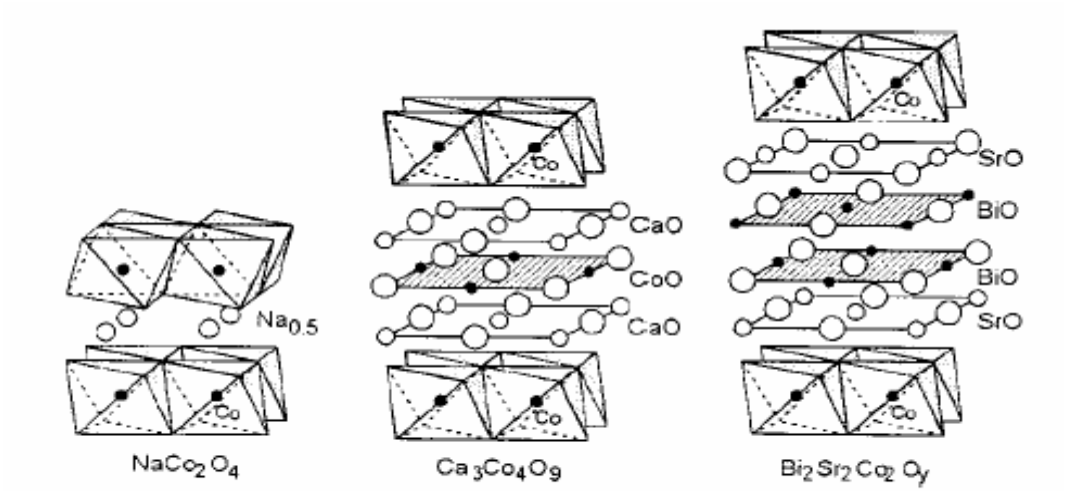

FIG. 1. Crystal structure of the layered cobalt oxides.

κ smaller in misfits

Influence of incommensurability?

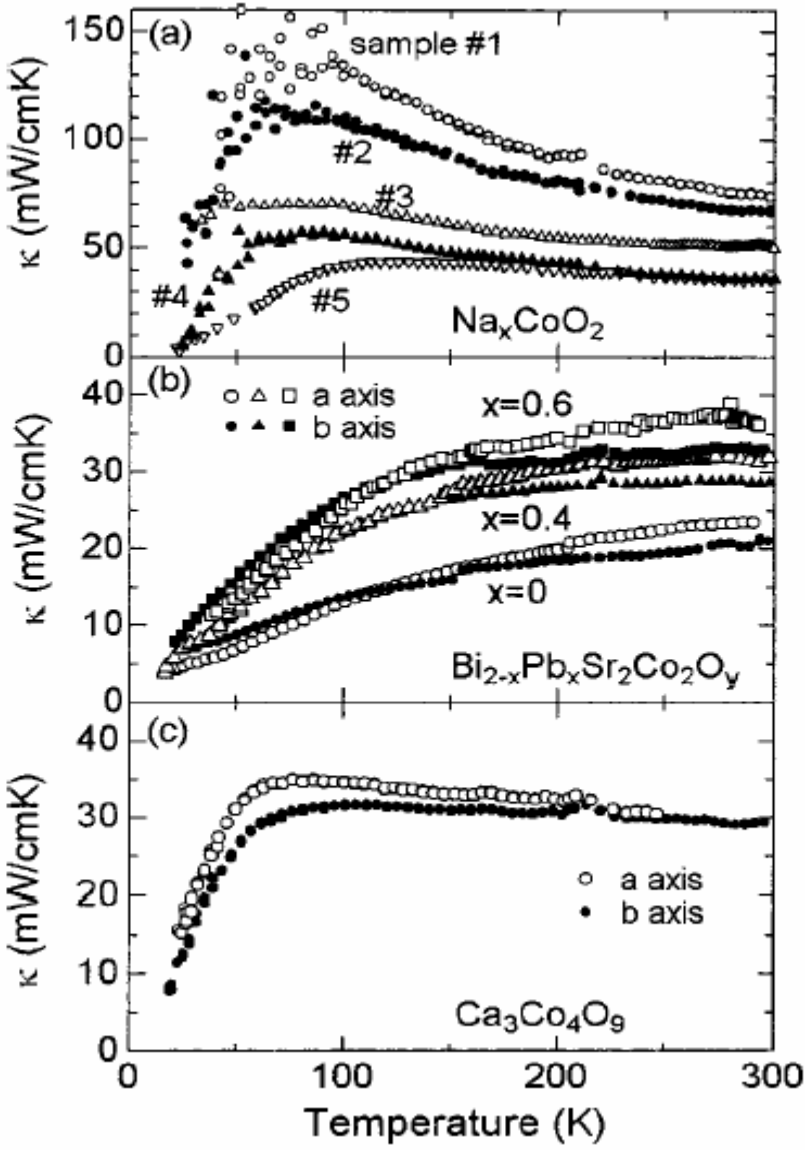

A. Satake et al., JAP96, 931 (2004)

Conclusion

- Charge transfer between the layers :
S_{300K} mostly depends on the ratio Co^{3+}/Co^{4+}

- Low T : electronic correlations influence ($S \sim \gamma T$) + S(H) term

- Small κ

↳ Power factor is constant : modification of the block layers?
↳Influence on thermal conductivity?

Nanostructuration

2D electron gas in $SrTiO_3$

H. Ohta et al., Nat. Mater. 6, 129 (2007)

$SrTi_{1-x}Nb_xO_3$

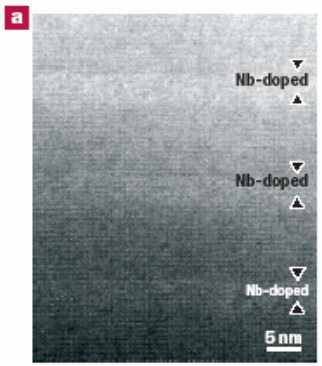

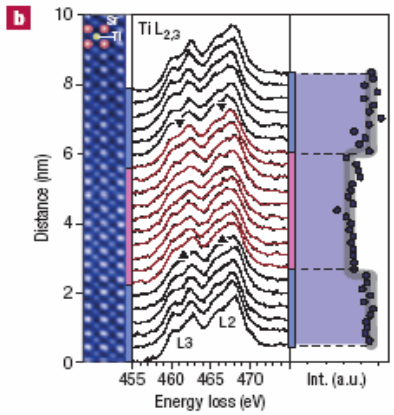

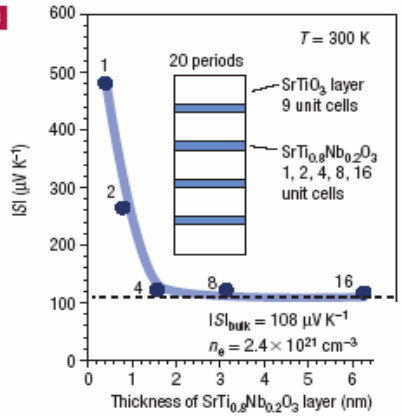

Nanostructuration : Increase of S

$$\sigma_{\text{eff.}} = \sigma_{\text{2DEG}}/(1+N_{\text{barrier}})$$

$$ZT_{\text{eff.}} = ZT_{\text{2DEG}}/(1+N_{\text{barrier}})$$

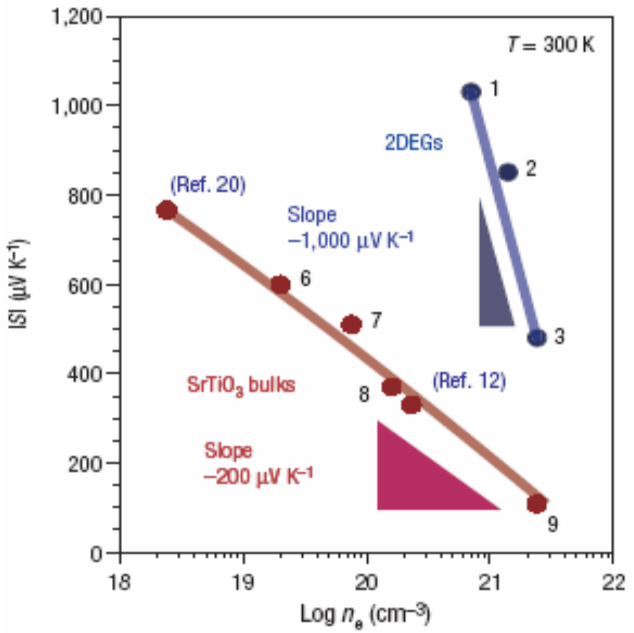

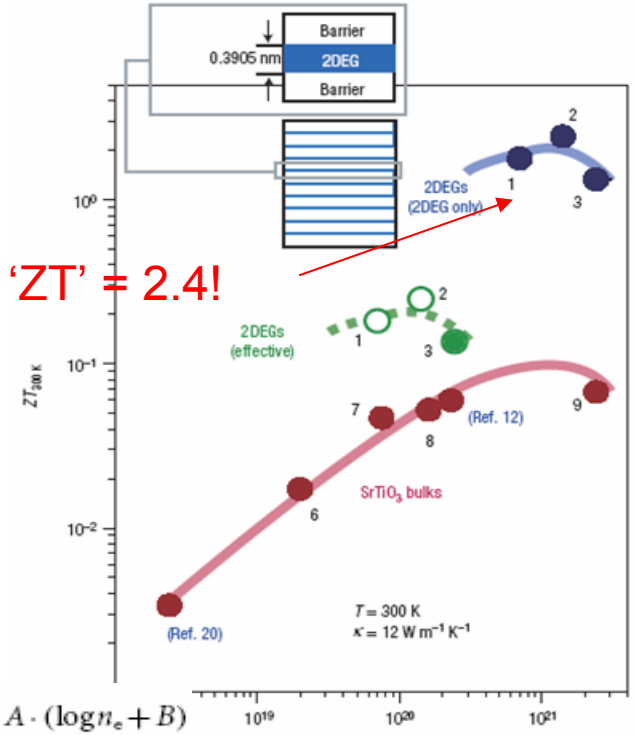

'ZT' = 2.4!

$$|S| = -k_B/e \cdot \ln 10 \cdot A \cdot (\log n_e + B)$$

κ of $SrTiO_3$ single crystals

Na_xCoO_2 nanowires

Sol-gel electrospinning

Same technique as for $Ca_3Co_4O_9$
Lin et al., J. Phys. Chem. C 114, 10061 (2010)

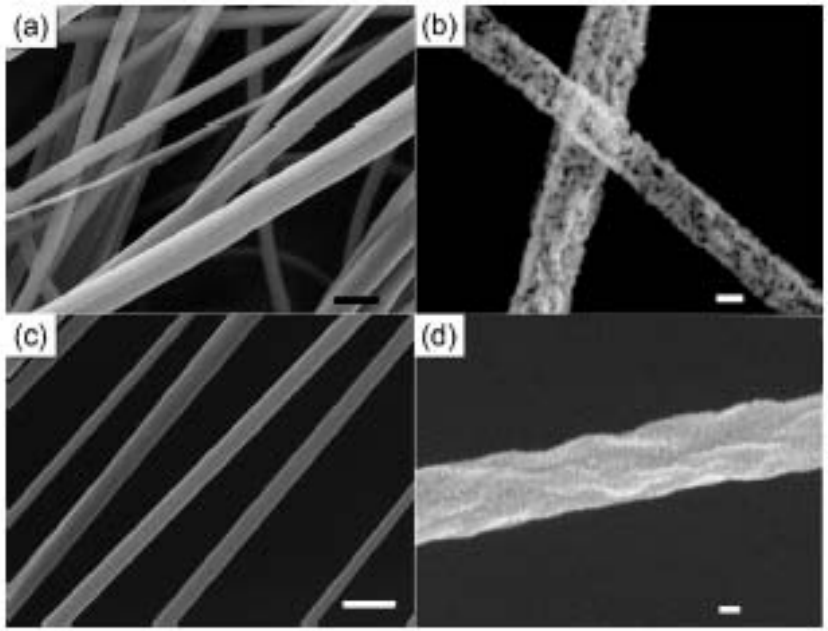

Figure 1. SEM image of $NaCo_2O_4$ nanofibers before and after annealing, synthesized with two different solvents; (a) and (b) methanol-based nanofibers before (a) and after (b) annealing; (c) and (d) water-based nanofibers before (c) and after (d) annealing; scale bars in (a) and (c) represent 1 μm, and in (b) and (d) represent 100 nm.

$\rho \sim \Omega.m$?
Resistivity overestimated by 3 orders of magnitude by the measurement technique?

F. Ma et al., J. Phys. Chem. C 114, 22038 (2010)

Strong correlations + Size effects

Thin films of BiSrCoO misfits

Correlation effect :

Behavior different from the one classical observed through the surface diffusion mechanism (Fuchs – Sondheimer model)

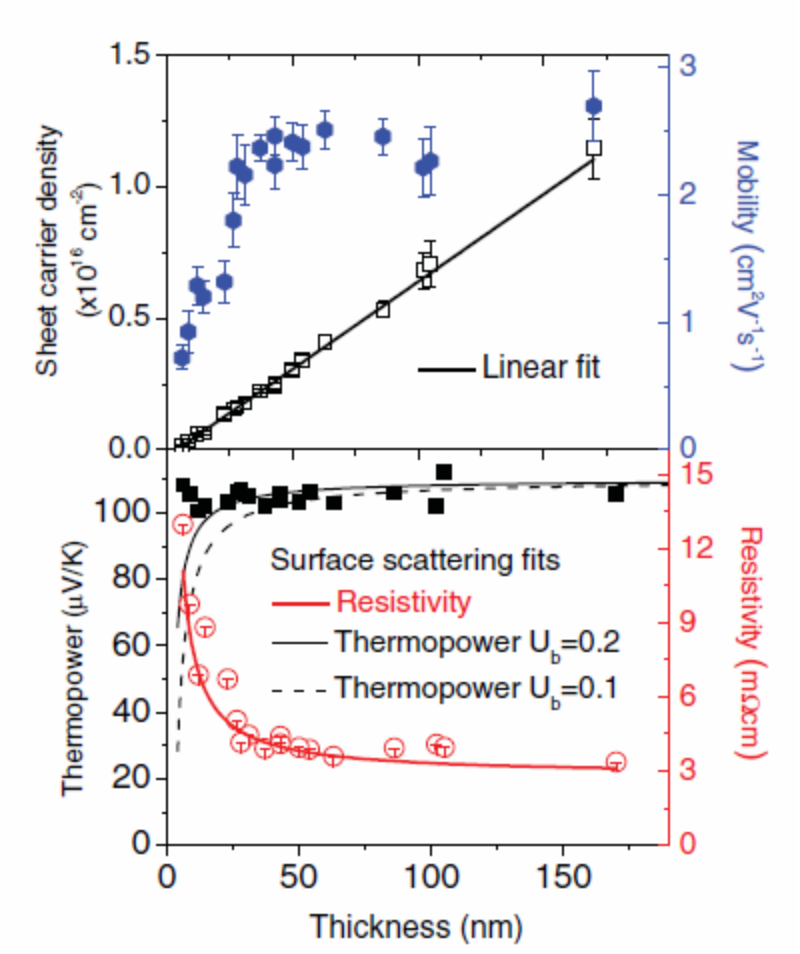

Decoupling of resistivity and Seebeck?

J. Ravichandran et al., PRB85, 085112 (2011)

Oxide modules

Oxide prototypes

1st prototype in 2000

n : $Ba_{0.4}Sr_{0.6}PbO_3$ Z = 2.10^{-4} K^{-1} at 673K (ZT = 0.13)
p : $Li_{0.025}Ni_{0.975}O$ Z = 0.75 10^{-4} K^{-1} at 1273K (ZT = 0.095)

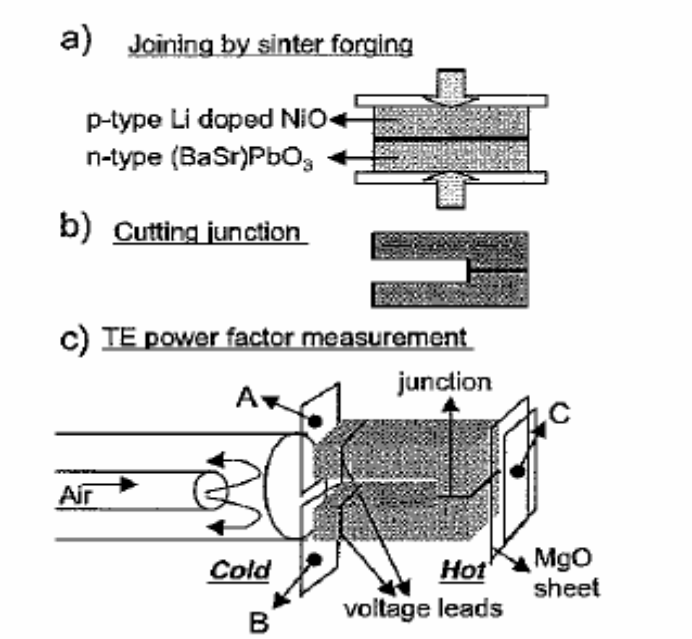

One leg : 4.8 ×4.9 × 17.5 mm^3

One pair : 7.91mW
T_H = 987K
ΔT = 552K

W. Shin et al., JJAP39, 1254 (2000)

Oxide prototypes

$n : Ca_{0.92}La_{0.08}MnO_3$ / $p : Ca_{2.75}Gd_{0.25}Co_4O_9$

8 pairs 3 × 5 × 30 mm^3

TABLE I. Thermoelectric power S, resistivity ρ, and power factor S^2/ρ of p and n legs used for fin-type device.

Materials	ρ-T	S (700 °C)	ρ (700 °C)	S^2/ρ (700 °C)
		μV/K	mΩ cm	10^{-4}W m^{-1} K^{-2}
$Ca_{2.75}Gd_{0.25}Co_4O_9$ (p leg)	Semiconducting	185	7.8	4.8
$Ca_{0.92}La_{0.08}MnO_3$ (n leg)	Metallic	−120	6.6	2.2

TABLE II. Thermal conditions, open circuit voltage V_o, and maximum output power P_{max} for fin-type device with eight $p-n$ couples.

Condition	T_h, °C	ΔT, °C	V_o, mV	P_{max}, mW
a	477	235	550	19.8
b	580	290	694	31.8
c	672	335	838	46.5
d	773	390	988	63.5

T_h: Hot side temperature.
ΔT: Temperature difference.

T_h = 1046K , ΔT = 390K,
P=63.5mW

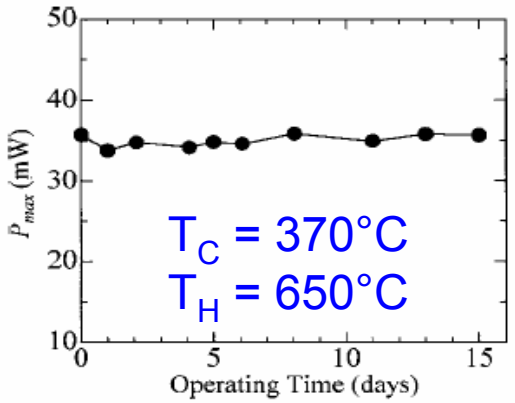

Stability

I. Matsubara et al., APL 78, 3627 (2001)

Modules

$La_{0.9}Bi_{0.1}NiO_3$ / $Ca_{2.7}Bi_{0.3}Co_4O_9$

n : $La_{0.9}Bi_{0.1}NiO_3$ / p : $Ca_{2.7}Bi_{0.3}Co_4O_9$
1 jonction : T_H = 1073K, ΔT = 500K, P = 94mW

140 paires
T_H = 1072K, ΔT = 551K

FIG. 4. (Color) Comparative photographs of the oxide module and a mobile phone, and a demonstration of charging a lithium-ion battery in the mobile phone. Red LED on the mobile phone indicates charging of the lithium-ion battery is in progress.

For mobile phone
T_H = 1072K!

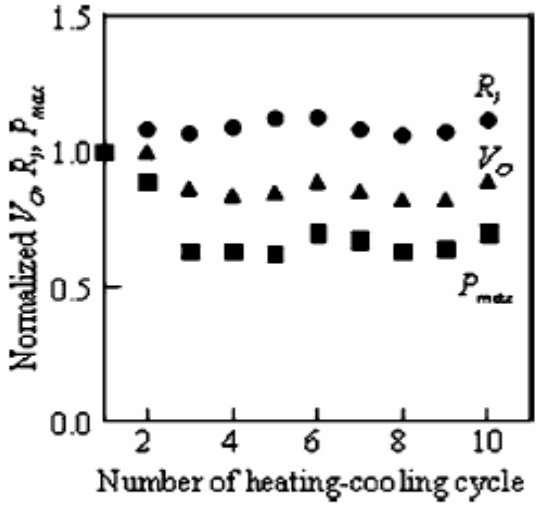

FIG. 3. Thermal resistance of the oxide module at T_H of ~723 K and ΔT of ~385 K. R_I (●), V_O (▲), and P_{max} (■) normalized by the values of the first trial are plotted against the number of heating-cooling cycles.

R. Funahashi et al., APL 85, 1036 (2004)
R. Funahashi et al., JAP99, 066117 (2006)

Comparison of modules

Manufacturing factor

$MF = R_{ideal} / R_{int}$,

Name	**Materials**	Type	Nb Couple	Power (W)	**MF**
Funahashi et al.	$Ca_{2.7}Bi_{0.3}Co_4O_9$ / $La_{0.9}Bi_{0.1}NiO_3$	PN	1	0.03	**0.15**
Shin et al.	(Li) NiO / (Ba, Sr) PbO_3	PN	2	0.034	**0.3**
Matsubara et al.	(Gd) $Ca_3Co_4O_9$ / (La) $CaMnO_3$	PN	8	0.089	**0.82**
Sudhakar et al.	$Ca_3Co_4O_9$ / $Ca_{0.95}Sm_{0.05}MnO_3$	PN	2	0.031	**0.57**
Present work	$Ca_{0.95}Sm_{0.05}MnO_3$/ $Ca_{0.95}Sm_{0.05}MnO_3$	N	2	0.016	**0.15**

Important to optimize the contacts quality!

S. Lemonnier, C. Goupil et al.

Modules and prototypes

JOURNAL OF APPLIED PHYSICS **109**, 124509 (2011)

Monolithic oxide–metal composite thermoelectric generators for energy harvesting

Shuichi Funahashi,[a] Takanori Nakamura, Keisuke Kageyama, and Hideharu Ieki
Research Center for Next Generation Technology, Murata Manufacturing Co., Ltd., 2288 Ohshinohara, Yasu, Shiga 520-2393, Japan

(Received 7 March 2011; accepted 11 May 2011; published online 27 June 2011)

Monolithic oxide–metal composite thermoelectric generators (TEGs) were fabricated using multilayer co-fired ceramic technology. These devices consisted of $Ni_{0.9}Mo_{0.1}$ and $La_{0.035}Sr_{0.965}TiO_3$ as p- and n-type thermoelectric materials, and $Y_{0.03}Zr_{0.97}O_2$ was used as an insulator, sandwiched between p- and n-type layers. To co-fire dissimilar materials, p-type layers contained 20 wt. % $La_{0.035}Sr_{0.965}TiO_3$; thus, these were oxide–metal composite layers. The fabricated device had 50 pairs of p–i–n junctions of 5.9 mm × 7.0 mm × 2.6 mm. The calculated maximum value of the electric power output from the device was 450 mW/cm^2 at $\Delta T = 360$ K. Furthermore, this device generated 100 μW at $\Delta T = 10$ K and operated a radio frequency (RF) transmitter circuit module assumed to be a sensor network system. © *2011 American Institute of Physics.*
[doi:10.1063/1.3599890]

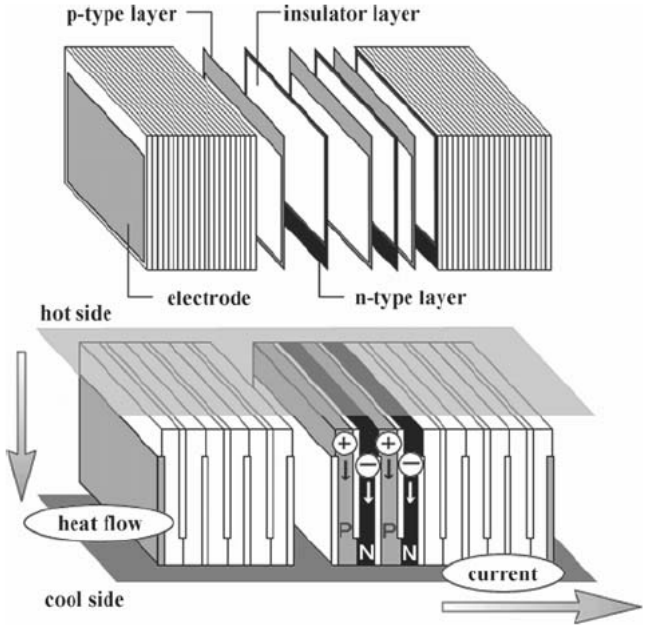

FIG. 1. Structure of the monolithic thermoelectric generator (TEG), based on multilayer ceramic capacitor (MLCC) technology. The p- and n-type layer printed insulators were stacked and co-fired.

Type n : $SrTiO_3$ dopé au La
450mW/cm^2 pour ΔT = 360K

Stability problems

Oxygen stoechiometry?

Oxides : can be synthesized in air or controlled atmosphere at 800°C – 1500°C

Misfits : 800 - 1000 °C in air, or controlled atmosphere

$La_{1-x}Sr_xCo^{3+}_{1-x}Co^{4+}_xO_3$: 1250°C

$Pr^{3+}_{1-x}Ca^{2+}_xCr^{3+/4+}O_3$: 1500°C in O_2

$CuCr_{1-x}Mg_xO_2$: 1200°C in air

$Ca_{0.9}M_{0.1}MnO_3$: 1300°C in air

$Zn_{1-x}Al_xO$: 1400°C in air

$Sr_{1-x}La_xTiO_3$: 1400°C

In_2O_3 : 1300°C in air

Thermal stability

Perovskites

Type n : manganese oxides

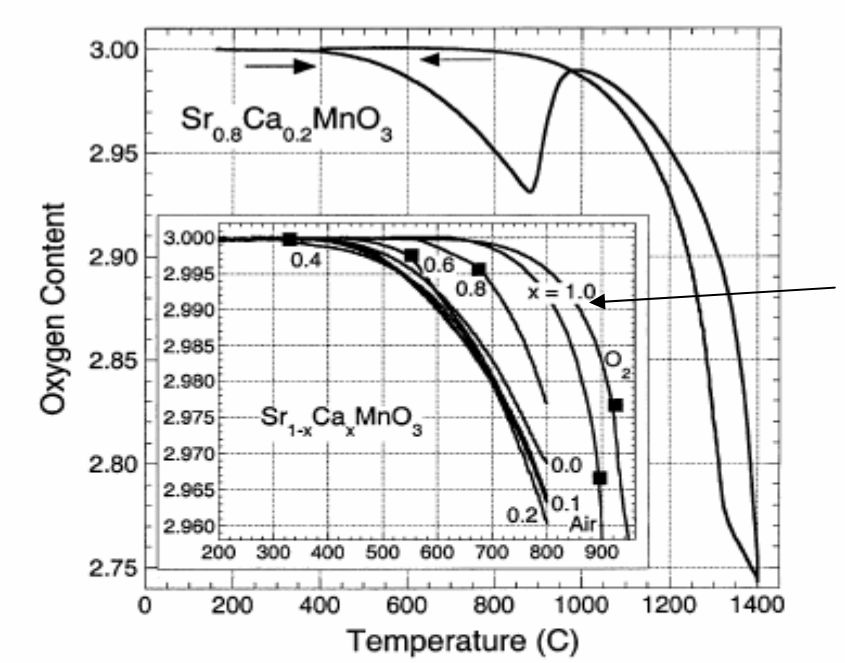

Fig. 2. Thermogravimetric analysis measurements on heating and cooling in a 20% O_2/Ar gas mixture for perovskite $Sr_{0.8}Ca_{0.2}MnO_3$. Inset: Oxygen nonstoichiometry during heating the perovskite phases $Sr_{1-x}Ca_xMnO_3$ ($x = 0.0, 0.1, 0.2, 0.4, 0.6, 0.8, 1.0$) in oxygen at low temperatures. Filled squares denote temperatures at which an increased formation of oxygen vacancies is observed on heating (legend the same as for main panel).

$CaMnO_3$
Stable jusqu'à ~ 700 -800°C
sous O_2

B. Dabrowski et al., JSSC170, 154 (2003)

Thermal stability

Misfits

Oxygen stoechiometry?

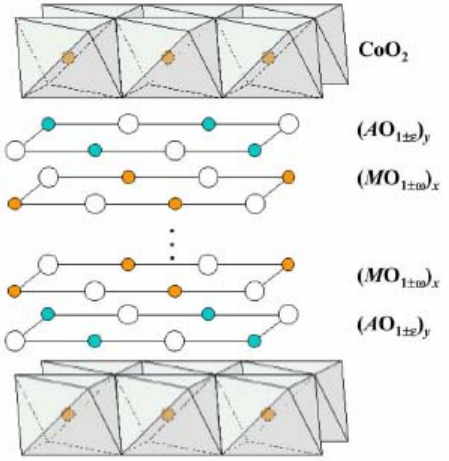

Fig. 1. Schematic illustration of the crystal structure of an ML cobalt-oxide phase, $[(MO_{1\pm\omega})_x]_m[(AO_{1\pm\varepsilon})_y]_nCoO_2$, consisting of two sub-systems, CoO_2 and $AO_{1\pm\varepsilon}$-$(MO_{1\pm\omega})_m$-$AO_{1\pm\varepsilon}$, that are incommensurate along the b-axis direction, but have the lattice parameters, a, c and β, in common.

N_2 annealing

Thermogravimetric
+ titration analysis

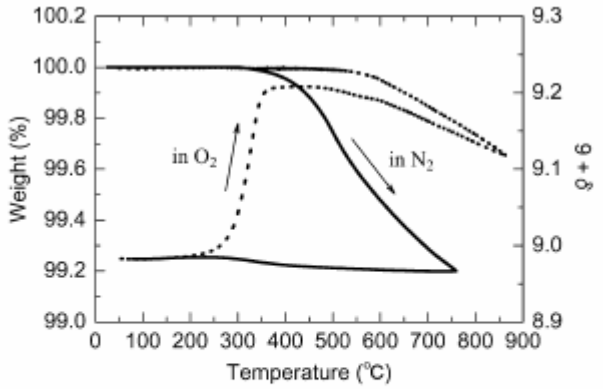

Fig. 2. TG curves for $Ca_3Co_{3.95}O_{9+\delta}$ showing its deoxygenation and oxygenation characteristics. First as-air-synthesized $Ca_3Co_{3.95}O_{9.24}$ is deoxygenated by heating (up to 750°C) and cooling in N_2 (—) and subsequently oxygenated by heating (up to 850°C) and cooling in O_2 (---). The mass of the sample was ~60 mg and the heating and cooling rates were 0.5°C/min.

Y. Morita et al., JSSC177, 3149 (2004)

Synthesis and measurements conditions : ZnO

Al-doped ZnO revisités : conditions de synthèse

Précurseurs identiques, préparation de lots de poudre (ball-milling, liant organique), séparation en 2 lots

1400°C, flux de N_2, 5h

15-20% pertes en masse
densité > 90%
barreaux bleu-nuit

1400°C, flux d'air sec, 5h

5% pertes en masse
densité > 90%
barreaux bleu-vert

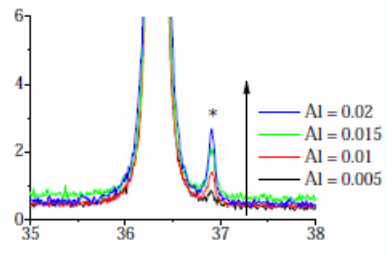

XRD (+ rietveld) :
pas de différence significative
présence de spinelle $ZnAl_2O_4$

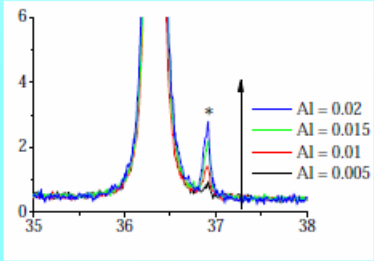

D Bérardan et al., J am ceram soc, dispo en ligne (2010)

D. Bérardan, GdR Thermoélectricité 06-2010

D. Bérardan et al., GDR Thermoélectricité, Grenoble, juin 2010

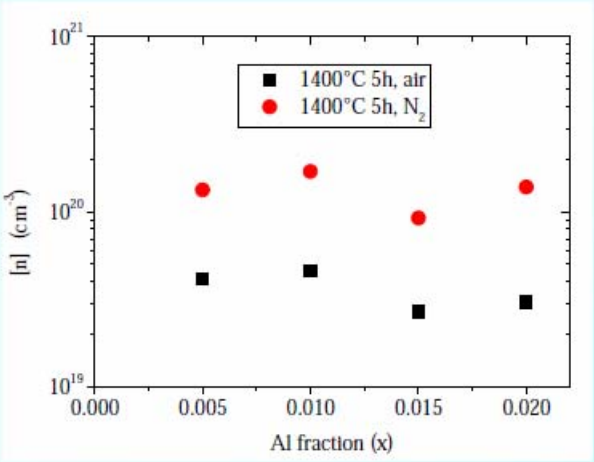

[n] nettement plus élevée après frittage N_2

$$Zn\,O \longrightarrow Zn_{Zn}^{X} + V_O^{\bullet\bullet} + 2\,e' + \frac{1}{2}O_2 \uparrow$$

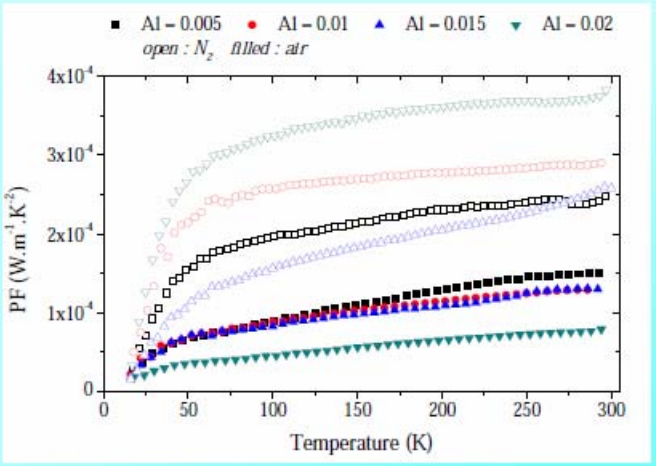

conséquence : frittage N_2 → $S^2\sigma$ *plus élevé*

(plus d'un facteur 2 d'écart)

D Bérardan et al., J am ceram soc, dispo en ligne (2010)

D. Bérardan, GdR Thermoélectricité 06-2010

D. Bérardan et al., GDR Thermoélectricité, Grenoble, juin 2010

Conclusion

ZT (n type) < ZT (p type)
Thermal conductivity : coming from the lattice

- n type oxides : degenerate semi-conductors

Seebeck described in a first approach by Mott's formula

- p type oxides

Seebeck coefficient : **Major role of the spin and orbital term**

Importance of electronic correlations

$$S = -\frac{k_B}{|e|} \ln(\beta \frac{1-x}{x})$$

How to enhance ZT??

↳Investigation of thermal conductivity

↳Nanostructuration and electronic correlations?

↳ Low dimensional structures

↳ Microstructures

↳ Anionic subsitutions (oxyselenides)

Collaborators

Laboratoire CRISMAT
Wataru Kobayashi (Tsukuba), Hidefumi Takahashi (Nagoya),
Antoine Maignan, Christine Martin,
Denis Pelloquin, Olivier Perez

Patrice Limelette, LEMA, Tours
Julien Bobroff, Véronique Brouet, LPS Orsay

This work is supported by FP7 European Initial Training Network
SOPRANO (GA-2008-214040)